

108p.

(NASA Contract No.)

N64-15788⁸

CODE-1

(NASA) CR-53063;

JPL TR-32-542

Technical Report No. 32-542

*Investigation of Liquid and Gaseous Secondary
Injection Phenomena on a Flat Plate
with $M = 2.01$ to $M = 4.54$*

*Mack W. Dowdy and
John F. Newton, Jr.*

OTS:PRICE

XEROX

\$ 9.10 ph.

MICROFILM \$

3.44 mf.



1304823 JET PROPULSION LABORATORY
CALIFORNIA INSTITUTE OF TECHNOLOGY
PASADENA, CALIFORNIA

December 23, 1963

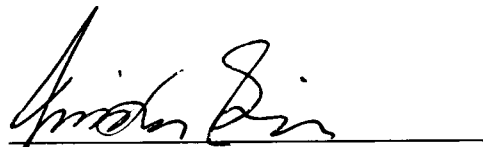
108p. ref

Technical Report No. 32-542

*Investigation of Liquid and Gaseous Secondary
Injection Phenomena on a Flat Plate
with $M = 2.01$ to $M = 4.54$*

Mack W. Dowdy

John F. Newton, Jr.



Winston Gin

**Winston Gin, Chief
Solid Propellant Engineering Section**

**JET PROPULSION LABORATORY
CALIFORNIA INSTITUTE OF TECHNOLOGY
PASADENA, CALIFORNIA**

December 23, 1963

**Copyright © 1963
Jet Propulsion Laboratory
California Institute of Technology**

**Prepared Under Contract No. NAS 7-100
National Aeronautics & Space Administration**

CONTENTS

I. Introduction	1
II. Description of Experiments	2
A. Flat Plate Design	2
B. Injection System	2
C. Instrumentation and Data Reduction	5
III. Test Results for Liquid Nitrogen Injection	7
A. General Considerations	7
B. Visual Data	7
C. Pressure Data	9
D. Temperature Data	12
E. Impinging Jet Injector	13
IV. Test Results for Gaseous Nitrogen Injection	14
A. General Considerations	14
B. Visual Data	14
C. Pressure Data	14
V. Separation Phenomena	17
A. General Considerations	17
B. Comparison of Laminar and Turbulent Boundary Layer Separation	17
C. Turbulent Boundary Layer Separation	18
D. Laminar Boundary Layer Separation	18
E. Stability of Separated Flows	19
VI. Conclusions and Recommendations	20
Appendix A. Liquid Nitrogen Data	21
Appendix B. Gaseous Nitrogen Data	59
Nomenclature	99
References	100

TABLES

1. Liquid nitrogen flow rate comparison	5
A-1. Liquid nitrogen injection	21
A-2. Pressure data for Run 4-1 (LN₂ injection)	22
A-3. Pressure data for Run 4-2 (LN₂ injection)	23
A-4. Pressure data for Run 4-3 (LN₂ injection)	24
A-5. Pressure data for Run 4-4 (LN₂ injection)	25
A-6. Pressure data for Run 4-5 (LN₂ injection)	26
A-7. Pressure data for Run 6-1 (LN₂ injection)	27
A-8. Pressure data for Run 6-2 (LN₂ injection)	28
A-9. Pressure data for Run 6-3 (LN₂ injection)	29
A-10. Pressure data for Run 6-4 (LN₂ injection)	30
A-11. Pressure data for Run 6-5 (LN₂ injection)	31
A-12. Pressure data for Run 6-6 (LN₂ injection)	32
A-13. Pressure data for Run 8-1 (LN₂ injection)	33
A-14. Pressure data for Run 8-2 (LN₂ injection)	34
A-15. Pressure data for Run 8-3 (LN₂ injection)	35
A-16. Pressure data for Run 8-4 (LN₂ injection)	36
A-17. Pressure data for Run 8-5 (LN₂ injection)	37
A-18. Pressure data for Run 10-1 (LN₂ injection)	38
A-19. Pressure data for Run 10-2 (LN₂ injection)	39
A-20. Pressure data for Run 12-1 (LN₂ injection)	40
A-21. Pressure data for Run 12-2 (LN₂ injection)	41
A-22. Pressure data for Run 12-3 (LN₂ injection)	42
A-23. Pressure data for Run 12-4 (LN₂ injection)	43
A-24. Pressure data for Run 12-5 (LN₂ injection)	44
A-25. Pressure data for Run 14-1 (LN₂ injection)	45
A-26. Pressure data for Run 14-2 (LN₂ injection)	46
A-27. Pressure data for Run 14-3 (LN₂ injection)	47
A-28. Pressure data for Run 14-4 (LN₂ injection)	48
A-29. Pressure data for Run 14-5 (LN₂ injection)	49
A-30. Pressure data for Run 15-1 (LN₂ injection)	50
A-31. Pressure data for Run 15-2 (LN₂ injection)	51
A-32. Pressure data for Run 15-3 (LN₂ injection)	52

TABLES (Cont'd)

A-33. Pressure data for Run 15-4 (LN₂ injection)	53
A-34. Pressure data for Run 15-5 (LN₂ injection)	54
B-1. Gaseous nitrogen injection	59
B-2. Pressure data for Run 19-1 (GN₂ injection)	60
B-3. Pressure data for Run 19-2 (GN₂ injection)	61
B-4. Pressure data for Run 19-3 (GN₂ injection)	62
B-5. Pressure data for Run 19-4 (GN₂ injection)	63
B-6. Pressure data for Run 24-1 (GN₂ injection)	64
B-7. Pressure data for Run 24-3 (GN₂ injection)	65
B-8. Pressure data for Run 24-4 (GN₂ injection)	66
B-9. Pressure data for Run 24-5 (GN₂ injection)	67
B-10. Pressure data for Run 24-6 (GN₂ injection)	68
B-11. Pressure data for Run 24-7 (GN₂ injection)	69
B-12. Pressure data for Run 26-1 (GN₂ injection)	70
B-13. Pressure data for Run 26-2 (GN₂ injection)	71
B-14. Pressure data for Run 26-3 (GN₂ injection)	72
B-15. Pressure data for Run 26-4 (GN₂ injection)	73
B-16. Pressure data for Run 26-5 (GN₂ injection)	74
B-17. Pressure data for Run 26-6 (GN₂ injection)	75
B-18. Pressure data for Run 28-1 (GN₂ injection)	76
B-19. Pressure data for Run 28-2 (GN₂ injection)	77
B-20. Pressure data for Run 28-4 (GN₂ injection)	78
B-21. Pressure data for Run 28-5 (GN₂ injection)	79
B-22. Pressure data for Run 28-6 (GN₂ injection)	80
B-23. Pressure data for Run 28-7 (GN₂ injection)	81
B-24. Pressure data for Run 28-8 (GN₂ injection)	82
B-25. Pressure data for Run 30-1 (GN₂ injection)	83
B-26. Pressure data for Run 30-2 (GN₂ injection)	84
B-27. Pressure data for Run 30-4 (GN₂ injection)	85
B-28. Pressure data for Run 30-5 (GN₂ injection)	86
B-29. Pressure data for Run 30-6 (GN₂ injection)	87
B-30. Pressure data for Run 32-1 (GN₂ injection)	88
B-31. Pressure data for Run 32-2 (GN₂ injection)	89

TABLES (Cont'd)

B-32. Pressure data for Run 32-3 (GN₂ injection)	90
B-33. Pressure data for Run 32-4 (GN₂ injection)	91
B-34. Pressure data for Run 32-5 (GN₂ injection)	92
B-35. Pressure data for Run 32-6 (GN₂ injection)	93
B-36. Pressure data for Run 32-7 (GN₂ injection)	94

FIGURES

1. Flat plate installation	2
2. Pressure tap locations on flat plate	2
3. Thermocouple locations on flat plate	3
4. Liquid nitrogen supply system	3
5. Comparison of injector inserts	4
6. Vapor pressure curve for nitrogen	7
7. Comparison of shadowgraphs for LN₂ injection at M = 2.01	8
8. Comparison of shadowgraphs for LN₂ injection at M = 3.26	9
9. Comparison of shadowgraphs for LN₂ injection with P_j/P_T ≈ 3.5	10
10. Typical pressure distribution for LN₂ injection at M = 2.61	11
11. Typical pressure distribution for LN₂ injection at M = 3.26	11
12. Separation distance for LN₂ injection	12
13. Length of downstream overpressure region for LN₂ injection	12
14. Integrated pressures in one forward quadrant for LN₂ injection	12
15. Typical temperature distributions for LN₂ injection	13
16. Comparison of pressure distribution produced by impinging jet injector and single hole injector for LN₂ injection	13
17. Comparison of shadowgraphs for GN₂ injection at M = 2.01	14
18. Typical shadowgraph for GN₂ injection at M = 2.61	15
19. Typical pressure distribution for GN₂ injection at M = 2.61	15
20. Separation distance for GN₂ injection	16

FIGURES (Cont'd)

21. Length of downstream overexpansion region for GN₂ injection	16
22. Stand-off distance for GN₂ injection	16
23. Comparison of centerline pressure distributions for laminar and turbulent separations	17
24. Pressure coefficient in separation zone for turbulent separation	18
25. Pressure coefficient in separation zone for laminar separation	19
A-1. Comparison of shadowgraphs for Run 4 (LN₂ injection)	55
A-2. Comparison of shadowgraphs for Run 6 (LN₂ injection)	56
A-3. Comparison of shadowgraphs for Run 15 (LN₂ injection)	57
B-1. Comparison of shadowgraphs for Run 24 (GN₂ injection)	95
B-2. Comparison of shadowgraphs for Run 26 (GN₂ injection)	96
B-3. Comparison of shadowgraphs for Run 30 (GN₂ injection)	97
B-4. Comparison of shadowgraphs for Run 32 (GN₂ injection)	98

ABSTRACT

15788

Author

An experimental program has been conducted in the 20-in. Supersonic Wind Tunnel at the Jet Propulsion Laboratory (JPL) to study the interaction effects produced when liquid or gaseous nitrogen is injected in a direction perpendicular to a supersonic stream on a flat plate. The tests provided useful information about the effects of free-stream Mach number, free-stream Reynolds number, and injection pressure on the shock structure and pressure distribution induced on the plate by the injection process. Pressure distributions in the injector region, schlierens, spark shadowgraphs, and motion pictures provided details about the flow interaction, which should assist in the development of more meaningful analytical models of secondary injection.

Author

I. INTRODUCTION

An experimental program has been conducted at the Jet Propulsion Laboratory (JPL) to investigate the interaction effects produced when a liquid or gas is injected in a direction perpendicular to a supersonic stream. The program was initiated to gain a better understanding of the side-force generation mechanisms associated with the injection of a secondary fluid into the expansion cone of a solid-propellant rocket nozzle for thrust-vector control.

Various organizations have devoted considerable effort to obtaining side-force data for specific rocket motors utilizing secondary injection for thrust-vector control. These efforts, with few exceptions, have placed little emphasis on obtaining the type of data needed for defining the mechanism producing the side-force. A notable exception is the work of Newton and Spaid (Ref. 1) at JPL where nozzle-wall pressure distributions in the injector region were obtained during rocket motor firings.

The present series of tests were conducted in the 20-in. Supersonic Wind Tunnel at JPL. Liquid and gaseous

nitrogen were injected perpendicularly to a supersonic stream on a flat plate. The purposes of the tests were to determine the effects of free-stream Mach number, of free-stream Reynolds number, and of injection pressure on the shock structure and pressure distribution induced on the plate by the injection process.

The primary data obtained were in the form of pressure distributions in the injector region. Schlierens and spark shadowgraphs were made for each run, and much information about the injectant body and shock structure was obtained from the pictures. Motion pictures (at 500 frames/sec) were made for a few selected liquid nitrogen runs to determine the steadiness of the flow disturbance.

A few liquid nitrogen runs were made using an impinging jet injector to determine what effect the increased atomization in the injector region would have on the nature of the disturbance created. The majority of the liquid nitrogen runs and all of the gaseous nitrogen runs were made using a single hole injector perpendicular to the plate surface.

II. DESCRIPTION OF EXPERIMENTS

A. Flat Plate Design

An 18 × 17.5-in. flat plate, 0.5-in. thick, was designed and fabricated from 321 stainless steel. Support for the plate was provided by two supporting struts running from the tunnel floor, and by a windshield support at the rear of the plate. A photograph showing the flat plate installed in the 20-in. Supersonic Wind Tunnel test section is given in Fig. 1.

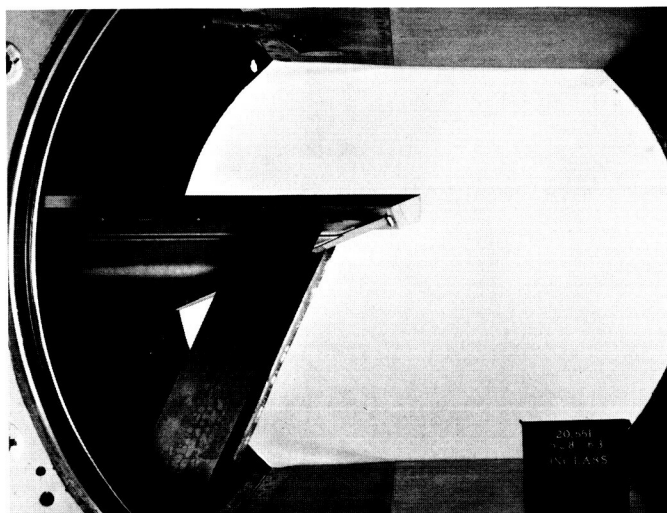


Fig. 1. Flat plate installation

A slotted hole was provided in the plate to allow two different injector inserts to be used. The injector station was located 7 in. from the leading edge of the plate. A trip wire 0.020-in. D was located 0.060 in. from the leading edge of the plate to increase the boundary-layer turbulence at the injector station.

The flat plate was instrumented with 96 pressure taps and 25 thermocouples. The pressure taps were closely spaced on the plate centerline and in one quadrant upstream of the injector. Five radial rows of pressure taps spaced $22\frac{1}{2}$ deg apart gave a good representation of the pressure distribution forward of the injector. The radial rows of pressure taps are designated A through F, beginning with the upstream row (Fig. 2). The 25 chromel-constantan plate thermocouples were located near the plate centerline and on one radial line from the injector in a direction perpendicular to the plate centerline (Fig. 3).

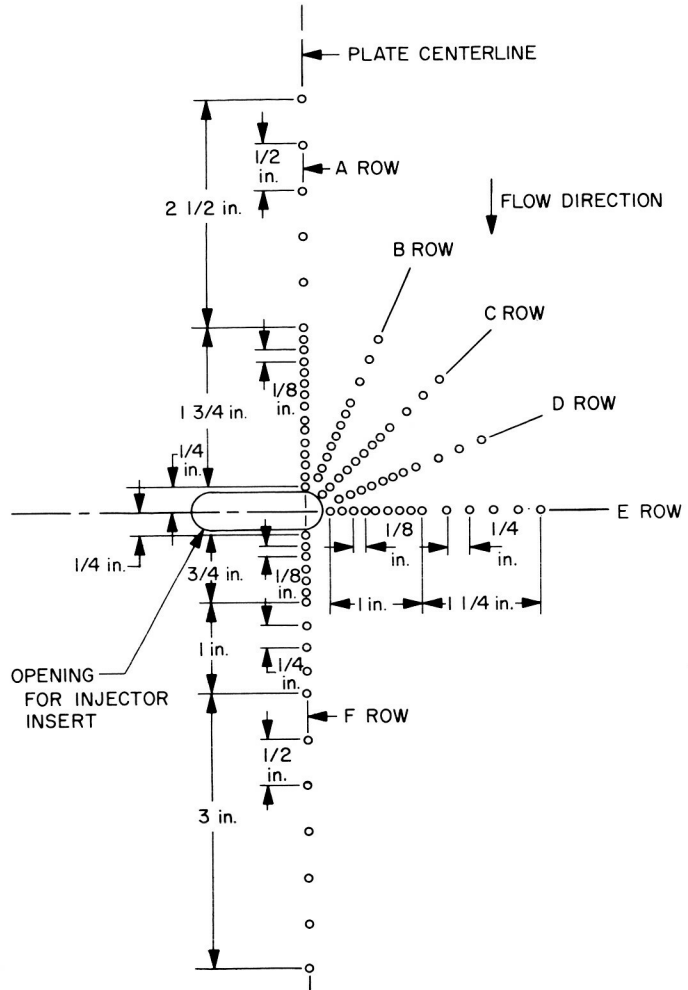


Fig. 2. Pressure tap locations on flat plate

B. Injection System

A 2600-gal, spherical Linde liquefied gas storage tank was used to supply pressurized liquid nitrogen to the injector. The liquid nitrogen storage tank was filled and then vented to the atmosphere for 12 hr prior to each day's test to insure saturated liquid nitrogen at atmospheric pressure in the supply tank. After venting, the supply tank was pressurized to approximately 175 psi.

Two by-pass lines were provided in the supply system outside the tunnel test section to decrease the piping cool-down time. An additional by-pass was provided in the tunnel test section by a solenoid valve located near the injector. The solenoid valve was left open upon start-

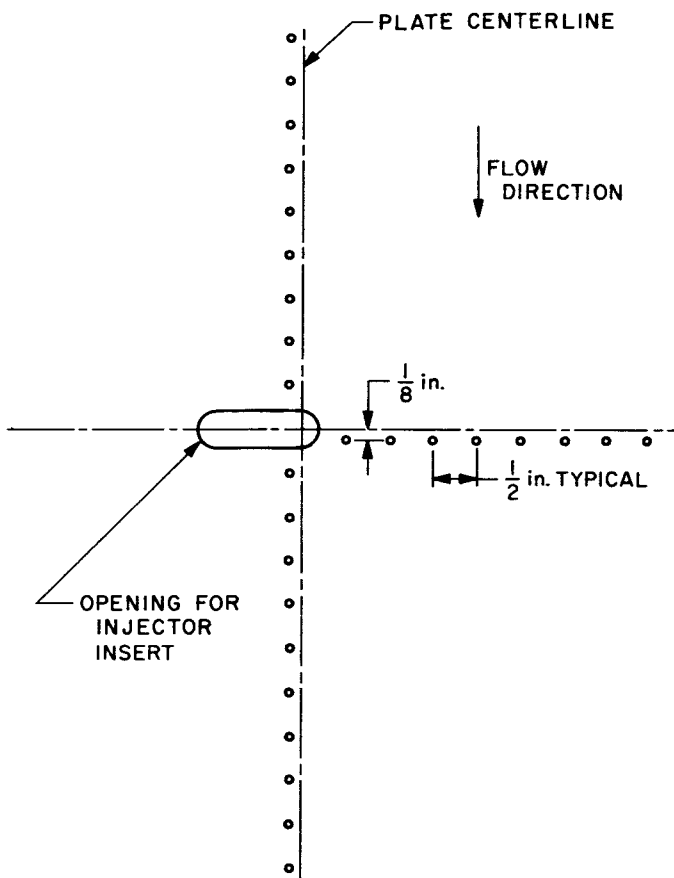


Fig. 3. Thermocouple locations on flat plate

ing the injection process to allow sufficient flow rate to rapidly cool the injection supply lines within the tunnel. After sufficient cooling of the lines, the solenoid valve was closed, forcing the total flow through the injector opening. A schematic diagram of the supply system used for the liquid nitrogen runs is given in Fig. 4.

The injection temperature and pressure were measured in the plenum immediately upstream of the injector. From the vapor-pressure curve for nitrogen, the temperature and pressure readings are sufficient to indicate whether or not zero quality liquid nitrogen exists in the plenum.

The two injector inserts used in these tests are shown in Fig. 5. The single hole injector was 0.100 in. in diameter with a length-to-diameter ratio of one. The cross-sectional area of the plenum was approximately 12 times the injector area. The impinging jet injector utilized two holes, 0.070-in. in diameter, inclined at 30 deg to the plate surface.

The liquid nitrogen supply lines from the storage tank to the wind tunnel test section were covered with thick foam insulation to reduce the heat input to the liquid nitrogen. Within the wind tunnel test section, the low-density air was assumed to provide sufficient insulation; however, the liquid nitrogen supply lines were shielded from the high-speed air flow by a windshield arrangement.

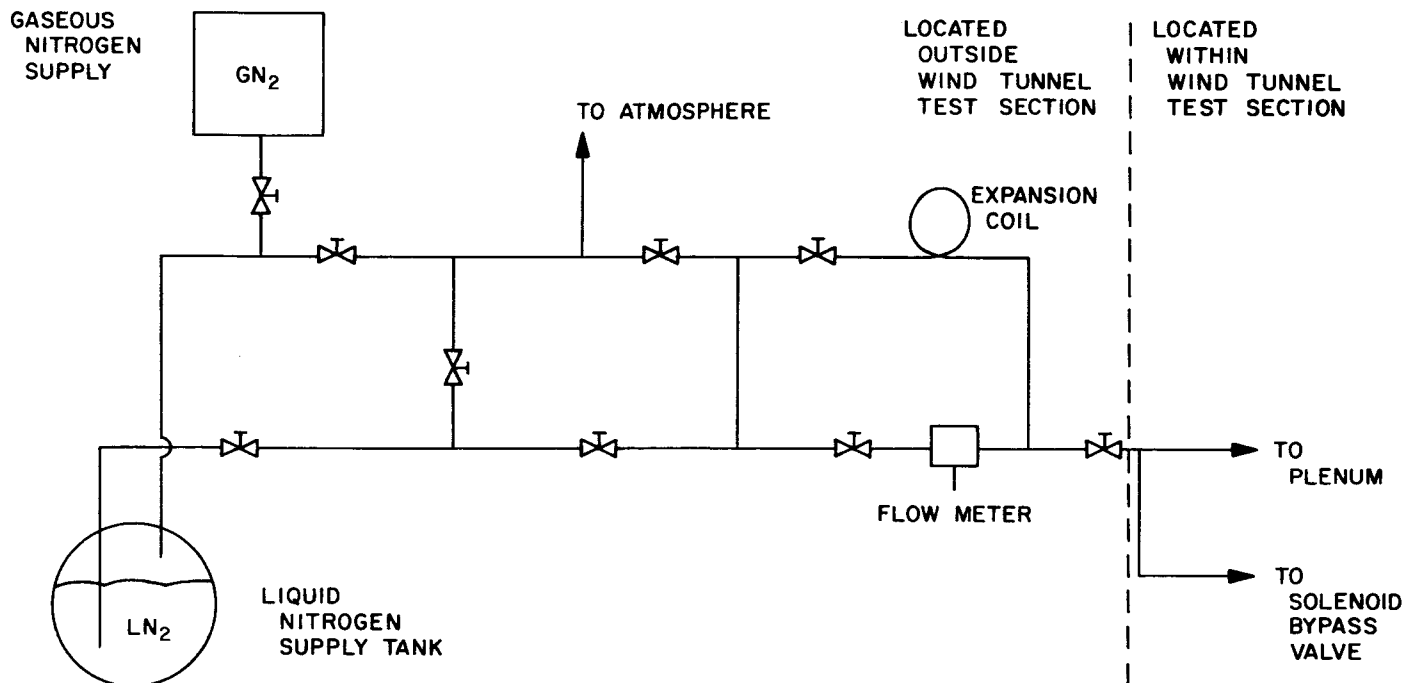


Fig. 4. Liquid nitrogen supply system

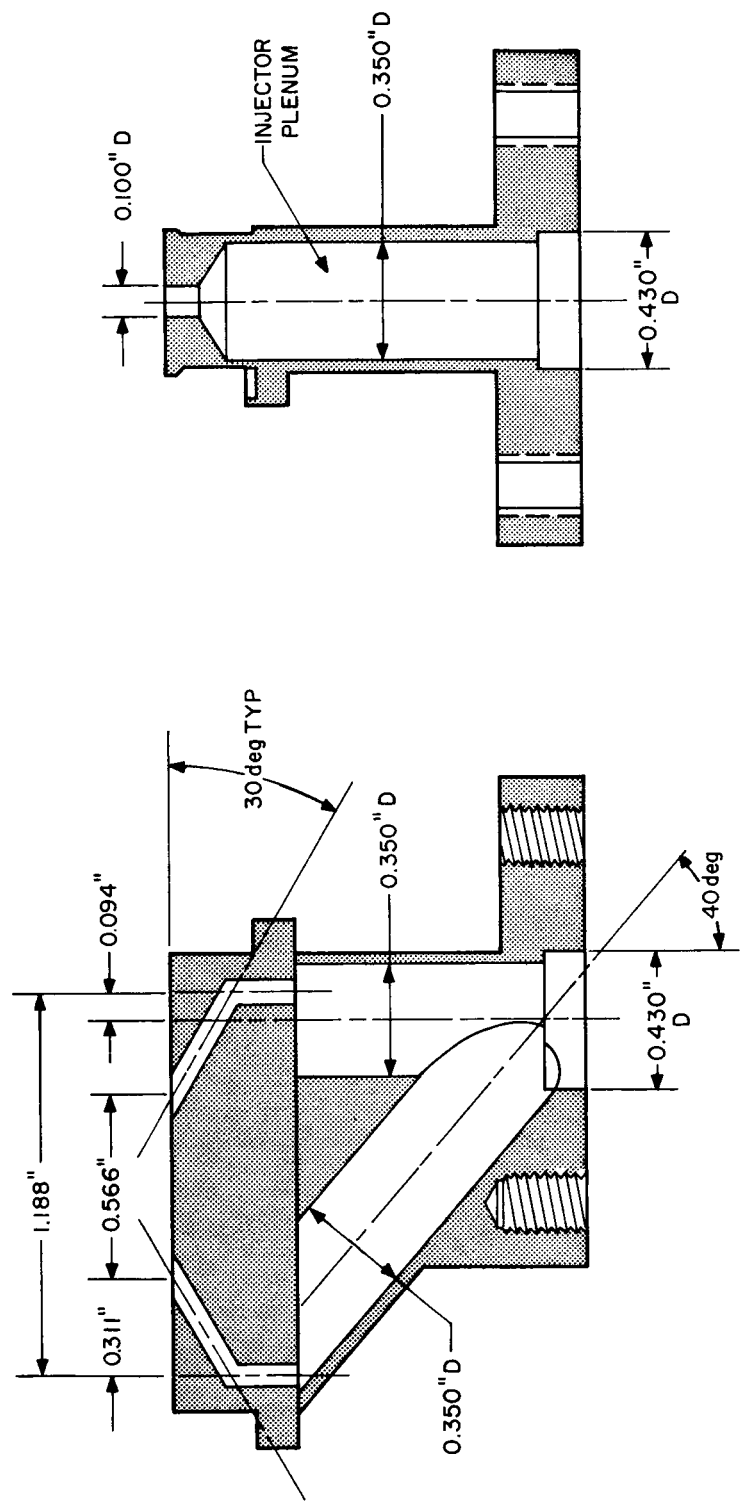


Fig. 5. Comparison of injector inserts

Several seal problems appeared because of the cryogenic temperatures of the injectant fluid. Flange joints with standard Parker #2-14 neoprene O-rings were found to provide good seals when the O-rings were under 80% compression (the compressed height of the O-ring was 20% of the uncompressed O-ring diameter). An insulating spacer was used between the solenoid valve and the remaining supply lines to reduce the heat flow from the valve to the injectant fluid. Initially, the spacer was made of Teflon; however, preliminary tests indicated the Teflon was unable to maintain an adequate seal at liquid nitrogen temperatures. A change in material from Teflon to nylon produced a satisfactory seal for the duration of the tests.

The gaseous nitrogen supply system used was considerably simpler than the liquid one. The gas was piped directly from the gaseous nitrogen supply through a control valve to the injector plenum.

C. Instrumentation and Data Reduction

Thin-walled 1/16-in. D stainless steel tubing was used from the pressure taps to a point outside the wind tunnel. Short lengths of flexible tubing connected the stainless steel tubing to the multi-pressure measuring system (MPMS), which is a 100-port pressure scanner. The pressures to be measured are connected to the lower plate or stator of the MPMS. There is an O-ring in the stator plate surrounding each pressure input tube. The upper lapped plate or rotor which contains the transducer is rotated with respect to the stator to bring the transducer in contact with each pressure input tube. There is an external adjustment of the load on the O-rings to prevent leakage between pressure ports. The entire assembly is covered with an evacuated dome providing evacuation of the transducer prior to each pressure reading. A vacuum reference, an atmospheric reference, and the dome pressure were included in the MPMS data scan. The MPMS scanning rate was 6 ports/sec (after a short settling time before the scan).

A 5-psia Statham transducer was used in the MPMS for most of the runs to obtain the necessary sensitivity; however, a 15-psia Statham was used for runs made at low Mach numbers and high tunnel pressures to provide the pressure range needed.

The outputs of the 25 chromel-constantan plate thermocouples were read by a slow speed thermocouple scanner and recorded by the main data scan for each run/point.

The injection temperature and pressure were measured in the plenum immediately upstream of the injector opening. The injection pressure was measured with a 500-psia Statham transducer and recorded during the main data scan. The chromel-constantan thermocouple for measuring the injection temperature was covered with nylon insulation and held in position by a metal clip.

Prior to the test, the two injectors were water-calibrated to determine the flow characteristics of each. Corrections were made for the differences in properties of liquid nitrogen and water to obtain calibration curves for liquid nitrogen. Realizing that cavitation would occur in the injector and introduce errors in the flow measurement because of the low tunnel static pressure, a SPACO Model R3/8-3J turbine flowmeter was installed in the supply system outside of the tunnel test section.

Care was exercised in starting the flow through the turbine flowmeter to prevent vaporization from damaging the flowmeter by overspeeding; however, the flowmeter was damaged two times during the series of tests. The damage was attributed to ice formation in the supply system upstream of the flowmeter. The source of the moisture is not known at present.

It is interesting to compare the flow rate which was measured by the turbine flowmeter during the test with the flow rate which was calculated using the injector calibration. The maximum pressure observed on the centerline pressure distribution for each run/point was used as the exit pressure encountered by the liquid jet upon entering the free stream. The pressure drop through the injector and the injection temperature were used to obtain a flow rate from the calibration curve. A comparison of the flow rates obtained by the two methods is given in Table 1 for the runs in which the turbine flowmeter was in operation. Notice that the flow rate measured by the turbine flowmeter was always less than the flow rate predicted by the calibration curve, indicating that the expected cavitation was occurring in the injector. The amount of cavitation occurring should be indicated

Table 1. Liquid nitrogen flow rate comparison

Run	w_c	w_{fm}	Δw	$\frac{\Delta w}{w_c} \times 100$	$\frac{P_{exit}}{P_{sp}}$
6	0.238	0.224	0.014	5.9	0.294
4	0.244	0.225	0.019	7.8	0.152
15	0.227	0.201	0.026	11.4	0.026
14	0.213	0.166	0.047	22.0	0.014

by the ratio of the exit pressure to the vapor pressure, which corresponds to the injection temperature. Lower values of this ratio of exit pressure to vapor pressure should result in greater amounts of cavitation and larger deviations in actual and calculated flow rates. This result is shown in the data and must be considered when flow

rates are estimated for the runs made without the turbine flowmeter in operation.

The flow rate for the gaseous nitrogen runs was obtained from a calibration of the injector which used gaseous nitrogen.

III. TEST RESULTS FOR LIQUID NITROGEN INJECTION

A. General Considerations

The vapor pressure curve for nitrogen is given in Fig. 6. The range of maximum observed pressures from the centerline pressure distributions is shown on this curve. Upon injection into the supersonic stream, the liquid nitrogen enters a region of low pressure, giving rise to the possibility of flash vaporization occurring.

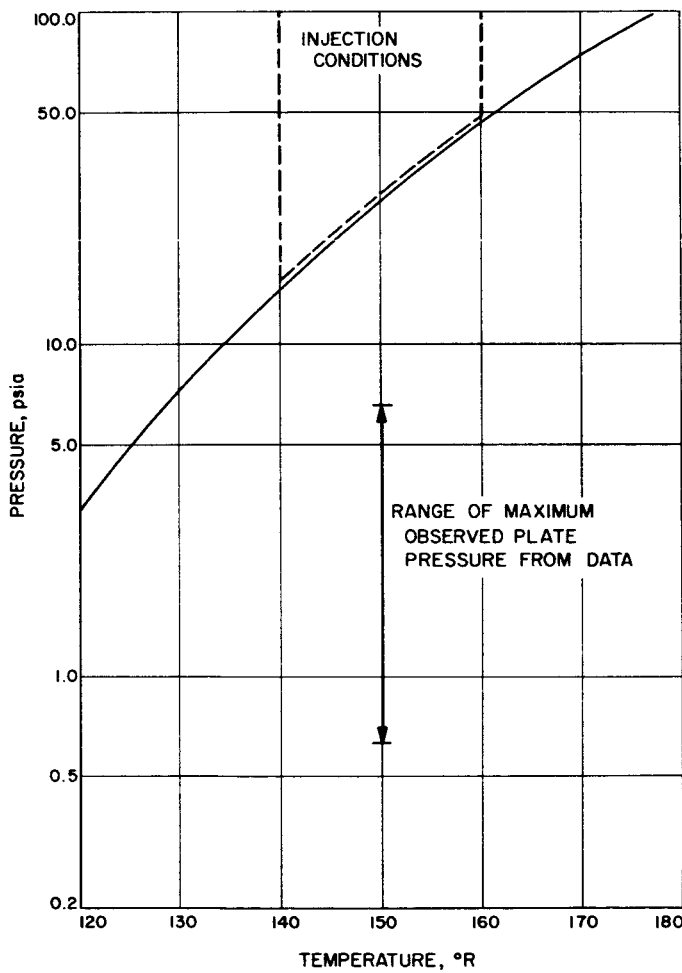


Fig. 6. Vapor pressure curve for nitrogen

Flash vaporization occurs when a liquid is suddenly brought into a region of low pressure where the liquid temperature exceeds the equilibrium temperature which corresponds to the surrounding pressure. This sudden drop in pressure causes the liquid to boil rapidly, producing large amounts of vapor. The latent heat of vaporization is supplied by the liquid itself since flash vaporization

occurs so rapidly that there is little time for heat transfer from the surrounding medium.

To place an upper limit on the percentage of liquid nitrogen which could be vaporized by flash vaporization for the conditions of these tests, an approximate calculation was made using a constant enthalpy model with the assumption that thermal equilibrium was realized upon completion of the flashing process. The equation governing such a process is given by

$$x h_{fg_0} = (1 - x) c_p (t_1 - t_0) \quad (1)$$

where

x percentage flash vaporization

h_{fg_0} heat of vaporization at surrounding pressure

c_p average specific heat between t_0 and t_1

t_1 injectant temperature

t_0 equilibrium temperature corresponding to the surrounding pressure

The maximum possible percentage flash vaporization varied from 9% for the higher exit pressures to a maximum of 15% for the lower exit pressures.

A discussion of the main trends observed for liquid nitrogen injection is given in this Section, and most of the liquid data is included in Appendix A.

B. Visual Data

Visual data in the form of schlierens and spark shadowgraphs were obtained for each run/point, and much information about the injectant body and shock structure resulted from these pictures.

Figure 7 shows a comparison of the spark shadowgraphs for Run 8 at a Mach number of 2.01, a tunnel total pressure of 75 cm Hg, and a Reynolds number per inch of approximately 0.293×10^6 . The effect of injection pressure is noticeable from this comparison. For the higher injection pressures, the liquid nitrogen jet penetrates further into the free stream, and the main body of the jet

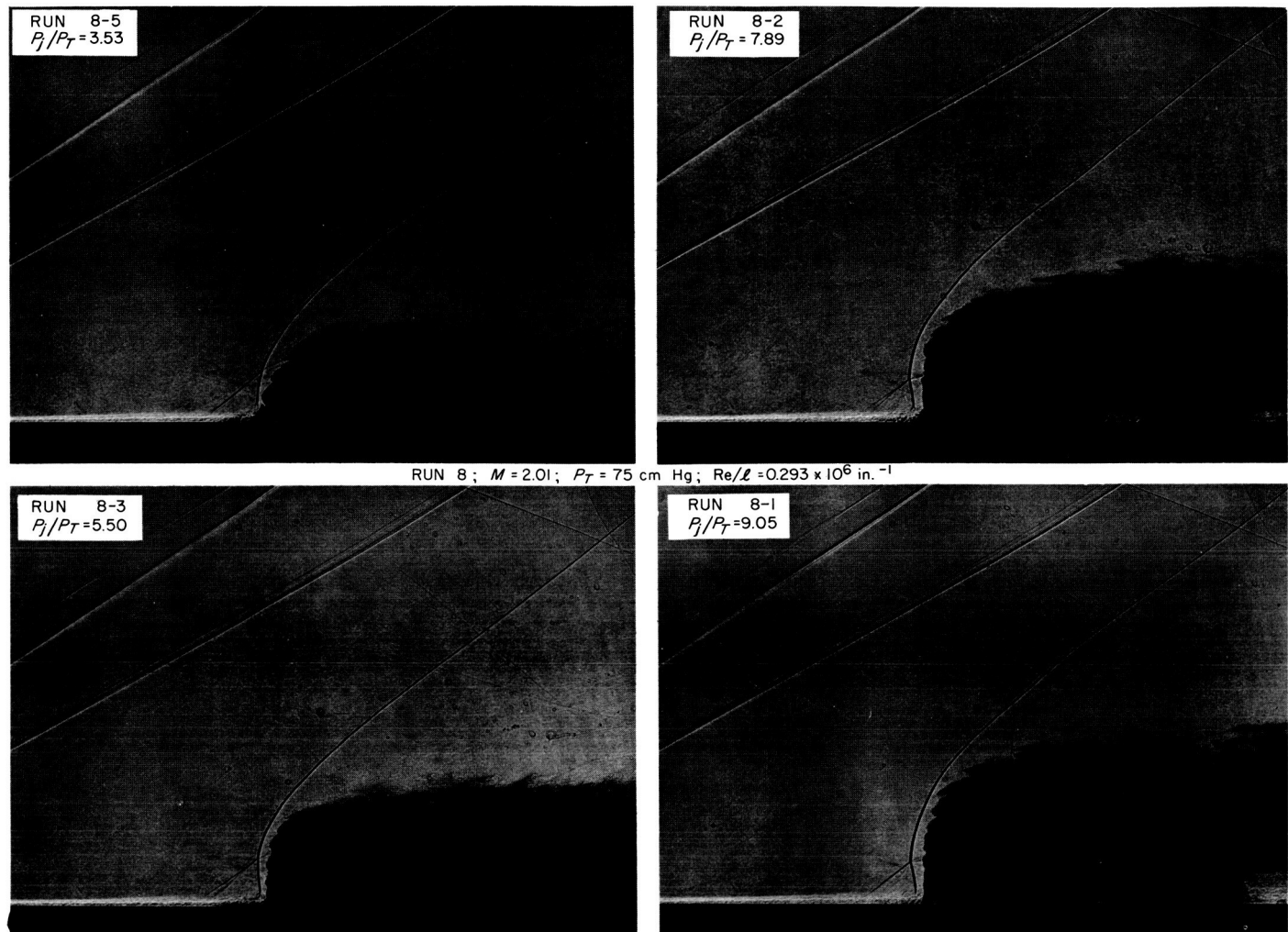


Fig. 7. Comparison of shadowgraphs for LN_2 injection at $M = 2.01$

remains away from the wall downstream of the injector. There is no noticeable difference in the separation distance forward of the injector as a function of injection pressure. The main curved shock produced by the injectant body splits into a λ -shock structure near the plate surface. The downstream slip line associated with the λ -shock structure is visible emanating from the junction point of the main shock and the λ -shock.

Figure 8 shows a comparison of the spark shadowgraphs for Runs 10 and 12 at a Mach number of 3.26, a tunnel total pressure of 152 cm Hg, and a Reynolds number per inch of approximately 0.298×10^6 . The injectant body is much larger and has a more ragged appearance than the injectant body for lower Mach number runs. The ragged injectant body produces an irregular shock shape, making it impossible to identify a λ -shock structure forward of

the injector; however, there is a forward shock associated with the separation region. The injectant body size again increases with injection pressure.

A comparison of the spark shadowgraphs for several runs with a ratio of injection pressure to tunnel total pressure of approximately 3.50 is given in Fig. 9. A comparison of Runs 8-5 and 6-2 gives an indication of the effect of free-stream Reynolds number. The run with the lower free-stream Reynolds number produced a larger disturbance and a greater separation distance forward of the injector. Runs 6-2, 4-2, and 10-2 are for the same tunnel total pressure and different free-stream Mach numbers. The higher Mach-number flows produced larger injectant bodies and larger separation zones; however, part of this change in the disturbance is attributable to the different free-stream Reynolds numbers for these run/points.

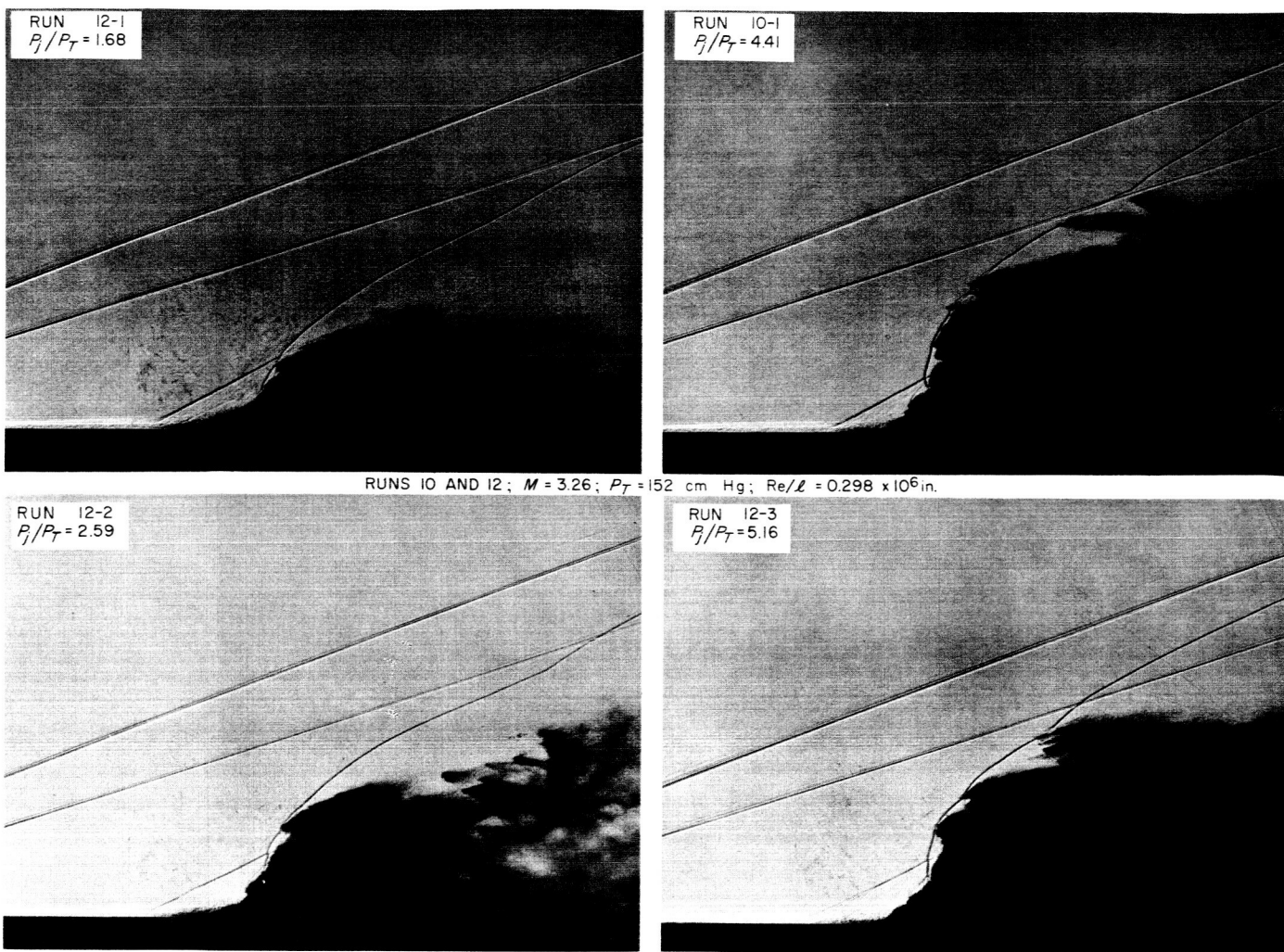


Fig. 8. Comparison of shadowgraphs for LN_2 injection at $M = 3.26$

C. Pressure Data

The pressure distribution for Run 4-3 is given in Fig. 10. The radial rows are lettered according to the key in Fig. 2. The local plate pressure is nondimensionalized by dividing it by the free-stream static pressure. The pressure disturbance is seen to spread considerably more to the side of the injector than forward of the injector, producing an elliptical disturbance region forward of the injector. The pressure peak shown on the centerline pressure distribution is the first peak pressure associated with a turbulent separation. The final pressure rise is not seen since no pressure taps were located closer than 0.25 in. to the injector. A comparison of the pressure distribution and the visual data for the run/point indicates the final pressure rise should be less than 0.25 in. from the injector. Notice a decrease in the peak pres-

sures observed in passing from the centerline distribution forward of the injector to the distribution in radial row E.

The centerline pressure distribution downstream of the injector shows an excess pressure for some distance downstream, which is typical of liquid injection runs. The break-up of the jet and vaporization of the liquid produces this excess pressure distribution. At higher injection rates and for higher free-stream Mach numbers, the liquid jet penetrates into the free stream to some extent before atomization and vaporization occur, and a subnormal pressure region is observed on the plate immediately downstream of the injector. Subsequent vaporization produces an excess pressure further downstream. Probably a small, subnormal pressure region

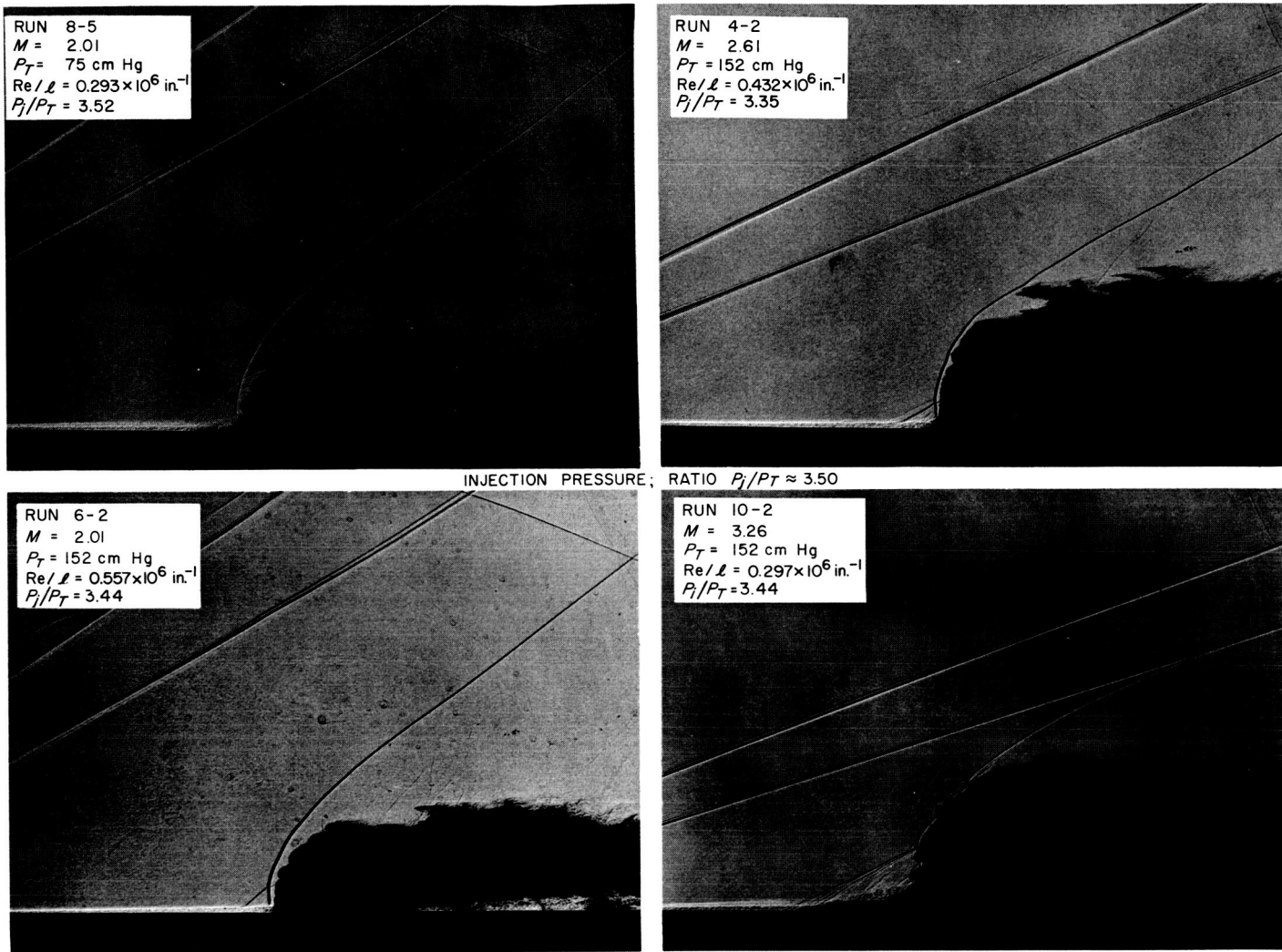


Fig. 9. Comparison of shadowgraphs for LN_2 injection with $P_j/P_T \approx 3.50$

exists downstream of the injector in all cases; however, pressure data sufficiently close to the injector was not obtained to verify this.

Figure 11 shows the pressure distribution for Run 12-1. The trends observed are similar to those mentioned previously for Run 4-3. For this particular run/point, there is a region of reduced pressure gradient in the turbulent separation zone. The final peak pressure rise decreases in passing from the distribution forward of the injector to the distribution in radial row E.

A plot of separation distance versus the ratio of injection pressure to tunnel total pressure P_j/P_T is shown in Fig. 12. The separation distance shown here is defined as the distance from the injector to the point forward of the injector where the local pressure rises above the

tunnel static pressure as measured from the centerline pressure distributions. No detectable change in separation distance with P_j/P_T was observed for Runs 4 and 6, possibly because of the smallness of the disturbance. A comparison of Runs 6 and 8 indicates an increase in separation distance with a decrease in tunnel total pressure for a constant Mach number. The data for Runs 10 and 12 show that the separation distance passes through a maximum value for $P_j/P_T \approx 2.5$ and then starts decreasing for further increases in P_j/P_T . If the disturbance area forward of the injector is plotted versus P_j/P_T for Runs 10 and 12, the area passes through a maximum for $P_j/P_T \approx 2.5$, also.

For liquid injection, a region of excess pressure exists downstream of the injector. The length of this downstream overpressure region is shown plotted versus the

ratio of injection pressure to tunnel total pressure P_j/P_T in Fig. 13. The length of the downstream overpressure region is defined as the distance from the injector to the point downstream where the local pressure decreases to the free stream static pressure. The data for most runs exhibit maximum points for various values of P_j/P_T .

The excess pressures in one forward quadrant were numerically integrated to get an indication of the induced force in that region. The integrated pressures for one forward quadrant are plotted versus the ratio of injection pressure to tunnel total pressure P_j/P_T in Fig. 14. No noticeable differences in integrated pressures were

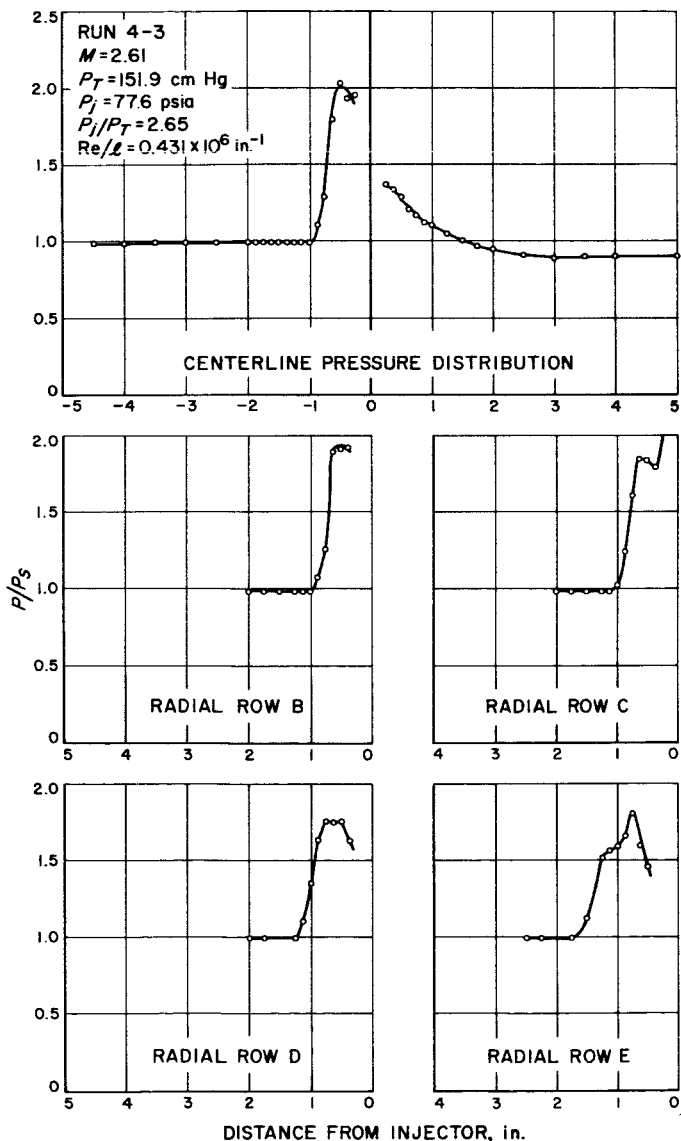


Fig. 10. Typical pressure distribution for LN_2 injection at $M = 2.61$

found for Run 6 because of the small size of the disturbance. A comparison of Runs 6 and 8 for a Mach number of 2.01 shows a higher integrated pressure for Run 8, which has the lower tunnel total pressure. The excess pressures in the forward quadrant for Run 8 were less than the excess pressures for Run 6; however, the much larger disturbance area for Run 8 resulted in a larger integrated pressure. The data indicate that the integrated pressures for a particular run pass through a maximum point at a certain value of P_j/P_T . The decrease in integrated pressure for one forward quadrant after a certain

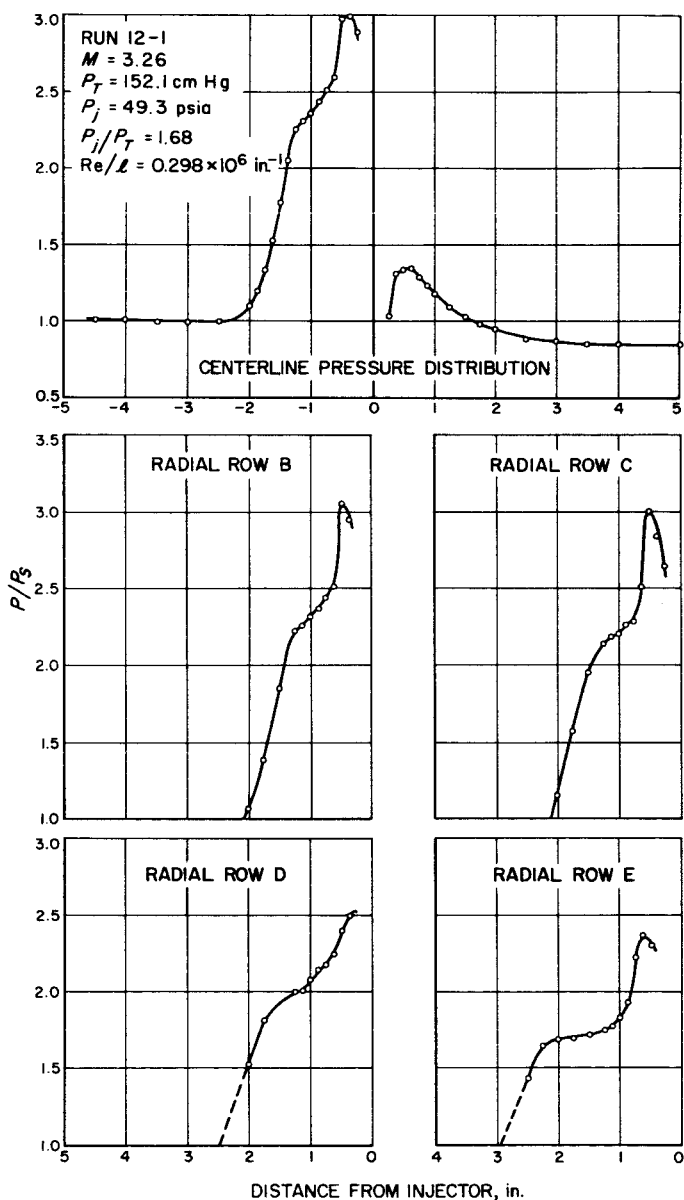


Fig. 11. Typical pressure distribution for LN_2 injection at $M = 3.26$

value of P_j/P_T is caused possibly by the increased penetration of the main body of the liquid jet before jet

break-up, resulting in a decrease in the amount of spreading of the disturbance on the plate surface forward of the injector.

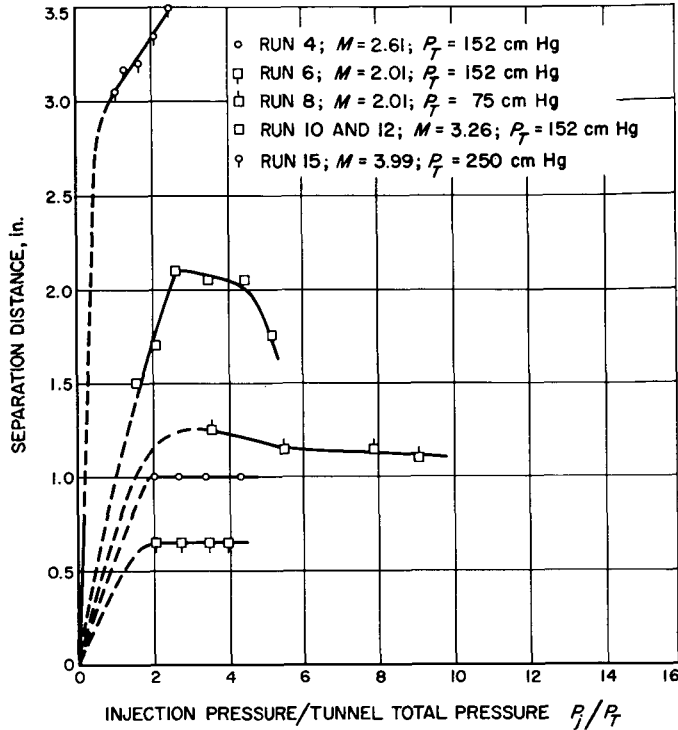


Fig. 12. Separation distance for LN₂ injection

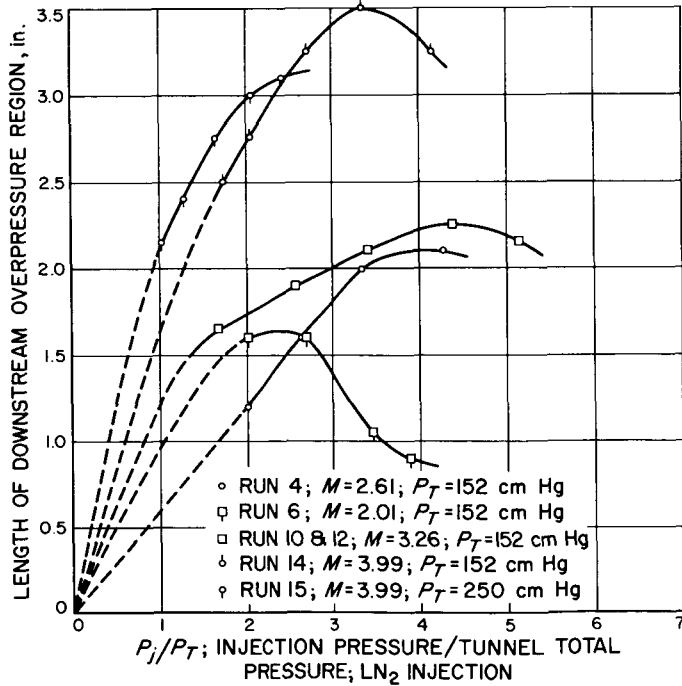


Fig. 13. Length of downstream overpressure region for LN₂ injection

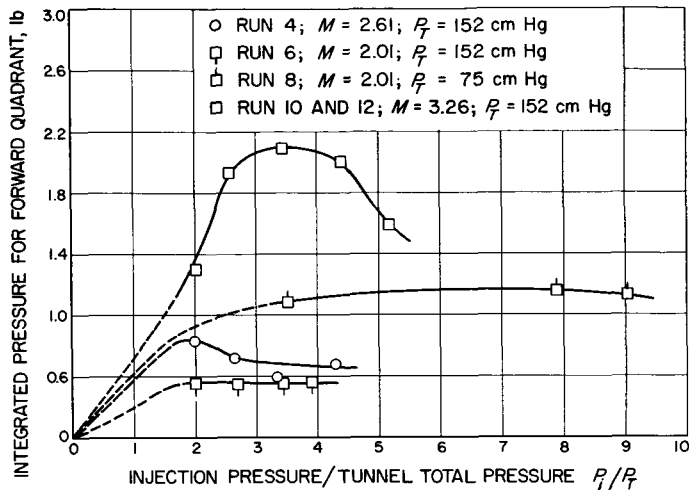


Fig. 14. Integrated pressures in one forward quadrant for LN₂ injection

D. Temperature Data

The temperature distribution in the injector region was obtained using chromel-constantan thermocouples located according to the key in Fig. 3. The thermocouples were mounted flush with the plate surface and surrounded by a potting compound to provide some insulation between the thermocouple and the stainless steel plate. However, the conduction of heat in the stainless steel plate did affect the thermocouple readings and produced a time-dependent temperature distribution in the injector region. One purpose of the temperature measurements was to determine the type of thermal environment present in the region forward of the injector where separation occurs. It is known that heat transfer effects are important in determining the nature of separation phenomena.

A comparison of the centerline temperature distribution for several run/points with $P_j/P_T \approx 3.4$ is given in Fig. 15. As the Mach number is increased for a constant tunnel total pressure, the injectant spreads out more, producing a larger temperature disturbance forward of the injector. The temperature distributions are smoothed somewhat by the conduction effects in the plate. A comparison of temperature profiles and separation distances shows that plate temperatures in the separation zone are about equal to the liquid nitrogen temperature. The temperature distribution for Run 6-2 indicates that the liquid nitrogen is not in direct contact with the plate

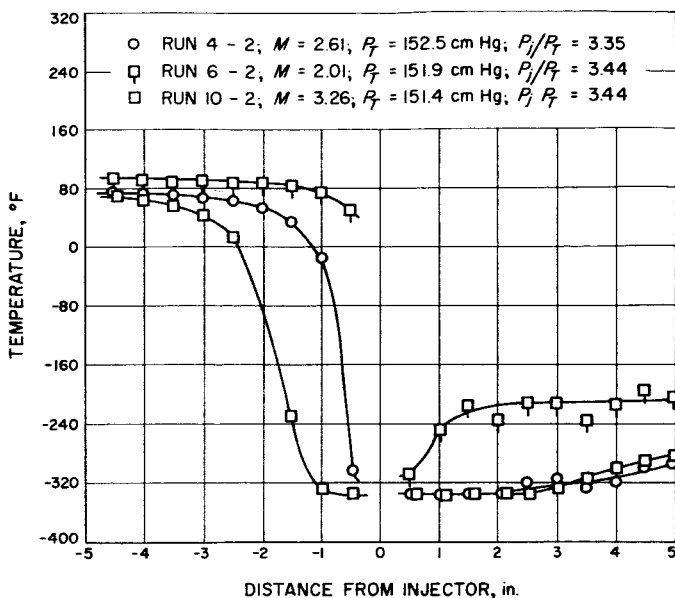


Fig. 15. Typical temperature distributions for LN_2 injection

surface downstream of the injector. The shadowgraph for Run 6-2, shown in Fig. 9, also indicates that the liquid nitrogen jet penetrates far into the free stream and remains away from the plate downstream of the injector.

E. Impinging Jet Injector

Several liquid nitrogen runs were made using an impinging jet injector to determine what effect the increased atomization in the injector region would have on the nature of the disturbance created. Some cold-flow nozzle tests utilizing the impinging jet principle have been made previously under NASA Contract No. NASW-249.

A comparison of the pressure disturbance produced by the impinging jet injector and the single hole injector for approximately the same flow rates is given in the contour-pressure plot of Fig. 16. The pressure contours are drawn for various values of the ratio of local pressure to free-stream static pressure. The solid lines are supported by measured pressures, and the dashed lines are reasonable extensions of the observed pressure data. The comparison points out several differences in the disturbance created by the two injector designs. The disturbance region forward of the impinging jet injector is much larger than

the disturbance region upstream of the single hole; however, the excess pressures are greater for the single hole injector. Downstream of the single hole injector there is a region of excess pressure, while a region of subnormal pressures similar to gas injector exists downstream of the impinging jet injector.

In an actual application for thrust vector control, the disturbance would occur in a region of favorable pressure gradient. The presence of a favorable pressure gradient would tend to reduce the area of the disturbance forward of the injector and modify the pressure distribution somewhat. The size of the region of excess pressure downstream of the single hole would increase, while the subnormal pressure region downstream of the impinging jet injector would decrease in size. On the basis of available data, no definite conclusions can be made concerning the relative merits of the two injector designs.

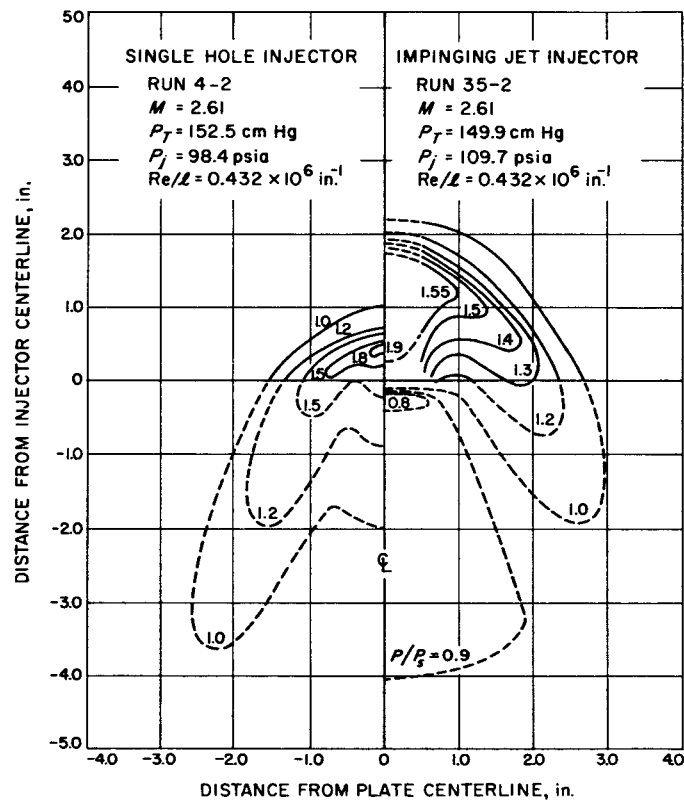


Fig. 16. Comparison of pressure distribution produced by impinging jet injector and single hole injector for LN_2 injection

IV. TEST RESULTS FOR GASEOUS NITROGEN INJECTION

A. General Considerations

Considerable experimental data are available in the literature on the fluid dynamics of gas injection. A recent survey of both theoretical and experimental work on gas injection for thrust-vector control was reported by Kallis and Adelburg (Ref. 2). Because of the large amount of gas data available, only part of the gas data is discussed here; however, most of the data is included in Appendix B.

B. Visual Data

Visual data in the form of schlierens and spark shadowgraphs were obtained for each run/point, and much information about the jet interaction and shock structure resulted from an examination of these pictures.

Figure 17 shows a comparison of the spark shadowgraphs for Run 30 at a Mach number of 2.01, a tunnel total pressure of 110 cm Hg, and a Reynolds number per inch of approximately 0.427×10^6 . The main shock produced by the nitrogen jet becomes much stronger and more curved as the injection pressure is increased. For higher injection pressures, the main shock splits into a λ -shock structure near the plate surface. The slip line associated with the λ -shock is visible emanating from the junction point of the λ -shock with the main curved shock. For higher injection pressures, a shock associated with the supersonic nitrogen jet becomes visible in the shadowgraphs. As will be pointed out later, the appearance of this jet shock coincides with a change in the type of centerline pressure distribution observed downstream of the injector.

Several interesting features observed for the high injection pressure runs are shown in Fig. 18, which is a shadowgraph for Run 28-8. For this high injection pressure and relatively low tunnel pressure, the gaseous nitrogen jet penetrates a considerable distance into the main stream. The curved main shock produced by the injectant jet looks similar to the shock produced by a free body in the main stream some distance away from the plate surface. The jet shock is clearly seen also in this picture. No forward shock associated with the separation region is detectable in the shadowgraph; however, this could be due to the low density flow and the weakness of this shock.

C. Pressure Data

The pressure distribution for Run 26-6 is given in Fig. 19. The radial rows are lettered according to the key

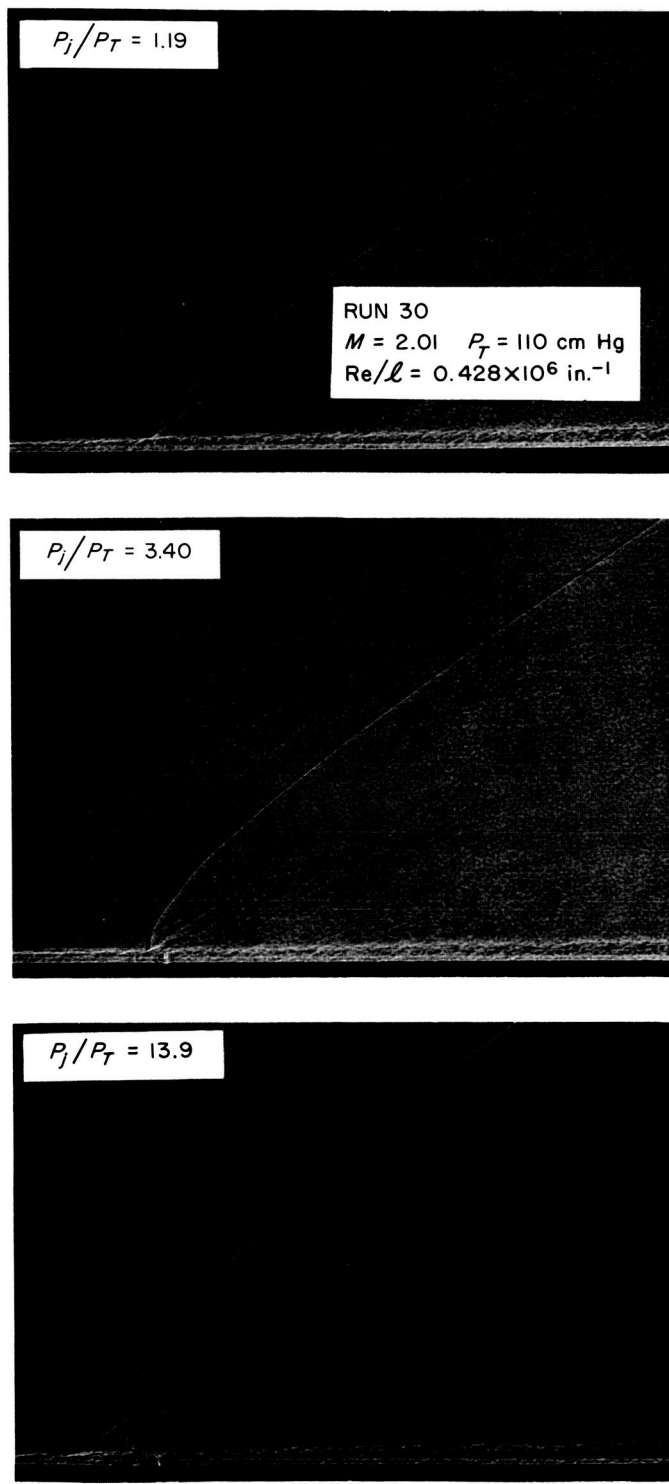


Fig. 17. Comparison of shadowgraphs for GN_2 injection at $M = 2.01$

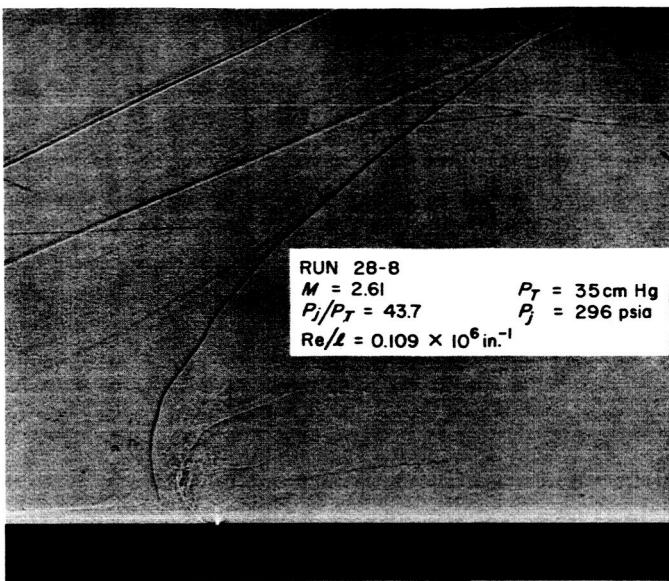


Fig. 18. Typical shadowgraph for GN_2 injection at $M = 2.61$

in Fig. 2. The local plate pressure is nondimensionalized by dividing it by the free-stream static pressure. Notice the first peak pressure associated with a turbulent separation zone. This peak pressure decreases in passing from the forward centerline distribution to the distribution in radial row E. The disturbance spreads more to the side of the injector, producing an elliptical disturbance zone ahead of the injector.

The centerline pressure distribution shows a subnormal pressure region immediately downstream of the injector, which is typical of gaseous injection. This subnormal pressure region results from an overexpansion of the primary flow in the wake of the injectant jet. Immediately downstream of this subnormal pressure region is a region of excess pressure. A comparison of the pressure distribution with its corresponding shadowgraph reveals that the excess pressure region is located approximately at the point where the jet shock contacts the plate surface. Runs with low injection pressures did not exhibit an excess pressure region, but rather showed a subnormal pressure region immediately downstream of the injector, followed by an asymptotic rise to free-stream static pressure. For all run/points which showed an asymptotic pressure recovery downstream, no jet shock was observed on the corresponding shadowgraph.

A plot of separation distance versus the ratio of injection pressure to tunnel total pressure P_j/P_t is shown in Fig. 20. The separation distance here is defined as the distance from the injector to the point forward of the

injector where the local pressure rises above tunnel static pressure, as measured from the centerline pressure distributions. The curves for laminar and turbulent separation both show an increase in separation distance with increasing injection pressure. Unlike the data for liquid nitrogen injection, the separation distance does not reach a maximum value for the available gaseous nitrogen data. The laminar separation distance increases for an increase

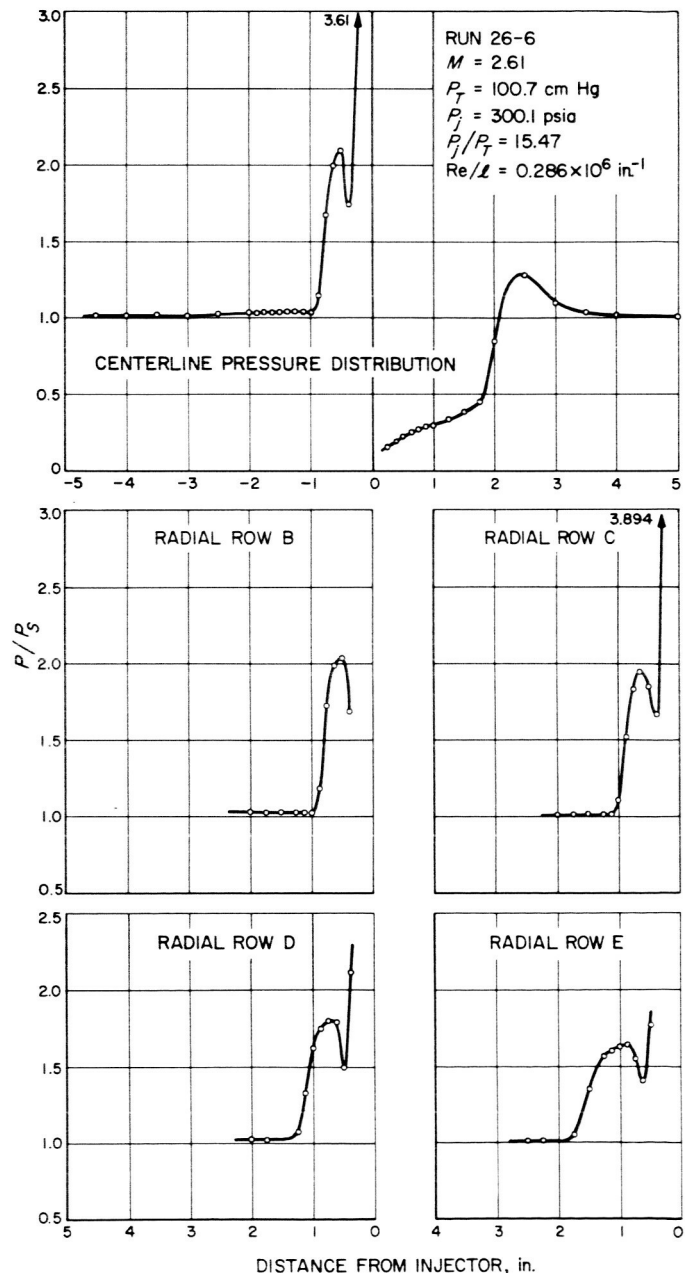
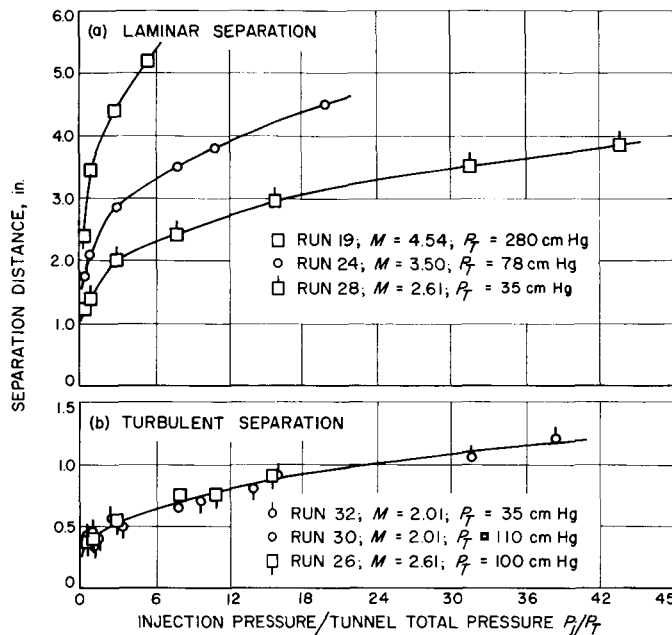


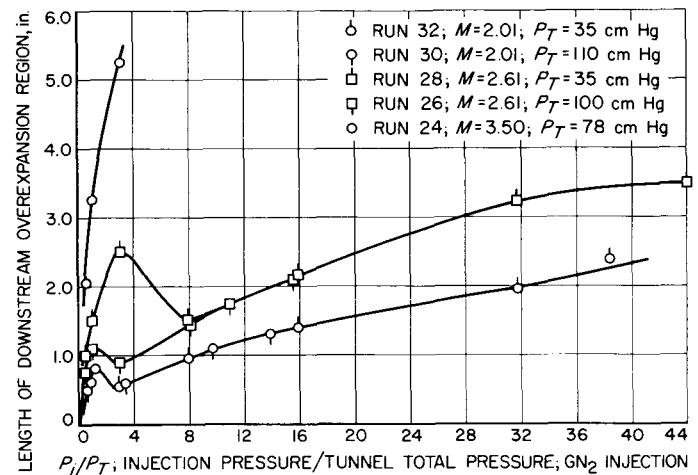
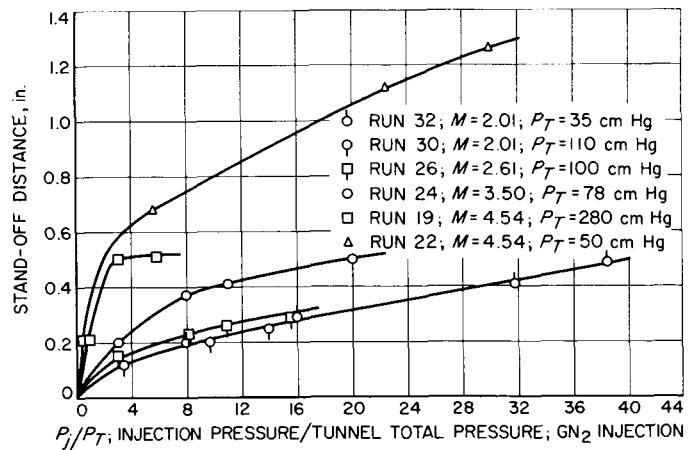
Fig. 19. Typical pressure distribution for GN_2 injection at $M = 2.61$

Fig. 20. Separation distance for GN_2 injection

in Mach number and/or a decrease in free-stream Reynolds number. This variation will be discussed further in Section V, on separation phenomena. The gaseous data for the turbulent separation distance was all for low Mach numbers and is adequately represented by a single curve.

The extent of the subnormal pressure region immediately downstream of the injector for gaseous injection is indicated by the length of the downstream overexpansion region, as measured from the centerline pressure distribution. The length of the downstream overexpansion region is the distance from the injector opening to the point downstream where the local pressure rises to the free-stream static pressure. The length of this downstream overexpansion region is plotted versus the ratio of injection pressure to tunnel total pressure P_j/P_T in Fig. 21. The first peak point in the data for a particular run corresponds to the maximum P_j/P_T for which the run/points exhibited an asymptotic pressure recovery downstream of the injector. For further increases in P_j/P_T , the data drop to a minimum value and then start increasing again.

Values of a shock stand-off distance were measured from the spark shadowgraphs for most runs. The stand-off distance is defined as the distance from the injector opening to the most forward point of the main curved shock associated with the injectant jet. The stand-off distance is shown plotted versus the ratio of injection pressure to tunnel total pressure P_j/P_T in Fig. 22. All runs show an increase in stand-off distance with increasing injection pressure.

Fig. 21. Length of downstream overexpansion region for GN_2 injectionFig. 22. Stand-off distance for GN_2 injection

V. SEPARATION PHENOMENA

A. General Considerations

Boundary-layer separation occurs whenever the streamwise pressure increases sufficiently to overcome the forces tending to accelerate the flow near a solid boundary. The only forces tending to accelerate the boundary-layer flow are the shear forces acting between adjacent layers of fluid. In laminar flows, a relatively small adverse pressure gradient imposed on the boundary layer is sufficient to cause separation since only viscous shearing forces are present to overcome this pressure force. The onset of turbulence increases the shearing forces because of the appearance of Reynolds stresses associated with the turbulent fluctuations. The increased shearing stresses, tending to accelerate the boundary-layer flow, delay the separation of the boundary layer.

B. Comparison of Laminar and Turbulent Boundary Layer Separation

The nature of the boundary layer has a large influence on separation phenomena. Available data on separated flows show that the pressure rise in a turbulent separa-

tion zone is greater than the pressure rise in a laminar separation zone, but the turbulent separation zone is smaller than the laminar separation zone. Considerable data, and many analyses, are available for treating separated flows; however, most of them are concerned with two-dimensional laminar and turbulent separations. The majority of the work done has been on separations associated with shock-wave boundary-layer reflections and separations produced by steps or wedges on the flow boundary. Indications are that for laminar separations the pressure level in the separation zone is independent of the geometry producing the separation, while for turbulent separations the pressure level in the separation zone often depends significantly on geometry.

In Fig. 23, the centerline pressure distributions forward of the single hole injector are compared for three run/points. The plate static pressures are nondimensionalized by dividing them by the free-stream static pressure. Notice that the pressure level in the separated region is much greater for turbulent separation than for laminar separation. The laminar separation zone extends

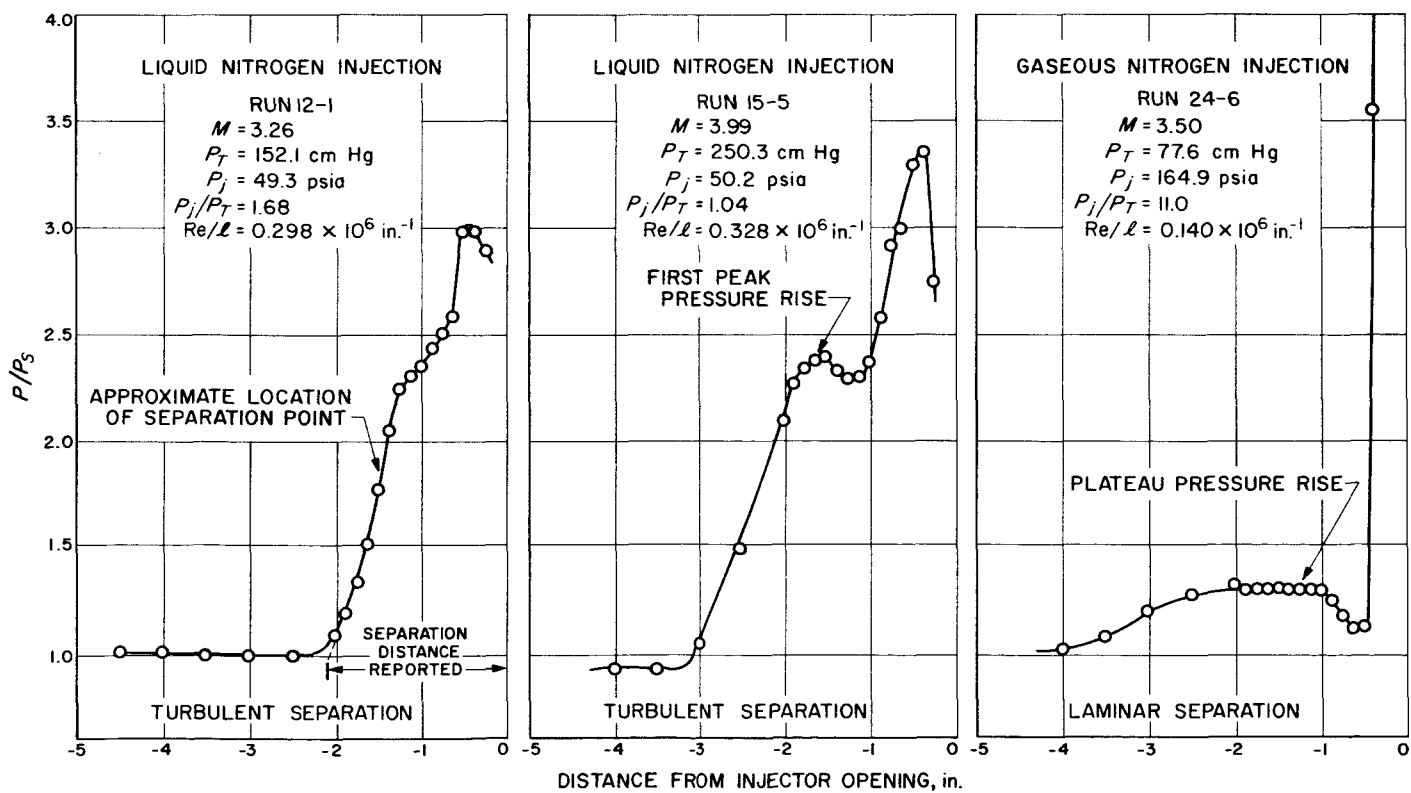


Fig. 23. Comparison of centerline pressure distributions for laminar and turbulent separations

further forward of the injector than the turbulent separation zone. It is very difficult to experimentally determine the boundary-layer separation point from static pressure measurements on the plate because of the steep pressure gradient which exists at the separation point. An approximate method of determining the separation point is to locate the separation point at the first inflection point in the pressure distribution curve drawn through the data points. Because of the difficulty in accurately locating the separation point from pressure distribution data, the separation distance is defined in this Report as the distance from the injector to the point forward of the injector where the plate static pressure rises above the free-stream static pressure. The actual separation distance is somewhat less than the values of separation distance reported, since both laminar and turbulent boundary layers will support some adverse pressure gradient before separating.

C. Turbulent Boundary Layer Separation

Bogdonoff and Kepler (Ref. 3) report on some experimental work on turbulent boundary-layer separation associated with flow over forward-facing steps and wedges, and turbulent separation caused by incident shocks. They obtained two different types of pressure distributions, depending on the geometry causing the separation. It is interesting to compare the results in Fig. 23 with the experimental work in Ref. 3. The pressure distribution for Run 15-5 is very similar in shape to the pressure distribution in the separation zone for a forward-facing step. The pressure increases to a peak, then drops slightly, and finally increases to the second, higher peak pressure. The pressure distribution for Run 12-1 is similar to the pressure distributions in the separation zone for a wedge or a shock-wave boundary-layer reflection. The pressure does not pass through a first peak, but continues to increase to the final peak pressure; however, there is a region of decreased pressure gradient where the pressure distribution passes through an inflection point.

Since the separation points cannot be located accurately on the pressure distributions, the runs are compared by using a characteristic point in the static-pressure distributions. The characteristic point was chosen as the first peak in the pressure distribution, or at the inflection point in the reduced pressure gradient region for runs which did not exhibit a first peak.

A pressure coefficient for the separation zone, based on the pressure at the characteristic point of the static pressure distribution, was calculated for each run/point which possessed a characteristic point. Figure 24 shows

the variation of pressure coefficient with free-stream Mach number. The pressure coefficient in the separation zone decreases with increasing Mach number in a manner similar to that indicated in the available data for turbulent separation ahead of two-dimensional steps and wedges; however, the pressure levels are lower. The lower pressure level can be attributed to the three-dimensional character of the separation ahead of the injectant jet, compared with the essentially two-dimensional character of the separation ahead of steps and wedges. Some of the scatter in the data at Mach numbers of 2.01 and 2.61 can be attributed to a slight variation of pressure coefficient with free-stream Reynolds number. The pressure coefficient decreases slightly with increasing free-stream Reynolds number. The data for steps and wedges similarly indicate a decreasing dependence on Reynolds number for increasing Mach number.

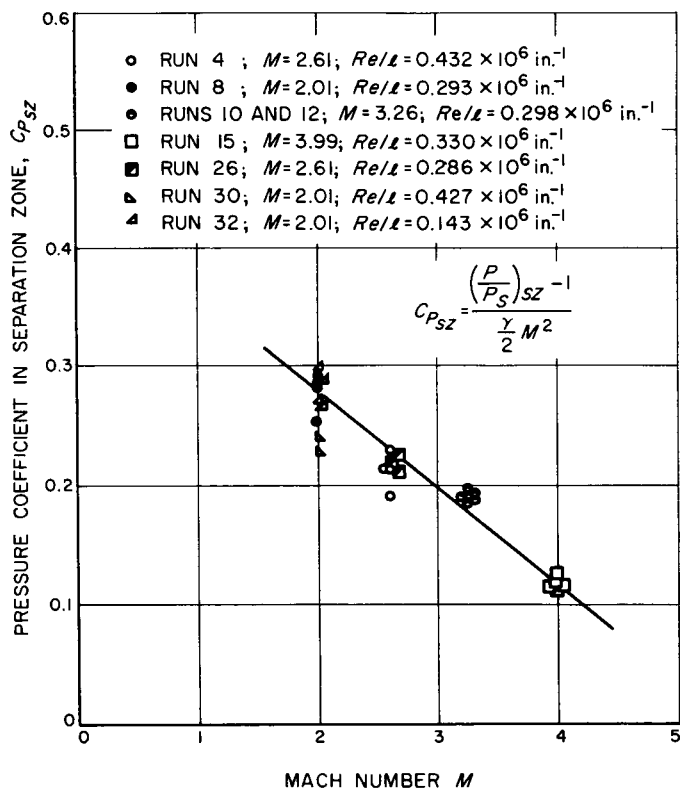


Fig. 24. Pressure coefficient in separation zone for turbulent separation

D. Laminar Boundary Layer Separation

Laminar boundary-layer separation differs considerably from turbulent separation. In Fig. 23, notice that a plateau region exists in the pressure distribution in the

laminar separation zone. This plateau pressure region is characteristic of laminar separations in general. The pressure level in this plateau region is much less than the first peak pressure in a turbulent separation zone; however, laminar separation zones cover larger areas than turbulent ones.

A pressure coefficient for the separation zone, based on the pressure in the plateau region of the static pressure distribution, was calculated for each run/point. Figure 25 shows a plot of this pressure coefficient versus the Reynolds number at the separation point for laminar separation. Notice the decreasing dependence on Reynolds number for increasing Mach-number flows. Curves similar to this are available for laminar separation ahead of steps and wedges. In laminar separations, the pressure level in the plateau region tends to be independent of the geometry causing the separation.

E. Stability of Separated Flows

The stability and steadiness of separated flows cannot be predicted with certainty, using present information. Motion pictures (at 500 frames/sec) were made of several of the liquid nitrogen injection runs to determine the steadiness of the flow interaction. Most of the runs exhibited an unsteadiness in the area of the separation zone forward of the injector. Unsteadiness can result from a hysteresis between laminar and turbulent separated zone conditions if the separation zone is near the transition point on the plate; however, some unsteadiness was observed for flows where the separation zone should have been well downstream of the transition point. A contributing factor to the unsteadiness of the flow disturb-

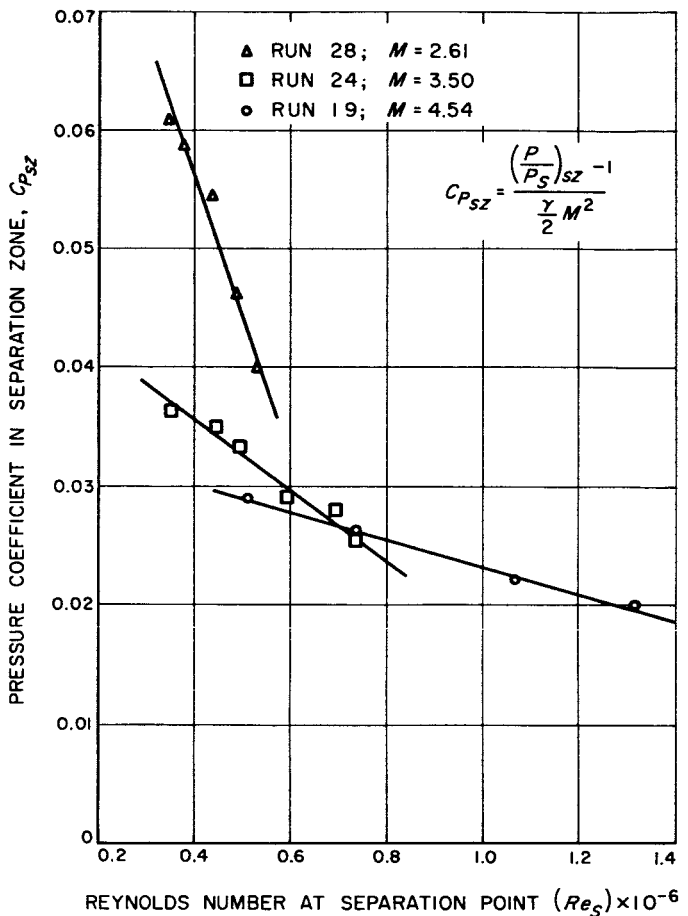


Fig. 25. Pressure coefficient in separation zone for laminar separation

ance could have been the cavitation condition present in the injector for liquid nitrogen injection.

VI. CONCLUSIONS AND RECOMMENDATIONS

These experiments have provided a systematic coverage of the effects of some of the more important parameters associated with the interaction of a liquid or gaseous injectant with a supersonic stream. The details about shock structure, separation distances, and pressure distributions in the injection region should assist in the development of more meaningful analytical models.

In general, the trends provided by the data are those which would be predicted by analysis. A notable exception was the apparent maximum in the curve of separation distance versus injection pressure for liquid injection. The importance of injector design and liquid jet break-up were illustrated by the greatly different pressure distributions observed for the two injector designs tested.

More information about the mixing of the secondary fluid with the main stream flow could be obtained by experimentally probing the downstream wake of the injectant jet. Measurements of composition, velocity, and temperature in the downstream wake would indicate how much entrainment and mixing occur. For liquid injection, the difficulties of making meaningful measurements in the downstream wake are increased because of the two-phase nature of the region. The Massachusetts Institute of Technology (Ref. 4) has done some work on two-phase velocity probes and composition probes for subsonic flow which has demonstrated that such measurements are practical if the probes are properly designed and calibrated. Composition measurements in the downstream wake region will be made for gas injection in the next wind tunnel test at JPL.

APPENDIX A
Liquid Nitrogen Data

Table A-1. Liquid nitrogen injection

Run	M	P _T , cm Hg	P _S , psia	T _T , °F	P _J , psia	T _J , °F	(P _J / P _T)	Re/l × 10 ⁻⁴ , in. ⁻¹	Separation distance, in.	w _{Jm} , lb/sec
4-1	2.61	152.0	1.494	106.0	125.5	-316	4.29	0.430	1.00	0.271
4-2	2.61	152.5	1.494	106.0	98.4	-319	3.35	0.432	1.00	0.239
4-3	2.61	151.9	1.492	105.5	77.6	-315	2.65	0.431	1.00	0.213
4-4	2.61	152.6	1.500	105.5	58.8	-313	2.00	0.433	1.00	0.179
4-5	2.61	152.1	1.495	105.5	48.4	-306	1.65	0.431	1.40	0.061
6-1	2.01	152.1	3.814	119.0	114.7	-315	3.91	0.558	0.65	0.259
6-2	2.01	151.9	3.807	119.0	100.8	-315	3.44	0.557	0.65	0.247
6-3	2.01	152.0	3.807	119.0	79.2	-314	2.70	0.558	0.65	0.212
6-4	2.01	152.0	3.807	119.0	59.2	-312	2.02	0.558	0.65	0.179
6-5	2.01	152.2	3.819	119.0	47.9	-306	1.63	0.559	1.00	0.079
6-6	2.01	152.1	3.809	119.0	36.8	-316	1.26	0.558	0.75	0.001
8-1	2.01	75.1	1.880	94.0	130.9	-310	9.05	0.293	1.05	0.270 ^a
8-2	2.01	75.0	1.875	94.0	114.0	-312	7.89	0.292	1.05	0.253 ^a
8-3	2.01	74.8	1.880	93.0	79.4	-310	5.50	0.292	1.15	0.209 ^a
8-4	2.01	74.9	1.895	93.0	58.5	-307	4.06	0.294	1.25	0.176 ^a
8-5	2.01	75.2	1.905	93.0	50.9	-308	3.52	0.293	1.15	0.165 ^a
10-1	3.26	151.8	0.548	110.0	129.0	-305	4.41	0.298	2.05	0.259 ^a
10-2	3.26	151.4	0.554	110.0	100.2	-305	3.44	0.297	2.05	0.229 ^a
12-1	3.26	152.1	0.539	110.0	49.3	-303	1.68	0.298	2.10	0.161 ^a
12-2	3.26	152.4	0.541	111.5	75.9	-304	2.59	0.299	2.15	0.199 ^a
12-3	3.26	151.9	0.540	110.5	151.1	-306	5.16	0.298	1.70	0.283 ^a
12-4	3.26	152.0	0.539	110.5	61.2	-307	2.09	0.298	1.70	0.180 ^a
12-5	3.26	152.1	0.540	110.5	45.1	-299	1.54	0.298	1.50	0.150 ^a
14-1	3.99	152.1	0.199	108.0	122.4	-299	4.18	0.204	—	0.211 ^a
14-2	3.99	151.7	0.190	109.0	98.9	-300	3.38	0.209	—	0.190
14-3	3.99	151.9	0.200	110.0	80.4	-301	2.75	0.204	—	0.175
14-4	3.99	151.9	0.198	110.0	60.6	-301	2.07	0.204	—	0.158
14-5	3.99	151.8	0.197	110.0	50.7	-301	1.73	0.203	—	0.140
15-1	3.99	249.9	0.320	113.0	62.1	-302	1.29	0.330	3.17	0.167
15-2	3.99	250.2	0.324	114.0	80.2	-302	1.66	0.330	3.20	0.209
15-3	3.99	250.6	0.324	114.0	99.7	-302	2.07	0.331	3.35	0.220
15-4	3.99	250.4	0.325	117.0	119.2	-301	2.47	0.328	3.50	0.247
15.5	3.99	250.3	0.324	117.0	50.2	-300	1.04	0.328	3.05	0.163

^aCalculated estimate

Table A-2. Pressure data for Run 4-1 (LN₂ injection)

Run	4-1	Re/L , in. ⁻¹	0.430×10^6
M	2.61	P_f , psia	125.5
P_T , cm Hg	152.1	T_f , °F	-316
P_s , psia	1.49	P_f/P_T	4.28
T_T , °F	106.0		

Pressure Tap	$\frac{P}{P_s}$										
A1	1.915	B1	1.982	C1	1.969	D1	1.619	E1	—	F1	1.298
A2	2.014	B2	2.009	C2	1.829	D2	1.777	E2	—	F2	1.287
A3	1.954	B3	1.781	C3	1.882	D3	1.772	E3	1.444	F3	1.276
A4	1.650	B4	1.093	C4	1.833	D4	1.978	E4	1.617	F4	1.217
A5	1.021	B5	1.081	C5	1.561	D5	1.620	E5	1.842	F5	1.189
A6	1.116	B6	0.990	C6	1.017	D6	1.234	E6	1.763	F6	1.162
A7	0.985	B7	0.992	C7	1.010	D7	1.056	E7	1.552	F7	1.155
A8	0.998	B8	0.990	C8	0.991	D8	0.992	E8	1.559	F8	1.115
A9	0.999	B9	0.992	C9	0.990	D9	—	E9	1.476	F9	1.089
A10	1.005	B10	0.996	C10	0.992	D10	0.990	E10	1.068	F10	1.083
A11	0.998	B11	0.994	C11	0.988	D11	0.989	E11	0.988	F11	1.026
A12	0.999	—	—	C12	0.997	—	—	E12	—	F12	0.909
A13	0.999	—	—	—	—	—	—	E13	0.992	F13	0.966
A14	1.003	—	—	—	—	—	—	E14	1.003	F14	0.902
A15	0.997	—	—	—	—	—	—	—	—	F15	0.883
A16	0.994	—	—	—	—	—	—	—	—	F16	—
A17	0.993	—	—	—	—	—	—	—	—	F17	0.900
A18	1.003	—	—	—	—	—	—	—	—	—	—
A19	0.988	—	—	—	—	—	—	—	—	—	—
A20	0.984	—	—	—	—	—	—	—	—	—	—

Table A-3. Pressure data for Run 4-2 (LN₂ injection)

Run	4-2	Re/l , in. ⁻¹	0.432×10^6
<i>M</i>	2.61	<i>P_j</i> , psia	98.4
<i>P_T</i> , cm Hg	152.5	<i>T_j</i> , °F	-319
<i>P_S</i> , psia	1.49	<i>P_j/P_T</i>	3.35
<i>T_T</i> , °F	106.0		

Pressure Tap	$\frac{P}{P_S}$										
A1	1.775	B1	1.907	C1	1.765	D1	1.691	E1	—	F1	1.393
A2	1.893	B2	1.839	C2	1.834	D2	1.746	E2	—	F2	1.371
A3	1.888	B3	1.564	C3	1.791	D3	1.946	E3	1.536	F3	1.333
A4	1.528	B4	0.978	C4	1.660	D4	1.651	E4	1.618	F4	1.263
A5	0.917	B5	1.107	C5	1.356	D5	1.522	E5	1.786	F5	1.221
A6	1.154	B6	0.991	C6	1.023	D6	1.047	E6	1.586	F6	1.186
A7	0.988	B7	0.994	C7	1.009	D7	1.072	E7	1.473	F7	1.170
A8	1.000	B8	0.993	C8	0.991	D8	0.988	E8	1.496	F8	1.123
A9	1.000	B9	0.992	C9	0.992	D9	—	E9	1.370	F9	1.091
A10	1.007	B10	0.996	C10	0.996	D10	0.990	E10	1.048	F10	1.069
A11	0.997	B11	0.996	C11	0.984	D11	0.991	E11	0.985	F11	1.003
A12	0.999	—	—	C12	0.993	—	—	E12	—	F12	0.902
A13	0.997	—	—	—	—	—	—	E13	0.992	F13	0.897
A14	1.002	—	—	—	—	—	—	E14	0.984	F14	0.890
A15	0.998	—	—	—	—	—	—	—	—	F15	0.889
A16	0.996	—	—	—	—	—	—	—	—	F16	—
A17	0.993	—	—	—	—	—	—	—	—	F17	0.900
A18	0.990	—	—	—	—	—	—	—	—	—	—
A19	0.990	—	—	—	—	—	—	—	—	—	—
A20	0.984	—	—	—	—	—	—	—	—	—	—

Table A-4. Pressure data for Run 4-3 (LN₂ injection)

Run	4-3	$Re/l, \text{in.}^{-1}$	0.431×10^6
M	2.61	P_j, psia	77.6
$P_T, \text{cm Hg}$	151.9	$T_j, {}^\circ\text{F}$	-315
P_S, psia	1.49	P_j/P_T	2.65
$T_{T_s}, {}^\circ\text{F}$	105.5		

Pressure Tap	$\frac{P}{P_S}$										
A1	1.952	B1	1.926	C1	2.009	D1	1.626	E1	—	F1	1.377
A2	1.934	B2	1.919	C2	1.793	D2	1.743	E2	—	F2	1.339
A3	2.038	B3	1.899	C3	1.845	D3	1.742	E3	1.449	F3	1.293
A4	1.797	B4	1.262	C4	1.849	D4	1.742	E4	1.591	F4	1.215
A5	1.294	B5	1.080	C5	1.608	D5	1.628	E5	1.795	F5	1.168
A6	1.107	B6	0.986	C6	1.247	D6	1.342	E6	1.656	F6	1.126
A7	0.983	B7	0.989	C7	1.025	D7	1.101	E7	1.584	F7	1.106
A8	0.995	B8	0.986	C8	0.986	D8	0.985	E8	1.561	F8	1.047
A9	0.995	B9	0.989	C9	0.986	D9	—	E9	1.504	F9	1.010
A10	0.999	B10	0.992	C10	0.990	D10	0.984	E10	1.120	F10	0.967
A11	0.994	B11	0.993	C11	0.984	D11	0.988	E11	0.985	F11	0.953
A12	0.995	—	—	C12	0.991	—	—	E12	—	F12	0.913
A13	0.998	—	—	—	—	—	—	E13	0.986	F13	0.898
A14	0.993	—	—	—	—	—	—	E14	0.988	F14	0.909
A15	0.994	—	—	—	—	—	—	—	—	F15	0.904
A16	0.992	—	—	—	—	—	—	—	—	F16	—
A17	0.994	—	—	—	—	—	—	—	—	F17	0.908
A18	0.989	—	—	—	—	—	—	—	—	—	—
A19	0.986	—	—	—	—	—	—	—	—	—	—
A20	0.981	—	—	—	—	—	—	—	—	—	—

Table A-5. Pressure data for Run 4-4 (LN₂ injection)

Run	4-4	$Re/l, \text{in.}^{-1}$	0.433×10^6
M	2.61	P_f, psia	58.8
$P_T, \text{cm Hg}$	152.6	$T_f, ^\circ\text{F}$	-313
P_S, psia	1.50	P_f/P_T	2.00
$T_f, ^\circ\text{F}$	105.5		

Pressure Tap	$\frac{P}{P_S}$										
A1	1.943	B1	1.861	C1	2.112	D1	1.610	E1	—	F1	1.366
A2	1.900	B2	1.883	C2	1.721	D2	1.696	E2	—	F2	1.310
A3	1.888	B3	2.043	C3	1.825	D3	1.716	E3	1.433	F3	1.245
A4	2.101	B4	1.486	C4	1.841	D4	1.766	E4	1.531	F4	1.166
A5	1.413	B5	1.165	C5	1.767	D5	1.783	E5	1.718	F5	1.115
A6	1.203	B6	0.990	C6	1.456	D6	1.523	E6	1.685	F6	1.074
A7	0.997	B7	0.984	C7	1.142	D7	1.174	E7	1.637	F7	1.048
A8	0.991	B8	0.982	C8	0.984	D8	1.041	E8	1.603	F8	0.989
A9	0.992	B9	0.986	C9	0.982	D9	—	E9	1.559	F9	0.956
A10	0.997	B10	0.989	C10	0.988	D10	0.980	E10	1.213	F10	0.912
A11	0.990	B11	0.990	C11	0.979	D11	0.979	E11	0.989	F11	0.893
A12	0.993	—	—	C12	0.989	—	—	E12	—	F12	0.870
A13	0.993	—	—	—	—	—	—	E13	0.982	F13	0.869
A14	0.993	—	—	—	—	—	—	E14	0.986	F14	0.872
A15	0.993	—	—	—	—	—	—	—	—	F15	0.887
A16	0.992	—	—	—	—	—	—	—	—	F16	—
A17	0.986	—	—	—	—	—	—	—	—	F17	0.913
A18	0.988	—	—	—	—	—	—	—	—	—	—
A19	0.984	—	—	—	—	—	—	—	—	—	—
A20	0.979	—	—	—	—	—	—	—	—	—	—

Table A-6. Pressure data for Run 4-5 (LN₂ injection)

Run	4-5	Re/\bar{L}, in.⁻¹	0.431×10^6
M	2.61	P_j, psia	48.4
P_T, cm Hg	152.1	T_j, °F	-306
P_s, psia	1.50	P_j/P_T	1.65
T_T, °F	105.5		

Pressure Tap	$\frac{P}{P_s}$										
A1	1.946	B1	1.735	C1	1.861	D1	1.639	E1	—	F1	0.644
A2	1.755	B2	1.664	C2	1.703	D2	1.490	E2	—	F2	0.789
A3	1.697	B3	1.797	C3	1.595	D3	1.467	E3	1.411	F3	0.813
A4	1.856	B4	1.856	C4	1.646	D4	1.539	E4	1.329	F4	0.830
A5	1.872	B5	1.747	C5	1.754	D5	1.617	E5	1.310	F5	0.831
A6	1.800	B6	1.430	C6	1.771	D6	1.634	E6	1.336	F6	0.821
A7	1.438	B7	1.124	C7	1.647	D7	1.551	E7	1.383	F7	0.780
A8	1.084	B8	1.038	C8	1.326	D8	1.392	E8	1.457	F8	0.770
A9	1.031	B9	0.987	C9	1.075	D9	—	E9	1.738	F9	0.797
A10	1.002	B10	0.989	C10	0.989	D10	0.984	E10	1.409	F10	0.794
A11	0.991	B11	0.991	C11	0.984	D11	0.980	E11	1.167	F11	0.808
A12	0.993	—	—	C12	0.990	—	—	E12	—	F12	0.838
A13	0.997	—	—	—	—	—	—	E13	0.987	F13	0.876
A14	0.994	—	—	—	—	—	—	E14	0.984	F14	0.901
A15	0.993	—	—	—	—	—	—	—	—	F15	0.918
A16	0.990	—	—	—	—	—	—	—	—	F16	—
A17	0.988	—	—	—	—	—	—	—	—	F17	0.948
A18	0.988	—	—	—	—	—	—	—	—	—	—
A19	0.985	—	—	—	—	—	—	—	—	—	—
A20	0.980	—	—	—	—	—	—	—	—	—	—

Table A-7. Pressure data for Run 6-1 (LN₂ injection)

Run	6-1	Re/l , in. ⁻¹	0.558×10^6
<i>M</i>	2.01	<i>P_j</i> , psia	114.7
<i>P_T</i> , cm Hg	152.1	<i>T_j</i> , °F	-315
<i>P_S</i> , psia	3.81	<i>P_j/P_T</i>	3.91
<i>T_T</i> , °F	119.0		

Pressure Tap	$\frac{P}{P_S}$										
A1	1.703	B1	1.584	C1	1.604	D1	1.532	E1	—	F1	1.182
A2	1.576	B2	1.364	C2	1.564	D2	1.486	E2	—	F2	1.117
A3	1.349	B3	1.023	C3	1.433	D3	1.372	E3	1.447	F3	1.126
A4	1.017	B4	1.010	C4	1.115	D4	1.156	E4	1.420	F4	0.957
A5	1.002	B5	1.009	C5	1.007	D5	1.002	E5	1.382	F5	1.053
A6	1.006	B6	1.009	C6	1.005	D6	0.987	E6	1.315	F6	0.994
A7	0.990	B7	1.009	C7	1.006	D7	0.984	E7	1.206	F7	0.999
A8	0.994	B8	1.008	C8	1.005	D8	0.981	E8	1.087	F8	0.973
A9	0.993	B9	1.003	C9	1.005	D9	—	E9	1.007	F9	0.943
A10	0.996	B10	1.000	C10	1.006	D10	0.980	E10	0.973	F10	0.936
A11	0.980	B11	0.995	C11	1.004	D11	0.976	E11	0.997	F11	0.947
A12	0.991	—	—	C12	1.007	—	—	E12	—	F12	0.966
A13	0.989	—	—	—	—	—	—	E13	1.018	F13	0.983
A14	0.990	—	—	—	—	—	—	E14	1.019	F14	0.973
A15	0.983	—	—	—	—	—	—	—	—	F15	0.984
A16	0.987	—	—	—	—	—	—	—	—	F16	—
A17	0.987	—	—	—	—	—	—	—	—	F17	1.033
A18	0.992	—	—	—	—	—	—	—	—	—	—
A19	0.996	—	—	—	—	—	—	—	—	—	—
A20	0.994	—	—	—	—	—	—	—	—	—	—

Table A-8. Pressure data for Run 6-2 (LN₂ injection)

Run	6-2	Re/l , in. ⁻¹	0.557×10^6
<i>M</i>	2.01	P_j , psia	100.8
P_T , cm Hg	151.9	T_j , °F	-315
P_S , psia	3.81	P_j/P_T	3.44
T_T , °F	119.0		

Pressure Tap	$\frac{P}{P_S}$										
A1	1.694	B1	1.584	C1	1.589	D1	1.536	E1	—	F1	1.195
A2	1.570	B2	1.362	C2	1.565	D2	1.490	E2	—	F2	1.148
A3	1.352	B3	1.023	C3	1.436	D3	1.378	E3	1.444	F3	1.140
A4	1.019	B4	1.010	C4	1.121	D4	1.162	E4	1.416	F4	1.247
A5	1.001	B5	1.009	C5	1.008	D5	1.004	E5	1.379	F5	1.151
A6	1.006	B6	1.009	C6	1.006	D6	0.987	E6	1.312	F6	1.053
A7	0.990	B7	1.008	C7	1.006	D7	0.984	E7	1.202	F7	1.018
A8	0.994	B8	1.008	C8	1.005	D8	0.981	E8	1.083	F8	0.925
A9	0.993	B9	1.003	C9	1.006	D9	—	E9	1.005	F9	0.937
A10	0.997	B10	1.001	C10	1.007	D10	0.981	E10	0.973	F10	0.931
A11	0.980	B11	0.995	C11	1.005	D11	0.975	E11	0.996	F11	0.922
A12	0.990	—	—	C12	1.008	—	—	E12	—	F12	0.944
A13	0.989	—	—	—	—	—	—	E13	1.018	F13	0.981
A14	0.989	—	—	—	—	—	—	E14	1.020	F14	0.971
A15	0.983	—	—	—	—	—	—	—	—	F15	1.001
A16	0.988	—	—	—	—	—	—	—	—	F16	—
A17	0.986	—	—	—	—	—	—	—	—	F17	1.056
A18	0.992	—	—	—	—	—	—	—	—	—	—
A19	0.997	—	—	—	—	—	—	—	—	—	—
A20	0.993	—	—	—	—	—	—	—	—	—	—

Table A-9. Pressure data for Run 6-3 (LN₂ injection)

Run	6-3	Re/l , in. ⁻¹	0.558×10^6
M	2.01	P_j , psia	79.2
P_T , cm Hg	152.0	T_j , °F	-314
P_B , psia	3.81	P_j/P_T	2.70
T_T , °F	119.0		

Pressure Tap	$\frac{P}{P_B}$										
A1	1.675	B1	1.579	C1	1.602	D1	1.530	E1	—	F1	1.218
A2	1.570	B2	1.357	C2	1.558	D2	1.481	E2	—	F2	1.153
A3	1.354	B3	1.024	C3	1.424	D3	1.365	E3	1.436	F3	1.220
A4	1.023	B4	1.009	C4	1.116	D4	1.144	E4	1.409	F4	1.199
A5	1.001	B5	1.008	C5	1.008	D5	1.001	E5	1.372	F5	1.223
A6	1.005	B6	1.008	C6	1.005	D6	0.988	E6	1.302	F6	1.004
A7	0.990	B7	1.009	C7	1.004	D7	0.983	E7	1.185	F7	1.320
A8	0.993	B8	1.007	C8	1.005	D8	0.980	E8	1.073	F8	1.028
A9	0.993	B9	1.002	C9	1.006	D9	—	E9	1.001	F9	1.163
A10	0.996	B10	1.000	C10	1.006	D10	0.978	E10	0.971	F10	0.945
A11	0.979	B11	0.993	C11	1.005	D11	0.974	E11	0.993	F11	0.891
A12	0.989	—	—	C12	1.008	—	—	E12	—	F12	0.913
A13	0.989	—	—	—	—	—	—	E13	1.016	F13	0.927
A14	0.989	—	—	—	—	—	—	E14	1.020	F14	0.982
A15	0.982	—	—	—	—	—	—	—	—	F15	1.004
A16	0.988	—	—	—	—	—	—	—	—	F16	—
A17	0.986	—	—	—	—	—	—	—	—	F17	1.037
A18	0.992	—	—	—	—	—	—	—	—	—	—
A19	0.997	—	—	—	—	—	—	—	—	—	—
A20	0.993	—	—	—	—	—	—	—	—	—	—

Table A-10. Pressure data for Run 6-4 (LN₂ injection)

Run	6-4	Re/l , in. ⁻¹	0.558×10^6
M	2.01	P_j , psia	59.2
P_T , cm Hg	152.0	T_j , °F	-312
P_S , psia	3.81	P_j/P_T	2.02
T_T , °F	119.0		

Pressure Tap	$\frac{P}{P_S}$										
A1	1.692	B1	1.588	C1	1.683	D1	1.546	E1	—	F1	1.223
A2	1.573	B2	1.385	C2	1.567	D2	1.479	E2	—	F2	1.128
A3	1.369	B3	1.023	C3	1.439	D3	1.373	E3	1.447	F3	1.086
A4	1.028	B4	1.008	C4	1.131	D4	1.156	E4	1.398	F4	1.211
A5	1.000	B5	1.007	C5	1.006	D5	1.002	E5	1.363	F5	1.169
A6	1.003	B6	1.006	C6	1.004	D6	0.984	E6	1.294	F6	0.937
A7	0.989	B7	1.007	C7	1.004	D7	0.981	E7	1.181	F7	1.296
A8	0.991	B8	1.007	C8	1.003	D8	0.979	E8	1.069	F8	1.152
A9	0.991	B9	1.001	C9	1.004	D9	—	E9	0.997	F9	1.230
A10	0.995	B10	0.998	C10	1.005	D10	0.977	E10	0.969	F10	0.904
A11	0.978	B11	0.993	C11	1.004	D11	0.973	E11	0.986	F11	0.906
A12	0.988	—	—	C12	1.006	—	—	E12	—	F12	0.931
A13	0.988	—	—	—	—	—	—	E13	1.015	F13	0.940
A14	0.988	—	—	—	—	—	—	E14	1.021	F14	0.967
A15	0.982	—	—	—	—	—	—	—	—	F15	0.986
A16	0.987	—	—	—	—	—	—	—	—	F16	—
A17	0.986	—	—	—	—	—	—	—	—	F17	1.016
A18	0.991	—	—	—	—	—	—	—	—	—	—
A19	0.996	—	—	—	—	—	—	—	—	—	—
A20	0.993	—	—	—	—	—	—	—	—	—	—

Table A-11. Pressure data for Run 6-5 (LN₂ injection)

Run	6-5	Re/l, in.⁻¹	0.559×10^6
M	2.01	P_j, psia	47.9
P_T, cm Hg	152.2	T_j, °F	-306
P_S, psia	3.82	P_j/P_T	1.63
T_T, °F	119.0		

Pressure Tap	$\frac{P}{P_S}$										
A1	1.666	B1	1.521	C1	1.684	D1	1.442	E1	—	F1	0.796
A2	1.501	B2	1.507	C2	1.493	D2	1.397	E2	—	F2	0.819
A3	1.501	B3	1.507	C3	1.489	D3	1.393	E3	1.263	F3	0.819
A4	1.482	B4	1.359	C4	1.489	D4	1.402	E4	1.272	F4	0.812
A5	1.438	B5	1.105	C5	1.381	D5	1.315	E5	1.272	F5	0.825
A6	1.179	B6	1.000	C6	1.120	D6	1.148	E6	1.272	F6	0.826
A7	1.000	B7	1.000	C7	1.010	D7	1.005	E7	1.203	F7	0.837
A8	0.985	B8	0.999	C8	0.997	D8	0.974	E8	1.210	F8	0.849
A9	0.984	B9	0.994	C9	0.999	D9	—	E9	1.155	F9	0.876
A10	0.988	B10	0.993	C10	0.999	D10	0.972	E10	1.003	F10	0.881
A11	0.973	B11	0.986	C11	0.999	D11	0.968	E11	0.981	F11	0.910
A12	0.982	—	—	C12	1.002	—	—	E12	—	F12	0.964
A13	0.982	—	—	—	—	—	—	E13	1.010	F13	0.983
A14	0.983	—	—	—	—	—	—	E14	1.016	F14	1.016
A15	0.978	—	—	—	—	—	—	—	—	F15	1.041
A16	0.982	—	—	—	—	—	—	—	—	F16	—
A17	0.981	—	—	—	—	—	—	—	—	F17	1.074
A18	0.987	—	—	—	—	—	—	—	—	—	—
A19	0.992	—	—	—	—	—	—	—	—	—	—
A20	0.990	—	—	—	—	—	—	—	—	—	—

Table A-12. Pressure data for Run 6-6 (LN₂ injection)

Run	6-6	$Re/l, \text{ in.}^{-1}$	0.558×10^6
M	2.01	$P_j, \text{ psia}$	36.8
$P_T, \text{ cm Hg}$	152.1	$T_j, ^\circ\text{F}$	-316
$P_S, \text{ psia}$	3.81	P_j/P_T	1.26
$T_T, ^\circ\text{F}$	119.0		

Pressure Tap	$\frac{P}{P_S}$										
A1	1.662	B1	1.623	C1	1.556	D1	1.487	E1	—	F1	0.922
A2	1.613	B2	1.578	C2	1.569	D2	1.455	E2	—	F2	0.897
A3	1.552	B3	1.204	C3	1.544	D3	1.440	E3	1.330	F3	0.877
A4	1.245	B4	1.015	C4	1.377	D4	1.313	E4	1.320	F4	0.855
A5	1.005	B5	1.001	C5	1.144	D5	1.145	E5	1.369	F5	0.856
A6	0.998	B6	1.001	C6	1.001	D6	0.995	E6	1.282	F6	0.857
A7	0.983	B7	1.003	C7	0.999	D7	0.977	E7	1.228	F7	0.874
A8	0.987	B8	1.002	C8	1.000	D8	0.974	E8	1.143	F8	0.887
A9	0.986	B9	0.997	C9	1.000	D9	—	E9	1.054	F9	0.920
A10	0.990	B10	0.995	C10	1.002	D10	0.975	E10	0.968	F10	0.879
A11	0.974	B11	0.989	C11	1.001	D11	0.971	E11	0.981	F11	0.914
A12	0.984	—	—	C12	1.005	—	—	E12	—	F12	0.942
A13	0.983	—	—	—	—	—	—	E13	1.013	F13	0.965
A14	0.985	—	—	—	—	—	—	E14	1.015	F14	1.006
A15	0.978	—	—	—	—	—	—	—	—	F15	1.011
A16	0.983	—	—	—	—	—	—	—	—	F16	—
A17	0.985	—	—	—	—	—	—	—	—	F17	1.000
A18	0.989	—	—	—	—	—	—	—	—	—	—
A19	0.994	—	—	—	—	—	—	—	—	—	—
A20	0.991	—	—	—	—	—	—	—	—	—	—

Table A-13. Pressure data for Run 8-1 (LN₂ injection)

Run	8-1	Re/L, in.⁻¹	0.293×10^6
M	2.01	P_j, psia	130.9
P_T, cm Hg	75.1	T_j, °F	-310
P_S, psia	1.88	P_j/P_T	9.05
T_T, °F	94.0		

Pressure Tap	$\frac{P}{P_S}$										
A1	1.928	B1	1.610	C1	2.220	D1	1.413	E1	—	F1	0.955
A2	1.679	B2	1.811	C2	1.398	D2	1.442	E2	—	F2	0.983
A3	1.807	B3	1.757	C3	1.700	D3	1.613	E3	1.342	F3	1.013
A4	1.753	B4	1.669	C4	1.700	D4	1.604	E4	1.270	F4	0.958
A5	1.660	B5	1.450	C5	1.673	D5	1.592	E5	1.453	F5	0.962
A6	1.449	B6	1.092	C6	1.577	D6	1.536	E6	1.460	F6	0.953
A7	1.092	B7	1.025	C7	1.352	D7	1.450	E7	1.489	F7	0.937
A8	1.011	B8	1.026	C8	1.052	D8	1.289	E8	1.464	F8	0.919
A9	1.003	B9	1.035	C9	0.996	D9	—	E9	1.447	F9	0.938
A10	1.002	B10	1.041	C10	0.994	D10	0.970	E10	1.402	F10	0.968
A11	0.988	B11	1.033	C11	0.990	D11	0.976	E11	1.316	F11	0.918
A12	0.994	—	—	C12	0.996	—	—	E12	—	F12	0.905
A13	0.994	—	—	—	—	—	—	E13	1.025	F13	0.887
A14	0.994	—	—	—	—	—	—	E14	1.003	F14	0.890
A15	0.989	—	—	—	—	—	—	—	—	F15	0.891
A16	0.987	—	—	—	—	—	—	—	—	F16	—
A17	0.989	—	—	—	—	—	—	—	—	F17	0.938
A18	0.994	—	—	—	—	—	—	—	—	—	—
A19	1.002	—	—	—	—	—	—	—	—	—	—
A20	0.999	—	—	—	—	—	—	—	—	—	—

Table A-14. Pressure data for Run 8-2 (LN₂ injection)

Run	8-2	Re/L, in.⁻¹	0.292×10^6
M	2.01	P_j, psia	114.0
P_T, cm Hg	75.0	T_j, °F	-312
P_S, psia	1.88	P_j/P_T	7.89
T_T, °F	94.0		

Pressure Tap	$\frac{P}{P_S}$										
A1	1.848	B1	1.675	C1	2.119	D1	1.436	E1	—	F1	1.002
A2	1.741	B2	1.823	C2	1.464	D2	1.493	E2	—	F2	1.020
A3	1.984	B3	1.790	C3	1.724	D3	1.640	E3	1.337	F3	1.052
A4	1.744	B4	1.633	C4	1.887	D4	1.743	E4	1.346	F4	0.995
A5	1.599	B5	1.391	C5	1.680	D5	1.622	E5	1.514	F5	0.987
A6	1.352	B6	1.072	C6	1.546	D6	1.530	E6	1.760	F6	0.977
A7	1.071	B7	1.030	C7	1.318	D7	1.421	E7	1.583	F7	0.973
A8	1.012	B8	1.027	C8	1.030	D8	1.239	E8	1.479	F8	0.940
A9	1.005	B9	1.039	C9	0.997	D9	—	E9	1.491	F9	0.909
A10	1.005	B10	1.048	C10	0.980	D10	0.981	E10	1.390	F10	0.976
A11	0.990	B11	1.037	C11	0.990	D11	0.972	E11	1.287	F11	0.905
A12	0.997	—	—	C12	0.996	—	—	E12	—	F12	0.867
A13	1.000	—	—	—	—	—	—	E13	1.024	F13	0.840
A14	0.995	—	—	—	—	—	—	E14	1.012	F14	0.866
A15	0.991	—	—	—	—	—	—	—	—	F15	0.884
A16	0.989	—	—	—	—	—	—	—	—	F16	—
A17	0.993	—	—	—	—	—	—	—	—	F17	0.944
A18	0.996	—	—	—	—	—	—	—	—	—	—
A19	1.002	—	—	—	—	—	—	—	—	—	—
A20	1.003	—	—	—	—	—	—	—	—	—	—

Table A-15. Pressure data for Run 8-3 (LN₂ injection)

Run	8-3	Re/l , in. ⁻¹	0.292×10^6
M	2.01	P_j , psia	79.4
P_T , cm Hg	74.8	T_j , °F	-310
P_S , psia	1.88	P_j/P_T	5.50
T_T , °F	93.0		

Pressure Tap	$\frac{P}{P_S}$										
A1	1.953	B1	1.611	C1	2.071	D1	1.478	E1	—	F1	1.013
A2	1.669	B2	1.783	C2	1.481	D2	1.453	E2	—	F2	1.015
A3	2.026	B3	1.881	C3	1.670	D3	1.813	E3	1.793	F3	0.970
A4	1.792	B4	1.861	C4	1.891	D4	1.601	E4	1.337	F4	0.952
A5	1.836	B5	1.410	C5	1.763	D5	2.732	E5	1.493	F5	0.944
A6	1.448	B6	1.203	C6	1.548	D6	1.514	E6	1.691	F6	0.949
A7	1.242	B7	1.039	C7	1.364	D7	1.412	E7	1.888	F7	0.915
A8	1.014	B8	1.023	C8	1.115	D8	1.255	E8	2.192	F8	0.917
A9	1.002	B9	1.035	C9	0.998	D9	—	E9	1.712	F9	0.938
A10	1.002	B10	1.041	C10	0.995	D10	0.973	E10	1.366	F10	0.894
A11	0.986	B11	1.035	C11	0.988	D11	0.968	E11	1.275	F11	0.876
A12	0.994	—	—	C12	0.994	—	—	E12	—	F12	0.869
A13	0.992	—	—	—	—	—	—	E13	1.021	F13	0.888
A14	0.994	—	—	—	—	—	—	E14	1.009	F14	0.905
A15	0.988	—	—	—	—	—	—	—	—	F15	—
A16	0.986	—	—	—	—	—	—	—	—	F16	—
A17	0.989	—	—	—	—	—	—	—	—	F17	0.963
A18	0.994	—	—	—	—	—	—	—	—	—	—
A19	0.999	—	—	—	—	—	—	—	—	—	—
A20	0.998	—	—	—	—	—	—	—	—	—	—

Table A-16. Pressure data for Run 8-4 (LN₂ injection)

Run	8-4	$Re/l, \text{in.}^{-1}$	0.294×10^6
M	2.01	P_j, psia	58.5
$P_T, \text{cm Hg}$	74.9	$T_j, ^\circ\text{F}$	-307
P_S, psia	1.90	P_j/P_T	4.06
$T_T, ^\circ\text{F}$	93.0		

Pressure Tap	$\frac{P}{P_S}$										
A1	1.971	B1	1.548	C1	2.005	D1	1.515	E1	—	F1	0.950
A2	1.629	B2	1.684	C2	1.450	D2	1.381	E2	—	F2	0.967
A3	2.150	B3	1.752	C3	1.609	D3	1.731	E3	1.364	F3	0.960
A4	1.667	B4	1.721	C4	1.799	D4	1.691	E4	1.279	F4	0.920
A5	1.800	B5	1.539	C5	1.765	D5	2.293	E5	1.415	F5	0.908
A6	1.530	B6	1.350	C6	1.654	D6	1.597	E6	1.607	F6	0.900
A7	1.396	B7	1.195	C7	1.463	D7	1.420	E7	1.895	F7	0.910
A8	1.171	B8	1.055	C8	1.149	D8	1.309	E8	1.977	F8	0.973
A9	1.005	B9	1.031	C9	1.145	D9	—	E9	1.718	F9	0.894
A10	0.999	B10	1.038	C10	0.991	D10	0.972	E10	1.357	F10	0.898
A11	0.985	B11	1.028	C11	1.005	D11	0.967	E11	1.294	F11	0.889
A12	0.991	—	—	C12	0.993	—	—	E12	—	F12	0.896
A13	0.990	—	—	—	—	—	—	E13	1.028	F13	0.901
A14	0.992	—	—	—	—	—	—	E14	0.992	F14	0.910
A15	0.985	—	—	—	—	—	—	—	—	F15	0.924
A16	0.985	—	—	—	—	—	—	—	—	F16	—
A17	0.988	—	—	—	—	—	—	—	—	F17	0.981
A18	0.993	—	—	—	—	—	—	—	—	—	—
A19	0.998	—	—	—	—	—	—	—	—	—	—
A20	1.000	—	—	—	—	—	—	—	—	—	—

Table A-17. Pressure data for Run 8-5 (LN₂ injection)

Run	8-5	Re/L , in. ⁻¹	0.293×10^6
M	2.01	P_j , psia	50.9
P_T , cm Hg	75.2	T_j , °F	-308
P_S , psia	1.91	P_j/P_T	3.52
T_T , °F	93.0		

Pressure Tap	$\frac{P}{P_S}$										
A1	1.917	B1	1.633	C1	1.961	D1	1.471	E1	—	F1	0.992
A2	1.656	B2	1.705	C2	1.529	D2	1.486	E2	—	F2	0.980
A3	1.707	B3	1.711	C3	1.644	D3	1.543	E3	1.336	F3	0.975
A4	1.709	B4	1.662	C4	1.640	D4	1.535	E4	1.373	F4	0.924
A5	1.673	B5	1.437	C5	1.621	D5	1.513	E5	1.416	F5	0.906
A6	1.491	B6	1.068	C6	1.575	D6	1.488	E6	1.405	F6	0.890
A7	1.093	B7	1.085	C7	1.322	D7	1.395	E7	1.400	F7	0.899
A8	1.041	B8	1.028	C8	1.014	D8	1.201	E8	1.388	F8	0.892
A9	1.000	B9	1.030	C9	1.041	D9	—	E9	1.388	F9	0.912
A10	1.000	B10	1.035	C10	0.988	D10	0.972	E10	1.351	F10	0.910
A11	0.986	B11	1.027	C11	0.983	D11	0.963	E11	1.218	F11	0.925
A12	0.991	—	—	C12	0.991	—	—	E12	—	F12	0.939
A13	0.991	—	—	—	—	—	—	E13	1.015	F13	0.938
A14	0.992	—	—	—	—	—	—	E14	1.002	F14	0.952
A15	0.988	—	—	—	—	—	—	—	—	F15	0.961
A16	0.986	—	—	—	—	—	—	—	—	F16	—
A17	0.988	—	—	—	—	—	—	—	—	F17	0.997
A18	0.993	—	—	—	—	—	—	—	—	—	—
A19	0.999	—	—	—	—	—	—	—	—	—	—
A20	0.999	—	—	—	—	—	—	—	—	—	—

Table A-18. Pressure data for Run 10-1 (LN₂ injection)

Run	10-1	Re/\bar{L} , in. ⁻¹	0.298×10^6
<i>M</i>	3.26	P_j , psia	129.0
P_T , cm Hg	151.8	T_j , °F	-305
P_s , psia	0.548	P_j/P_T	4.41
T_T , °F	110.0		

Pressure Tap	$\frac{P}{P_s}$										
A1	2.788	B1	3.175	C1	2.396	D1	2.813	E1	—	F1	0.810
A2	3.224	B2	2.997	C2	3.092	D2	2.954	E2	—	F2	1.227
A3	3.006	B3	2.902	C3	3.000	D3	2.914	E3	2.632	F3	1.353
A4	2.822	B4	2.383	C4	2.948	D4	3.245	E4	2.761	F4	1.353
A5	2.472	B5	2.414	C5	2.402	D5	2.086	E5	2.819	F5	1.340
A6	2.448	B6	2.377	C6	2.310	D6	2.083	E6	2.374	F6	1.328
A7	2.423	B7	2.365	C7	2.242	D7	2.043	E7	1.902	F7	1.304
A8	2.411	B8	2.346	C8	2.221	D8	2.012	E8	1.868	F8	1.230
A9	2.374	B9	2.024	C9	2.230	D9	—	E9	1.831	F9	1.166
A10	2.254	B10	1.310	C10	2.119	D10	1.935	E10	1.782	F10	1.077
A11	2.012	B11	1.021	C11	1.699	D11	1.724	E11	1.751	F11	1.024
A12	1.626	—	—	C12	1.138	—	—	E12	—	F12	0.966
A13	1.297	—	—	—	—	—	—	E13	1.705	F13	0.954
A14	1.110	—	—	—	—	—	—	E14	1.638	F14	0.926
A15	1.028	—	—	—	—	—	—	—	—	F15	0.917
A16	0.985	—	—	—	—	—	—	—	—	F16	—
A17	0.991	—	—	—	—	—	—	—	—	F17	0.890
A18	0.997	—	—	—	—	—	—	—	—	—	—
A19	1.003	—	—	—	—	—	—	—	—	—	—
A20	1.006	—	—	—	—	—	—	—	—	—	—

Table A-19. Pressure data for Run 10-2 (LN₂ injection)

Run	10-2	$Re/L, \text{ in.}^{-1}$	0.297×10^6
M	3.26	$P_j, \text{ psia}$	100.2
$P_T, \text{ cm Hg}$	151.4	$T_j, ^\circ\text{F}$	-305
$P_S, \text{ psia}$	0.554	P_j/P_T	3.44
$T_T, ^\circ\text{F}$	110.0		

Pressure Tap	$\frac{P}{P_S}$										
A1	2.861	B1	3.112	C1	2.624	D1	2.770	E1	—	F1	0.897
A2	3.130	B2	2.958	C2	3.009	D2	2.921	E2	—	F2	1.279
A3	2.958	B3	2.858	C3	2.949	D3	3.091	E3	2.573	F3	1.373
A4	2.755	B4	2.470	C4	3.003	D4	2.594	E4	2.749	F4	1.364
A5	2.549	B5	2.406	C5	2.394	D5	2.109	E5	2.952	F5	1.361
A6	2.452	B6	2.364	C6	2.343	D6	2.091	E6	2.279	F6	1.330
A7	2.412	B7	2.337	C7	2.243	D7	2.049	E7	1.909	F7	1.303
A8	2.385	B8	2.337	C8	2.212	D8	2.012	E8	1.788	F8	1.233
A9	2.318	B9	2.024	C9	2.218	D9	—	E9	1.794	F9	1.139
A10	2.179	B10	1.352	C10	2.103	D10	1.918	E10	1.764	F10	1.076
A11	1.982	B11	1.039	C11	1.694	D11	1.727	E11	1.733	F11	1.003
A12	1.624	—	—	C12	1.164	—	—	E12	—	F12	0.939
A13	1.324	—	—	—	—	—	—	E13	1.694	F13	0.924
A14	1.152	—	—	—	—	—	—	E14	1.639	F14	0.906
A15	1.039	—	—	—	—	—	—	—	—	F15	0.894
A16	0.988	—	—	—	—	—	—	—	—	F16	—
A17	0.988	—	—	—	—	—	—	—	—	F17	0.873
A18	1.003	—	—	—	—	—	—	—	—	—	—
A19	1.000	—	—	—	—	—	—	—	—	—	—
A20	1.006	—	—	—	—	—	—	—	—	—	—

Table A-20. Pressure data for Run 12-1 (LN₂ injection)

Run	12-1	$Re/L, \text{ in.}^{-1}$	0.298×10^6
<i>M</i>	3.26	$P_j, \text{ psia}$	49.3
$P_T, \text{ cm Hg}$	152.1	$T_j, ^\circ\text{F}$	-303
$P_s, \text{ psia}$	0.539	P_j/P_T	1.68
$T_T, ^\circ\text{F}$	110.0		

Pressure Tap	$\frac{P}{P_s}$										
A1	2.884	B1	2.957	C1	2.650	D1	2.498	E1	—	F1	1.028
A2	2.986	B2	3.059	C2	2.845	D2	2.394	E2	—	F2	1.308
A3	2.976	B3	2.508	C3	3.008	D3	2.247	E3	2.300	F3	1.336
A4	2.585	B4	2.441	C4	2.512	D4	2.179	E4	2.368	F4	1.343
A5	2.507	B5	2.372	C5	2.285	D5	2.142	E5	2.225	F5	1.281
A6	2.434	B6	2.308	C6	2.264	D6	2.079	E6	1.931	F6	1.222
A7	2.356	B7	2.259	C7	2.202	D7	2.007	E7	1.831	F7	1.175
A8	2.306	B8	2.223	C8	2.188	D8	2.000	E8	1.772	F8	1.088
A9	2.244	B9	1.844	C9	2.144	D9	—	E9	1.750	F9	1.027
A10	2.048	B10	1.380	C10	1.952	D10	1.811	E10	1.719	F10	0.976
A11	1.776	B11	1.065	C11	1.569	D11	1.528	E11	1.699	F11	0.947
A12	1.516	—	—	C12	1.153	—	—	E12	—	F12	0.879
A13	1.338	—	—	—	—	—	—	E13	1.644	F13	0.874
A14	1.194	—	—	—	—	—	—	E14	1.434	F14	0.853
A15	1.094	—	—	—	—	—	—	—	—	F15	0.850
A16	0.989	—	—	—	—	—	—	—	—	F16	—
A17	0.992	—	—	—	—	—	—	—	—	F17	0.850
A18	0.997	—	—	—	—	—	—	—	—	—	—
A19	1.004	—	—	—	—	—	—	—	—	—	—
A20	1.008	—	—	—	—	—	—	—	—	—	—

Table A-21. Pressure data for Run 12-2 (LN₂ injection)

Run	12-2	$Re/L, \text{in.}^{-1}$	0.299×10^6
M	3.26	P_j, psia	75.9
$P_T, \text{cm Hg}$	152.4	$T_j, ^\circ\text{F}$	-304
P_s, psia	0.541	P_j/P_T	2.59
$T_T, ^\circ\text{F}$	111.5		

Pressure Tap	$\frac{P}{P_s}$										
A1	2.796	B1	2.992	C1	2.601	D1	2.720	E1	—	F1	0.943
A2	3.030	B2	2.977	C2	2.895	D2	2.897	E2	—	F2	1.306
A3	2.974	B3	3.108	C3	2.990	D3	3.216	E3	2.453	F3	1.368
A4	3.012	B4	2.481	C4	3.117	D4	2.347	E4	2.594	F4	1.349
A5	2.544	B5	2.407	C5	2.385	D5	2.207	E5	2.477	F5	1.320
A6	2.496	B6	2.353	C6	2.373	D6	2.101	E6	2.035	F6	1.298
A7	2.430	B7	2.330	C7	2.236	D7	2.024	E7	1.933	F7	1.265
A8	2.379	B8	2.798	C8	2.203	D8	2.021	E8	1.867	F8	1.172
A9	2.370	B9	2.025	C9	2.182	D9	—	E9	1.830	F9	1.110
A10	2.276	B10	1.447	C10	2.084	D10	1.883	E10	1.777	F10	1.050
A11	2.076	B11	1.103	C11	1.655	D11	1.639	E11	1.746	F11	0.982
A12	1.689	—	—	C12	1.152	—	—	E12	—	F12	0.913
A13	1.369	—	—	—	—	—	—	E13	1.701	F13	0.883
A14	1.172	—	—	—	—	—	—	E14	1.572	F14	0.875
A15	1.088	—	—	—	—	—	—	—	—	F15	0.866
A16	0.986	—	—	—	—	—	—	—	—	F16	—
A17	0.990	—	—	—	—	—	—	—	—	F17	0.851
A18	0.996	—	—	—	—	—	—	—	—	—	—
A19	1.004	—	—	—	—	—	—	—	—	—	—
A20	1.010	—	—	—	—	—	—	—	—	—	—

Table A-22. Pressure data for Run 12-3 (LN_2 injection)

Run	12-3	Re/L, in.$^{-1}$	0.298×10^6
M	3.26	P_j, psia	151.1
P_T, cm Hg	151.9	T_j, °F	-306
P_s, psia	0.540	P_j/P_T	5.16
T_T, °F	110.5		

Pressure Tap	$\frac{P}{P_s}$										
A1	3.019	B1	3.249	C1	2.698	D1	3.027	E1	—	F1	1.080
A2	3.310	B2	2.844	C2	3.224	D2	2.975	E2	—	F2	1.399
A3	2.881	B3	2.401	C3	2.855	D3	3.073	E3	2.803	F3	1.466
A4	2.570	B4	2.466	C4	2.923	D4	2.084	E4	2.787	F4	1.450
A5	2.490	B5	2.453	C5	2.280	D5	2.117	E5	3.067	F5	1.441
A6	2.480	B6	2.494	C6	2.305	D6	2.119	E6	1.927	F6	1.401
A7	2.465	B7	2.722	C7	2.295	D7	2.077	E7	1.917	F7	1.362
A8	2.399	B8	2.281	C8	2.310	D8	2.105	E8	1.902	F8	1.271
A9	2.239	B9	1.384	C9	2.248	D9	—	E9	1.899	F9	1.181
A10	1.855	B10	1.055	C10	1.835	D10	1.825	E10	1.824	F10	1.140
A11	1.435	B11	0.987	C11	1.127	D11	1.286	E11	1.784	F11	1.013
A12	1.139	—	—	C12	0.998	—	—	E12	—	F12	1.001
A13	1.031	—	—	—	—	—	—	E13	1.722	F13	0.990
A14	0.995	—	—	—	—	—	—	E14	1.412	F14	0.972
A15	0.983	—	—	—	—	—	—	—	—	F15	0.959
A16	0.986	—	—	—	—	—	—	—	—	F16	—
A17	0.992	—	—	—	—	—	—	—	—	F17	0.934
A18	0.999	—	—	—	—	—	—	—	—	—	—
A19	1.003	—	—	—	—	—	—	—	—	—	—
A20	1.010	—	—	—	—	—	—	—	—	—	—

Table A-23. Pressure data for Run 12-4 (LN₂ injection)

Run	12-4	Re/L , in. ⁻¹	0.298×10^6
<i>M</i>	3.26	P_i , psia	61.2
P_T , cm Hg	152.0	T_j , °F	-307
P_S , psia	0.539	P_j/P_T	2.09
T_T , °F	110.5		

Pressure Tap	$\frac{P}{P_S}$										
A1	3.104	B1	3.055	C1	3.013	D1	3.029	E1	—	F1	1.568
A2	3.021	B2	2.562	C2	3.060	D2	3.254	E2	—	F2	1.616
A3	2.990	B3	2.499	C3	2.820	D3	2.824	E3	3.036	F3	1.602
A4	2.531	B4	2.406	C4	2.545	D4	2.227	E4	3.283	F4	1.551
A5	2.445	B5	2.375	C5	2.340	D5	2.127	E5	2.162	F5	1.507
A6	2.394	B6	2.309	C6	2.266	D6	2.107	E6	1.999	F6	1.444
A7	2.312	B7	2.185	C7	2.248	D7	2.076	E7	1.940	F7	1.383
A8	2.135	B8	1.874	C8	2.218	D8	2.069	E8	1.865	F8	1.274
A9	1.781	B9	1.142	C9	2.109	D9	—	E9	1.839	F9	1.157
A10	1.379	B10	1.005	C10	1.371	D10	1.348	E10	1.807	F10	1.121
A11	1.166	B11	0.993	C11	1.028	D11	1.085	E11	1.727	F11	1.026
A12	1.049	—	—	C12	1.001	—	—	E12	—	F12	0.960
A13	0.996	—	—	—	—	—	—	E13	1.408	F13	0.941
A14	0.988	—	—	—	—	—	—	E14	1.102	F14	0.919
A15	0.983	—	—	—	—	—	—	—	—	F15	0.905
A16	0.992	—	—	—	—	—	—	—	—	F16	—
A17	0.995	—	—	—	—	—	—	—	—	F17	0.891
A18	1.002	—	—	—	—	—	—	—	—	—	—
A19	1.007	—	—	—	—	—	—	—	—	—	—
A20	1.012	—	—	—	—	—	—	—	—	—	—

Table A-24. Pressure data for Run 12-5 (LN₂ injection)

Run	12-5	Re/l, in.⁻¹	0.298×10^6
M	3.26	P_j, psia	45.1
P_T, cm Hg	152.1	T_j, °F	-299
P_S, psia	0.540	P_j/P_T	1.54
T_T, °F	110.5		

Pressure Tap	$\frac{P}{P_S}$										
A1	2.383	B1	1.928	C1	2.315	D1	1.903	E1	—	F1	0.544
A2	1.997	B2	1.630	C2	2.007	D2	1.716	E2	—	F2	0.821
A3	1.831	B3	1.441	C3	1.644	D3	1.443	E3	1.636	F3	0.963
A4	1.669	B4	1.290	C4	1.360	D4	1.307	E4	1.610	F4	0.946
A5	1.393	B5	1.052	C5	1.219	D5	1.220	E5	1.508	F5	0.951
A6	1.128	B6	1.069	C6	1.093	D6	1.137	E6	1.305	F6	0.938
A7	1.081	B7	0.999	C7	1.133	D7	1.122	E7	1.183	F7	0.931
A8	1.038	B8	1.002	C8	1.084	D8	1.102	E8	1.125	F8	0.900
A9	1.004	B9	0.990	C9	1.039	D9	—	E9	1.097	F9	0.885
A10	1.035	B10	0.994	C10	1.040	D10	1.009	E10	1.086	F10	0.873
A11	1.008	B11	0.996	C11	1.000	D11	1.010	E11	1.012	F11	0.863
A12	0.989	—	—	C12	1.007	—	—	E12	—	F12	0.867
A13	0.991	—	—	—	—	—	—	E13	1.002	F13	0.889
A14	0.990	—	—	—	—	—	—	E14	1.001	F14	0.907
A15	0.988	—	—	—	—	—	—	—	—	F15	0.928
A16	0.994	—	—	—	—	—	—	—	—	F16	—
A17	0.998	—	—	—	—	—	—	—	—	F17	0.954
A18	1.004	—	—	—	—	—	—	—	—	—	—
A19	1.009	—	—	—	—	—	—	—	—	—	—
A20	1.013	—	—	—	—	—	—	—	—	—	—

Table A-25. Pressure data for Run 14-1 (LN₂ injection)

Run	14-1	Re/l , in. ⁻¹	0.204×10^6
M	3.99	P_j , psia	122.4
P_T , cm Hg	152.1	T_j , °F	-299
P_S , psia	0.199	P_j/P_T	4.18
T_T , °F	108.0		

Pressure Tap	$\frac{P}{P_S}$										
A1	2.377	B1	1.245	C1	2.293	D1	1.282	E1	—	F1	2.200
A2	1.211	B2	1.515	C2	1.239	D2	1.242	E2	—	F2	1.327
A3	1.493	B3	2.070	C3	1.504	D3	1.459	E3	0.989	F3	0.817
A4	2.096	B4	2.932	C4	1.918	D4	2.197	E4	1.262	F4	0.583
A5	3.020	B5	2.944	C5	2.755	D5	2.766	E5	1.504	F5	0.662
A6	2.938	B6	2.560	C6	2.760	D6	2.521	E6	1.989	F6	0.727
A7	2.614	B7	2.276	C7	2.529	D7	2.315	E7	2.453	F7	0.806
A8	2.338	B8	2.070	C8	2.284	D8	2.127	E8	2.313	F8	0.986
A9	2.127	B9	1.831	C9	2.062	D9	—	E9	2.124	F9	1.093
A10	1.983	B10	1.766	C10	1.791	D10	1.648	E10	1.851	F10	1.144
A11	1.938	B11	1.724	C11	1.699	D11	1.577	E11	1.625	F11	1.144
A12	1.842	—	—	C12	1.648	—	—	E12	—	F12	1.076
A13	1.803	—	—	—	—	—	—	E13	1.451	F13	1.028
A14	1.789	—	—	—	—	—	—	E14	1.417	F14	0.980
A15	1.763	—	—	—	—	—	—	—	—	F15	0.946
A16	1.749	—	—	—	—	—	—	—	—	F16	—
A17	1.763	—	—	—	—	—	—	—	—	F17	0.904
A18	1.735	—	—	—	—	—	—	—	—	—	—
A19	1.690	—	—	—	—	—	—	—	—	—	—
A20	1.600	—	—	—	—	—	—	—	—	—	—

Table A-26. Pressure data for Run 14-2 (LN₂ injection)

Run	14-2	Re/L , in. ⁻¹	0.209×10^6
M	3.99	P_f , psia	98.9
P_T , cm Hg	151.7	T_f , °F	-300
P_s , psia	0.190	P_f/P_T	3.38
T_T , °F	109.0		

Pressure Tap	$\frac{P}{P_s}$										
A1	1.376	B1	1.474	C1	1.485	D1	1.053	E1	—	F1	1.253
A2	1.676	B2	2.359	C2	1.224	D2	1.559	E2	—	F2	0.874
A3	2.453	B3	3.194	C3	2.159	D3	2.529	E3	1.100	F3	0.612
A4	3.244	B4	3.241	C4	2.994	D4	2.741	E4	1.779	F4	0.600
A5	3.341	B5	3.129	C5	3.053	D5	2.697	E5	2.356	F5	0.709
A6	3.206	B6	2.894	C6	2.971	D6	2.612	E6	2.326	F6	0.841
A7	2.997	B7	2.626	C7	2.826	D7	2.471	E7	2.303	F7	0.968
A8	2.712	B8	2.371	C8	2.556	D8	2.259	E8	2.259	F8	1.121
A9	2.462	B9	2.006	C9	2.276	D9	—	E9	2.173	F9	1.232
A10	2.241	B10	1.829	C10	1.871	D10	1.650	E10	1.859	F10	1.229
A11	2.150	B11	1.744	C11	1.723	D11	1.579	E11	1.635	F11	1.182
A12	1.979	—	—	C12	1.659	—	—	E12	—	F12	1.094
A13	1.926	—	—	—	—	—	—	E13	1.444	F13	1.041
A14	1.882	—	—	—	—	—	—	E14	1.406	F14	0.994
A15	1.853	—	—	—	—	—	—	—	—	F15	0.962
A16	1.835	—	—	—	—	—	—	—	—	F16	—
A17	1.832	—	—	—	—	—	—	—	—	F17	0.918
A18	1.812	—	—	—	—	—	—	—	—	—	—
A19	1.744	—	—	—	—	—	—	—	—	—	—
A20	1.650	—	—	—	—	—	—	—	—	—	—

Table A-27. Pressure data for Run 14-3 (LN₂ injection)

Run	14-3	Re/L , in. ⁻¹	0.204×10^6
M	3.99	P_j , psia	80.4
P_T , cm Hg	151.9	T_j , °F	-301
P_S , psia	0.200	P_j/P_T	2.75
T_{T_1} , °F	110.0		

Pressure Tap	$\frac{P}{P_S}$										
A1	1.345	B1	1.546	C1	1.454	D1	1.064	E1	—	F1	1.151
A2	1.717	B2	2.717	C2	1.246	D2	1.849	E2	—	F2	0.824
A3	2.807	B3	3.081	C3	2.504	D3	2.555	E3	1.252	F3	0.594
A4	3.137	B4	3.017	C4	2.877	D4	2.560	E4	2.042	F4	0.653
A5	3.104	B5	2.908	C5	2.852	D5	2.541	E5	2.261	F5	0.770
A6	2.964	B6	2.742	C6	2.807	D6	2.448	E6	2.196	F6	0.927
A7	2.711	B7	2.482	C7	2.692	D7	2.325	E7	2.196	F7	1.045
A8	2.619	B8	2.235	C8	2.504	D8	2.160	E8	2.126	F8	1.216
A9	2.510	B9	1.927	C9	2.098	D9	—	E9	2.031	F9	1.238
A10	2.126	B10	1.804	C10	1.798	D10	1.569	E10	1.804	F10	1.188
A11	1.989	B11	1.689	C11	1.686	D11	1.532	E11	1.529	F11	1.143
A12	1.880	—	—	C12	1.597	—	—	E12	—	F12	1.064
A13	1.826	—	—	—	—	—	—	E13	1.384	F13	1.017
A14	1.784	—	—	—	—	—	—	E14	1.378	F14	0.972
A15	1.720	—	—	—	—	—	—	—	—	F15	0.941
A16	1.751	—	—	—	—	—	—	—	—	F16	—
A17	1.748	—	—	—	—	—	—	—	—	F17	0.905
A18	1.720	—	—	—	—	—	—	—	—	—	—
A19	1.639	—	—	—	—	—	—	—	—	—	—
A20	1.541	—	—	—	—	—	—	—	—	—	—

Table A-28. Pressure data for Run 14-4 (LN₂ injection)

Run	14-4	Re/l , in. ⁻¹	0.204×10^6
M	3.99	P_j , psia	60.6
P_T , cm Hg	151.9	T_j , °F	-301
P_S , psia	0.198	P_j/P_T	2.07
T_T , °F	110.0		

Pressure Tap	$\frac{P}{P_S}$										
A1	1.398	B1	1.633	C1	1.545	D1	1.102	E1	—	F1	1.136
A2	1.799	B2	2.785	C2	1.319	D2	2.056	E2	—	F2	0.811
A3	2.904	B3	2.960	C3	2.618	D3	2.497	E3	1.407	F3	0.573
A4	3.025	B4	2.875	C4	2.779	D4	2.480	E4	2.118	F4	0.630
A5	2.940	B5	2.743	C5	2.751	D5	2.455	E5	2.206	F5	0.788
A6	2.791	B6	2.497	C6	2.731	D6	2.350	E6	2.155	F6	0.955
A7	2.480	B7	2.330	C7	2.463	D7	2.169	E7	2.172	F7	1.102
A8	2.424	B8	2.102	C8	2.237	D8	1.943	E8	1.994	F8	1.209
A9	2.480	B9	1.859	C9	1.977	D9	—	E9	1.909	F9	1.189
A10	2.037	B10	1.743	C10	1.706	D10	1.539	E10	1.689	F10	1.133
A11	1.960	B11	1.658	C11	1.661	D11	1.514	E11	1.472	F11	1.090
A12	1.825	—	—	C12	1.568	—	—	E12	—	F12	1.017
A13	1.791	—	—	—	—	—	—	E13	1.361	F13	0.977
A14	1.757	—	—	—	—	—	—	E14	1.356	F14	0.941
A15	1.717	—	—	—	—	—	—	—	—	F15	0.929
A16	1.706	—	—	—	—	—	—	—	—	F16	—
A17	1.709	—	—	—	—	—	—	—	—	F17	0.898
A18	1.650	—	—	—	—	—	—	—	—	—	—
A19	1.568	—	—	—	—	—	—	—	—	—	—
A20	1.458	—	—	—	—	—	—	—	—	—	—

Table A-29. Pressure data for Run 14-5 (LN₂ injection)

Run	14-5	Re/l, in.⁻¹	0.203×10^6
M	3.99	P_s, psia	50.7
P_T, cm Hg	151.8	T_s, °F	-301
P_s, psia	0.197	P_s/P_T	1.73
T_s, °F	110.0		

Pressure Tap	$\frac{P}{P_s}$										
A1	1.557	B1	1.696	C1	1.687	D1	1.159	E1	—	F1	1.205
A2	1.852	B2	2.773	C2	1.398	D2	2.128	E2	—	F2	0.835
A3	2.903	B3	2.906	C3	2.633	D3	2.454	E3	1.477	F3	0.574
A4	2.980	B4	2.812	C4	2.730	D4	2.452	E4	2.108	F4	0.625
A5	2.838	B5	2.619	C5	2.784	D5	2.415	E5	2.207	F5	0.795
A6	2.668	B6	2.358	C6	2.486	D6	2.250	E6	2.125	F6	0.983
A7	2.264	B7	2.151	C7	2.321	D7	2.048	E7	2.145	F7	1.136
A8	2.270	B8	1.980	C8	2.162	D8	1.852	E8	1.903	F8	1.185
A9	2.284	B9	1.801	C9	1.878	D9	—	E9	1.824	F9	1.162
A10	2.014	B10	1.702	C10	1.705	D10	1.509	E10	1.628	F10	1.099
A11	1.869	B11	1.636	C11	1.625	D11	1.503	E11	1.423	F11	1.062
A12	1.776	—	—	C12	1.551	—	—	E12	—	F12	1.003
A13	1.756	—	—	—	—	—	—	E13	1.347	F13	0.955
A14	1.713	—	—	—	—	—	—	E14	1.361	F14	0.926
A15	1.685	—	—	—	—	—	—	—	—	F15	0.906
A16	1.679	—	—	—	—	—	—	—	—	F16	—
A17	1.673	—	—	—	—	—	—	—	—	F17	0.875
A18	1.599	—	—	—	—	—	—	—	—	—	—
A19	1.503	—	—	—	—	—	—	—	—	—	—
A20	1.403	—	—	—	—	—	—	—	—	—	—

Table A-30. Pressure data for Run 15-1 (LN₂ injection)

Run	15-1	Re/l, in.⁻¹	0.330×10^6
M	3.99	P_j, psia	62.1
P_T, cm Hg	249.9	T_j, °F	-302
P_S, psia	0.320	P_j/P_T	1.29
T_T, °F	113.0		

Pressure Tap	$\frac{P}{P_S}$										
A1	2.958	B1	3.444	C1	2.411	D1	2.888	E1	—	F1	0.716
A2	3.520	B2	3.481	C2	3.191	D2	3.033	E2	—	F2	0.849
A3	3.457	B3	3.222	C3	3.404	D3	3.012	E3	2.572	F3	1.264
A4	3.275	B4	2.842	C4	3.243	D4	2.655	E4	2.595	F4	1.399
A5	3.005	B5	2.651	C5	2.760	D5	2.572	E5	2.464	F5	1.415
A6	2.677	B6	2.413	C6	2.656	D6	2.226	E6	2.355	F6	1.394
A7	2.392	B7	2.297	C7	2.441	D7	2.094	E7	2.184	F7	1.355
A8	2.399	B8	2.226	C8	2.173	D8	1.942	E8	1.881	F8	1.256
A9	2.324	B9	2.262	C9	2.129	D9	—	E9	1.846	F9	1.187
A10	2.303	B10	2.266	C10	2.059	D10	1.853	E10	1.685	F10	1.115
A11	2.339	B11	2.154	C11	2.098	D11	1.884	E11	1.576	F11	1.066
A12	2.331	—	—	C12	2.100	—	—	E12	—	F12	0.989
A13	2.317	—	—	—	—	—	—	E13	1.646	F13	0.938
A14	2.275	—	—	—	—	—	—	E14	1.674	F14	0.897
A15	2.206	—	—	—	—	—	—	—	—	F15	0.870
A16	1.685	—	—	—	—	—	—	—	—	F16	—
A17	1.150	—	—	—	—	—	—	—	—	F17	0.841
A18	0.932	—	—	—	—	—	—	—	—	—	—
A19	0.921	—	—	—	—	—	—	—	—	—	—
A20	0.936	—	—	—	—	—	—	—	—	—	—

Table A-31. Pressure data for Run 15-2 (LN₂ injection)

Run	15-2	Re/l , in. ⁻¹	0.330×10^6
M	3.99	P_j , psia	80.2
P_T , cm Hg	250.2	T_j , °F	-302
P_S , psia	0.324	P_j/P_T	1.66
T_T , °F	114.0		

Pressure Tap	$\frac{P}{P_S}$										
A1	2.802	B1	3.292	C1	2.370	D1	2.674	E1	—	F1	0.702
A2	3.456	B2	3.479	C2	3.301	D2	2.968	E2	—	F2	0.811
A3	3.522	B3	3.297	C3	3.486	D3	3.000	E3	2.513	F3	1.244
A4	3.306	B4	2.859	C4	3.294	D4	2.948	E4	2.669	F4	1.398
A5	3.115	B5	2.792	C5	2.825	D5	2.721	E5	2.548	F5	1.444
A6	2.816	B6	2.382	C6	2.479	D6	2.282	E6	2.491	F6	1.424
A7	2.472	B7	2.223	C7	2.545	D7	2.138	E7	2.351	F7	1.394
A8	2.346	B8	2.180	C8	2.174	D8	1.886	E8	1.946	F8	1.303
A9	2.276	B9	2.206	C9	2.107	D9	—	E9	1.991	F9	1.233
A10	2.276	B10	2.230	C10	2.003	D10	1.809	E10	1.588	F10	1.152
A11	2.318	B11	2.155	C11	2.062	D11	1.847	E11	1.545	F11	1.105
A12	2.309	—	—	C12	2.090	—	—	E12	—	F12	1.021
A13	2.297	—	—	—	—	—	—	E13	1.612	F13	0.960
A14	2.259	—	—	—	—	—	—	E14	1.657	F14	0.915
A15	2.192	—	—	—	—	—	—	—	—	F15	0.891
A16	1.723	—	—	—	—	—	—	—	—	F16	—
A17	1.199	—	—	—	—	—	—	—	—	F17	0.849
A18	0.953	—	—	—	—	—	—	—	—	—	—
A19	0.924	—	—	—	—	—	—	—	—	—	—
A20	0.936	—	—	—	—	—	—	—	—	—	—

Table A-32. Pressure data for Run 15-3 (LN₂ injection)

Run	15-3	Re/l , in. ⁻¹	0.331×10^6
<i>M</i>	3.99	<i>P_j</i> , psia	99.7
<i>P_T</i> , cm Hg	250.6	<i>T_j</i> , °F	-302
<i>P_S</i> , psia	0.324	<i>P_j/P_T</i>	2.07
<i>T_T</i> , °F	114.0		

Pressure Tap	$\frac{P}{P_S}$										
A1	2.647	B1	3.195	C1	2.242	D1	2.498	E1	—	F1	0.692
A2	3.280	B2	3.474	C2	2.918	D2	2.917	E2	—	F2	0.744
A3	3.498	B3	3.356	C3	3.326	D3	3.067	E3	2.456	F3	1.112
A4	3.422	B4	3.140	C4	3.304	D4	3.017	E4	2.669	F4	1.334
A5	3.153	B5	2.937	C5	3.032	D5	2.806	E5	2.641	F5	1.408
A6	2.891	B6	2.475	C6	2.680	D6	2.496	E6	2.576	F6	1.441
A7	2.552	B7	2.245	C7	2.479	D7	2.143	E7	2.484	F7	1.424
A8	2.360	B8	2.238	C8	2.193	D8	1.870	E8	2.055	F8	1.337
A9	2.238	B9	2.190	C9	2.020	D9	—	E9	1.972	F9	1.275
A10	2.240	B10	2.221	C10	1.960	D10	1.785	E10	1.598	F10	1.190
A11	2.283	B11	2.178	C11	2.027	D11	1.825	E11	1.540	F11	1.145
A12	2.297	—	—	C12	2.074	—	—	E12	—	F12	1.055
A13	2.302	—	—	—	—	—	—	E13	1.609	F13	0.989
A14	2.283	—	—	—	—	—	—	E14	1.655	F14	0.941
A15	2.247	—	—	—	—	—	—	—	—	F15	0.908
A16	1.873	—	—	—	—	—	—	—	—	F16	—
A17	1.341	—	—	—	—	—	—	—	—	F17	0.863
A18	0.993	—	—	—	—	—	—	—	—	—	—
A19	0.929	—	—	—	—	—	—	—	—	—	—
A20	0.939	—	—	—	—	—	—	—	—	—	—

Table A-33. Pressure data for Run 15-4 (LN₂ injection)

Run	15-4	Re/l , in. ⁻¹	0.328×10^6
M	3.99	P_j , psia	119.2
P_T , cm Hg	250.4	T_j , °F	-301
P_s , psia	0.325	P_j/P_T	2.47
T_T , °F	117.0		

Pressure Tap	$\frac{P}{P_s}$										
A1	2.536	B1	2.923	C1	2.181	D1	2.229	E1	—	F1	0.679
A2	2.948	B2	3.374	C2	2.555	D2	2.726	E2	—	F2	0.645
A3	3.355	B3	3.433	C3	3.131	D3	3.029	E3	2.229	F3	0.983
A4	3.405	B4	3.231	C4	3.286	D4	3.078	E4	2.531	F4	1.210
A5	3.238	B5	2.900	C5	3.169	D5	2.829	E5	2.598	F5	1.348
A6	2.926	B6	2.566	C6	2.742	D6	2.552	E6	2.604	F6	1.409
A7	2.666	B7	2.278	C7	2.407	D7	2.424	E7	2.286	F7	1.404
A8	2.319	B8	2.205	C8	2.252	D8	1.931	E8	2.126	F8	1.338
A9	2.323	B9	2.100	C9	2.069	D9	—	E9	2.093	F9	1.286
A10	2.190	B10	2.148	C10	1.879	D10	1.724	E10	1.664	F10	1.202
A11	2.216	B11	2.142	C11	1.941	D11	1.785	E11	1.512	F11	1.155
A12	2.210	—	—	C12	1.998	—	—	E12	—	F12	1.066
A13	2.242	—	—	—	—	—	—	E13	1.583	F13	1.004
A14	2.250	—	—	—	—	—	—	E14	1.604	F14	0.948
A15	2.247	—	—	—	—	—	—	—	—	F15	0.917
A16	2.017	—	—	—	—	—	—	—	—	F16	—
A17	1.519	—	—	—	—	—	—	—	—	F17	0.869
A18	1.062	—	—	—	—	—	—	—	—	—	—
A19	0.941	—	—	—	—	—	—	—	—	—	—
A20	0.922	—	—	—	—	—	—	—	—	—	—

Table A-34. Pressure data for Run 15-5 (LN₂ injection)

Run	15-5	$Re/L, \text{in.}^{-1}$	0.328×10^6
M	3.99	P_j, psia	50.2
$P_T, \text{cm Hg}$	250.3	$T_j, ^\circ\text{F}$	-300
P_s, psia	0.324	P_j/P_T	1.04
$T_T, ^\circ\text{F}$	117.0		

Pressure Tap	$\frac{P}{P_s}$										
A1	2.744	B1	3.325	C1	2.275	D1	2.667	E1	—	F1	0.739
A2	3.345	B2	3.193	C2	3.028	D2	2.858	E2	—	F2	0.801
A3	3.281	B3	3.152	C3	3.041	D3	2.863	E3	2.515	F3	1.243
A4	2.991	B4	2.755	C4	3.010	D4	2.584	E4	2.497	F4	1.347
A5	2.915	B5	2.423	C5	2.627	D5	2.409	E5	2.342	F5	1.349
A6	2.575	B6	2.313	C6	2.437	D6	2.081	E6	2.257	F6	1.316
A7	2.368	B7	2.221	C7	2.193	D7	2.074	E7	2.029	F7	1.287
A8	2.299	B8	2.212	C8	2.114	D8	1.853	E8	1.729	F8	1.188
A9	2.287	B9	2.276	C9	2.062	D9	—	E9	1.819	F9	1.124
A10	2.328	B10	2.224	C10	2.012	D10	1.836	E10	1.546	F10	1.055
A11	2.395	B11	2.095	C11	2.102	D11	1.917	E11	1.535	F11	1.014
A12	2.373	—	—	C12	2.107	—	—	E12	—	F12	0.952
A13	2.340	—	—	—	—	—	—	E13	1.649	F13	0.905
A14	2.262	—	—	—	—	—	—	E14	1.670	F14	0.855
A15	2.095	—	—	—	—	—	—	—	—	F15	0.853
A16	1.496	—	—	—	—	—	—	—	—	F16	—
A17	1.048	—	—	—	—	—	—	—	—	F17	0.829
A18	0.921	—	—	—	—	—	—	—	—	—	—
A19	0.921	—	—	—	—	—	—	—	—	—	—
A20	0.927	—	—	—	—	—	—	—	—	—	—

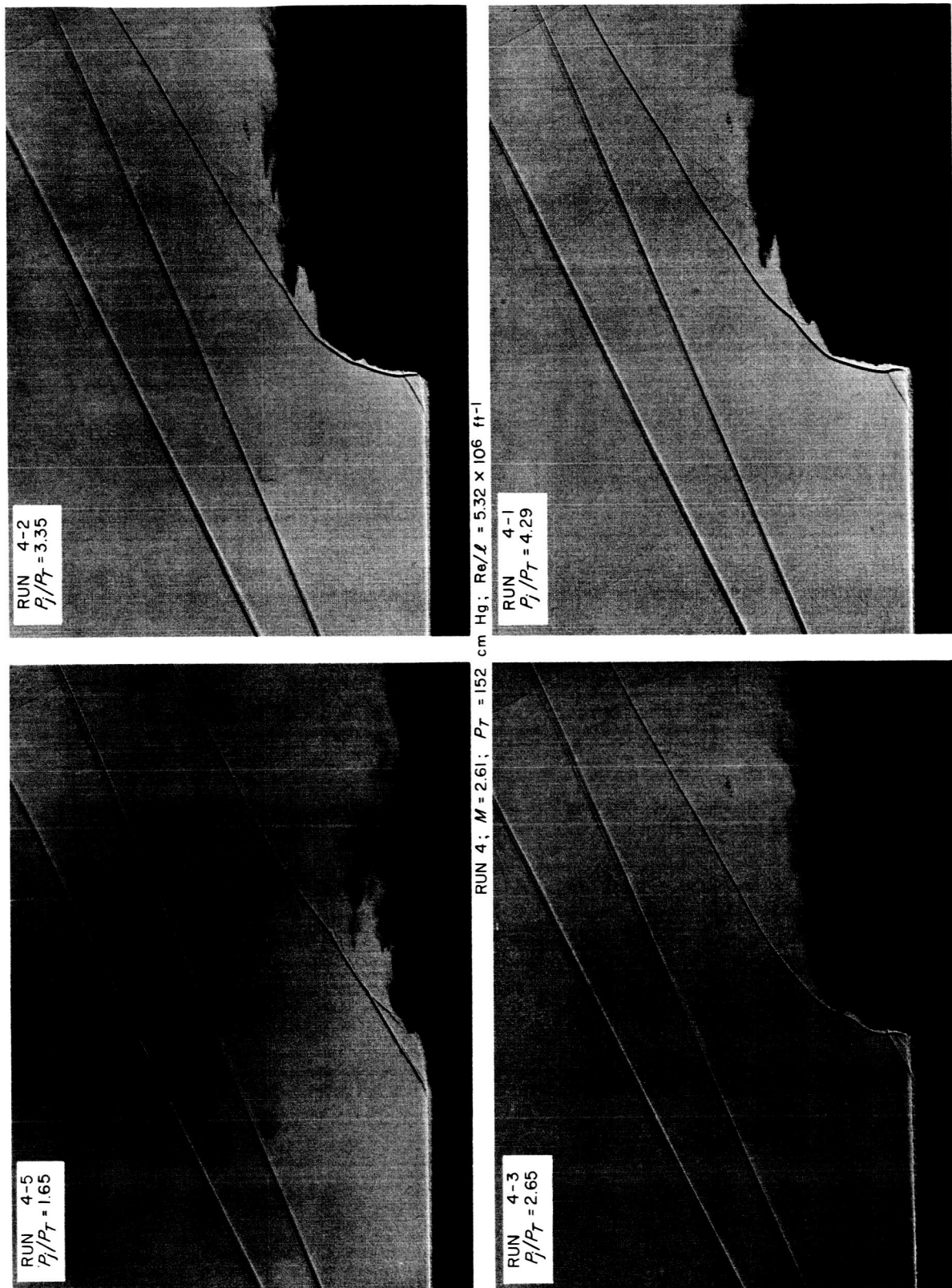


Fig. A-1. Comparison of shadowgraphs for Run 4 (LN_2 injection)

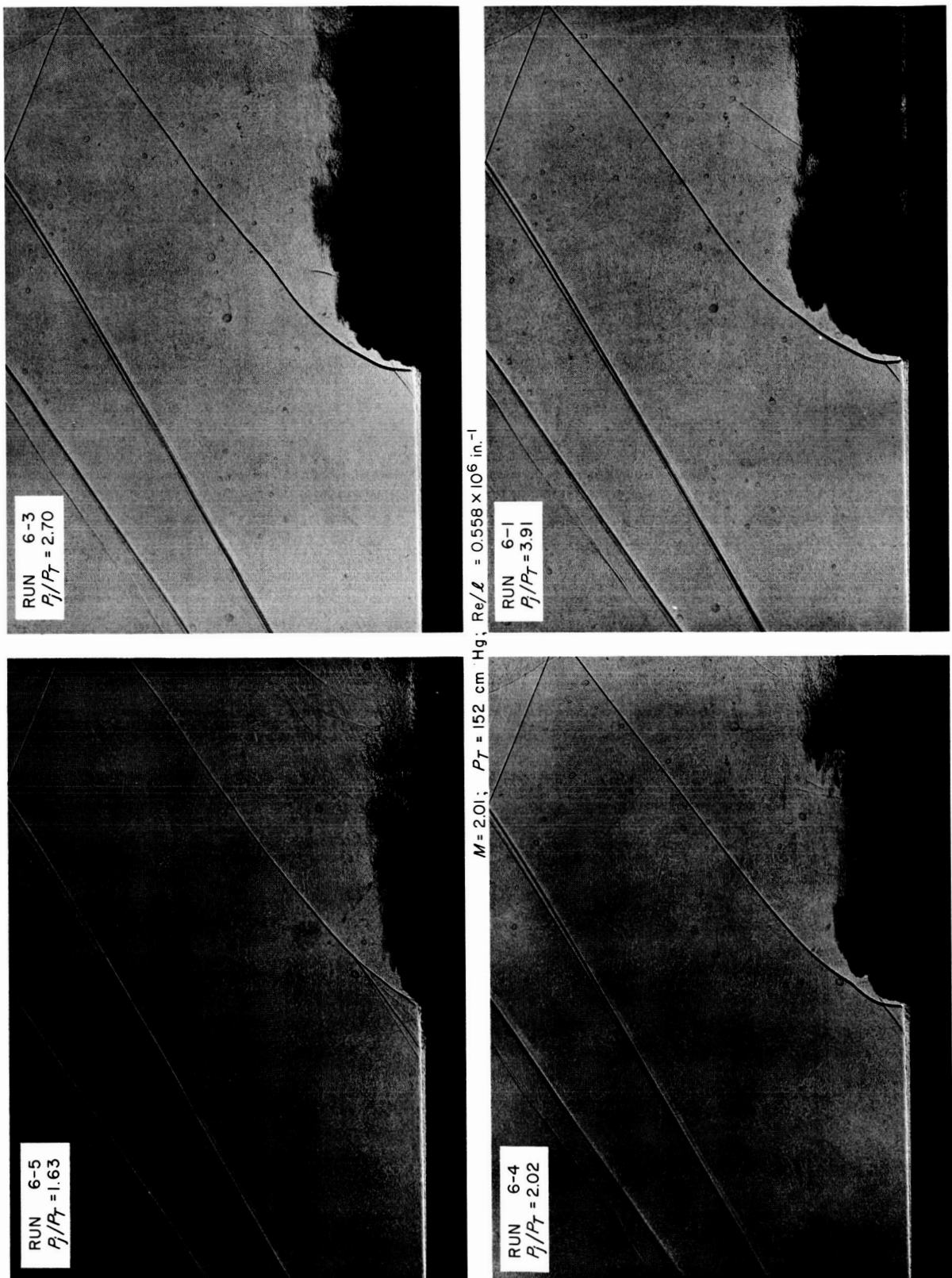


Fig. A-2. Comparison of shadowgraphs for Run 6 (LN_2 injection)

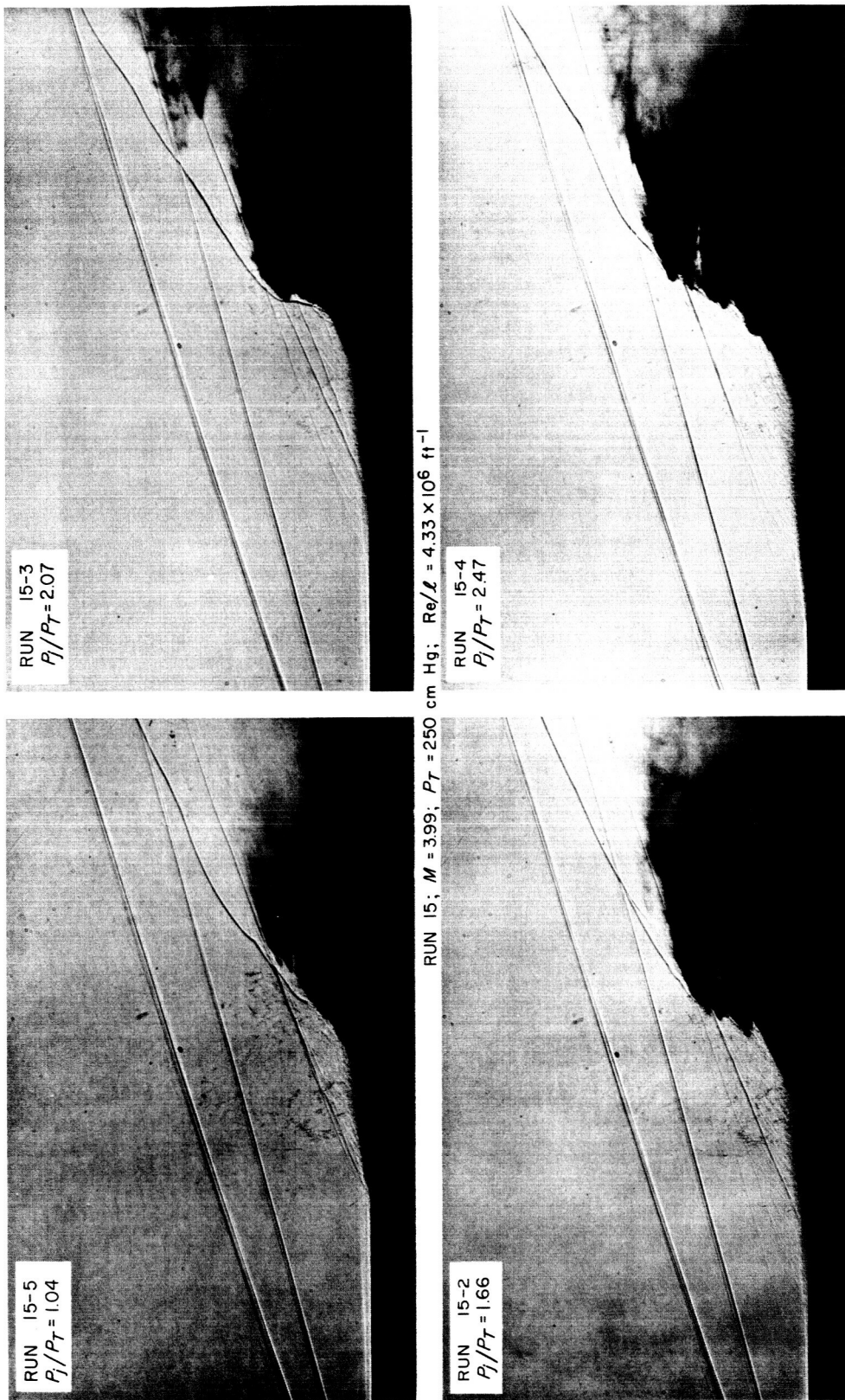


Fig. A-3. Comparison of shadowgraphs for Run 15 (LN_2 injection)

APPENDIX B
Gaseous Nitrogen Data

Table B-1. Gaseous nitrogen injection

Run	M	P _T , cm Hg	P _S , psia	T _T , °F	P _j , psia	T _j , °F	($\frac{P_j}{P_T}$)	Re/l × 10 ⁻⁴ , in. ⁻¹	Separation distance, in.	w _c , lb/min
19-1	4.54	280.1	0.170	111.5	27.0	76	0.50	0.286	2.40	0.268
19-2	4.54	280.1	0.169	111.5	53.7	76	0.99	0.286	3.25	0.538
19-3	4.54	280.2	0.169	112.0	161.9	78	3.00	0.284	4.40	1.65
19-4	4.54	280.0	0.169	112.0	301.0	78	5.58	0.284	5.20	3.11
24-1	3.50	77.2	0.195	91.5	7.2	72	0.48	0.140	1.75	—
24-3	3.50	77.7	0.195	92.0	14.8	72	0.99	0.141	2.10	—
24-4	3.50	77.7	0.195	92.0	45.4	74	3.03	0.141	2.85	0.454
24-5	3.50	77.7	0.194	92.0	119.5	74	7.99	0.141	3.50	1.21
24-6	3.50	77.6	0.195	92.0	164.9	74	11.0	0.140	3.80	1.69
24-7	3.50	77.6	0.194	92.0	301.3	75	20.2	0.140	4.50	3.12
26-1	2.61	100.2	0.969	101.0	9.3	73	0.48	0.287	0.375	—
26-2	2.61	100.3	0.973	102.0	18.8	74	0.97	0.287	0.40	—
26-3	2.61	100.1	0.973	103.0	57.3	74	2.97	0.285	0.55	0.576
26-4	2.61	100.5	0.978	104.0	156.2	74	8.07	0.285	0.75	1.60
26-5	2.61	100.7	0.978	104.0	212.0	74	10.9	0.286	0.75	2.19
26-6	2.61	100.7	0.976	105.0	300.1	74	15.5	0.286	0.90	3.11
28-1	2.61	35.4	0.351	85.0	3.5	71	0.51	0.105	1.25	—
28-2	2.61	35.4	0.351	84.0	6.4	71	0.93	0.106	1.40	—
28-4	2.61	35.4	0.351	82.5	20.8	72	3.05	0.106	2.00	—
28-5	2.61	35.4	0.351	82.5	54.1	72	7.95	0.106	2.40	—
28-6	2.61	35.5	0.353	82.0	108.4	73	15.9	0.107	2.95	1.10
28-7	2.61	35.5	0.351	82.0	216.7	73	31.7	0.107	3.50	2.25
28-8	2.61	35.2	0.351	81.5	296.0	73	43.7	0.109	3.85	3.09
30-1	2.01	110.3	2.717	96.0	12.7	73	0.60	0.428	0.375	—
30-2	2.01	110.7	2.727	97.0	25.3	74	1.19	0.428	0.40	0.25
30-4	2.01	110.5	2.720	97.5	72.4	74	3.40	0.427	0.50	0.73
30-5	2.01	110.5	2.722	98.0	205.6	74	9.66	0.427	0.70	2.10
30-6	2.01	110.6	2.723	98.0	296.1	74	13.9	0.427	0.80	3.09
32-1	2.01	35.5	0.897	81.5	3.2	70	0.46	0.143	0.42	—
32-2	2.01	35.8	0.906	81.0	6.2	71	0.90	0.144	0.42	—
32-3	2.01	35.6	0.902	80.0	19.8	72	2.89	0.143	0.55	0.195
32-4	2.01	35.0	0.890	77.0	53.7	73	7.97	0.142	0.65	0.537
32-5	2.01	35.2	0.892	77.0	107.5	73	15.9	0.143	0.90	1.09
32-6	2.01	35.6	0.902	77.0	217.5	73	31.7	0.145	1.05	2.25
32-7	2.01	34.7	0.879	77.0	256.4	73	38.4	0.141	1.20	2.65

Table B-2. Pressure data for Run 19-1 (GN₂ injection)

Run	19-1	Re/L , in. ⁻¹	0.286×10^6
<i>M</i>	4.54	P_j , psia	27.0
P_T , cm Hg	280.1	T_j , °F	76
P_S , psia	0.170	P_j/P_T	0.50
T_T , °F	111.5		

Pressure Tap	$\frac{P}{P_S}$										
A1	2.379	B1	1.211	C1	2.336	D1	1.518	E1	—	F1	0.482
A2	1.297	B2	1.178	C2	1.267	D2	0.983	E2	—	F2	0.521
A3	1.214	B3	1.247	C3	1.092	D3	1.089	E3	0.921	F3	0.554
A4	1.287	B4	1.257	C4	1.195	D4	1.168	E4	0.950	F4	0.640
A5	1.300	B5	1.257	C5	1.214	D5	1.158	E5	1.046	F5	0.716
A6	1.280	B6	1.254	C6	1.221	D6	1.168	E6	1.099	F6	0.776
A7	1.294	B7	1.254	C7	1.231	D7	1.175	E7	1.109	F7	0.785
A8	1.287	B8	1.261	C8	1.224	D8	1.188	E8	1.109	F8	0.822
A9	1.284	B9	1.231	C9	1.228	D9	—	E9	1.122	F9	0.858
A10	1.277	B10	1.195	C10	1.218	D10	1.162	E10	1.142	F10	0.861
A11	1.271	B11	1.152	C11	1.188	D11	1.135	E11	1.125	F11	0.871
A12	1.247	—	—	C12	1.148	—	—	E12	—	F12	0.891
A13	1.182	—	—	—	—	—	—	E13	1.079	F13	0.891
A14	1.198	—	—	—	—	—	—	E14	1.073	F14	0.908
A15	1.165	—	—	—	—	—	—	—	—	F15	0.917
A16	1.000	—	—	—	—	—	—	—	—	F16	—
A17	1.026	—	—	—	—	—	—	—	—	F17	0.947
A18	1.033	—	—	—	—	—	—	—	—	—	—
A19	1.043	—	—	—	—	—	—	—	—	—	—
A20	1.063	—	—	—	—	—	—	—	—	—	—

Table B-3. Pressure data for Run 19-2 (GN₂ injection)

Run	19-2	Re/l, in.⁻¹	0.286×10^6
M	4.54	P_j, psia	53.7
P_T, cm Hg	280.1	T_j, °F	76
P_S, psia	0.169	P_j/P_T	0.99
T_T, °F	111.5		

Pressure Tap	$\frac{P}{P_S}$										
A1	2.904	B1	2.063	C1	2.977	D1	2.545	E1	—	F1	0.452
A2	2.253	B2	1.179	C2	2.286	D2	1.372	E2	—	F2	0.455
A3	1.292	B3	1.196	C3	1.196	D3	0.983	E3	1.900	F3	0.492
A4	1.216	B4	1.263	C4	1.110	D4	1.070	E4	0.957	F4	0.542
A5	1.282	B5	1.296	C5	1.199	D5	1.153	E5	0.940	F5	0.581
A6	1.322	B6	1.289	C6	1.249	D6	1.196	E6	1.000	F6	0.658
A7	1.319	B7	1.296	C7	1.263	D7	1.203	E7	1.073	F7	0.701
A8	1.316	B8	1.289	C8	1.246	D8	1.213	E8	1.120	F8	0.804
A9	1.316	B9	1.289	C9	1.253	D9	—	E9	1.140	F9	0.831
A10	1.319	B10	1.286	C10	1.259	D10	1.216	E10	1.173	F10	0.851
A11	1.329	B11	1.266	C11	1.259	D11	1.199	E11	1.183	F11	0.874
A12	1.302	—	—	C12	1.243	—	—	E12	—	F12	0.880
A13	1.312	—	—	—	—	—	—	E13	1.123	F13	0.894
A14	1.309	—	—	—	—	—	—	E14	1.113	F14	0.884
A15	1.289	—	—	—	—	—	—	—	—	F15	0.914
A16	1.206	—	—	—	—	—	—	—	—	F16	—
A17	1.070	—	—	—	—	—	—	—	—	F17	0.924
A18	1.030	—	—	—	—	—	—	—	—	—	—
A19	1.043	—	—	—	—	—	—	—	—	—	—
A20	1.070	—	—	—	—	—	—	—	—	—	—

Table B-4. Pressure data for Run 19-3 (GN₂ injection)

Run	19-3	Re/L , in. ⁻¹	0.284×10^6
M	4.54	P_j , psia	161.9
P_T , cm Hg	280.2	T_j , °F	78
P_s , psia	0.169	P_j/P_T	3.00
T_T , °F	112.0		

Pressure Tap	$\frac{P}{P_s}$										
A1	3.605	B1	3.366	C1	2.980	D1	3.173	E1	—	F1	0.395
A2	3.303	B2	2.944	C2	3.515	D2	2.947	E2	—	F2	0.415
A3	2.957	B3	1.920	C3	2.897	D3	2.518	E3	2.871	F3	0.425
A4	2.176	B4	1.253	C4	2.166	D4	1.465	E4	2.874	F4	0.449
A5	1.399	B5	1.196	C5	1.269	D5	1.037	E5	2.176	F5	0.482
A6	1.236	B6	1.249	C6	1.120	D6	1.050	E6	1.209	F6	0.502
A7	1.269	B7	1.292	C7	1.183	D7	1.110	E7	0.924	F7	0.502
A8	1.312	B8	1.329	C8	1.223	D8	1.179	E8	0.967	F8	0.552
A9	1.346	B9	1.349	C9	1.236	D9	—	E9	1.037	F9	0.601
A10	1.372	B10	1.349	C10	1.319	D10	1.316	E10	1.133	F10	0.704
A11	1.392	B11	1.352	C11	1.329	D11	1.296	E11	1.243	F11	0.784
A12	1.382	—	—	C12	1.316	—	—	E12	—	F12	0.867
A13	1.376	—	—	—	—	—	—	E13	1.256	F13	0.904
A14	1.379	—	—	—	—	—	—	E14	1.186	F14	0.904
A15	1.376	—	—	—	—	—	—	—	—	F15	0.924
A16	1.372	—	—	—	—	—	—	—	—	F16	—
A17	1.356	—	—	—	—	—	—	—	—	F17	0.934
A18	1.279	—	—	—	—	—	—	—	—	—	—
A19	1.126	—	—	—	—	—	—	—	—	—	—
A20	1.070	—	—	—	—	—	—	—	—	—	—

Table B-5. Pressure data for Run 19-4 (GN₂ injection)

Run	19-4	Re/l, in.⁻¹	0.284 × 10⁶
M	4.54	P_j, psia	301.0
P_T, cm Hg	280.0	T_j, °F	78
P_S, psia	0.169	P_j/P_T	5.58
T_T, °F	112.0		

Pressure Tap	$\frac{P}{P_S}$										
A1	3.608	B1	4.980	C1	2.884	D1	3.067	E1	—	F1	0.369
A2	4.917	B2	3.864	C2	4.764	D2	3.990	E2	—	F2	0.389
A3	3.831	B3	3.153	C3	4.113	D3	3.515	E3	2.718	F3	0.389
A4	3.166	B4	2.113	C4	3.200	D4	2.934	E4	3.515	F4	0.425
A5	2.332	B5	1.432	C5	2.369	D5	1.877	E5	3.535	F5	0.422
A6	1.545	B6	1.243	C6	1.482	D6	1.206	E6	2.884	F6	0.445
A7	1.309	B7	1.263	C7	1.209	D7	1.093	E7	1.887	F7	0.439
A8	1.299	B8	1.299	C8	1.193	D8	1.143	E8	1.196	F8	0.472
A9	1.332	B9	1.356	C9	1.243	D9	—	E9	1.010	F9	0.478
A10	1.356	B10	1.392	C10	1.316	D10	1.342	E10	1.103	F10	0.522
A11	1.392	B11	1.399	C11	1.376	D11	1.382	E11	1.193	F11	0.558
A12	1.399	—	—	C12	1.392	—	—	E12	—	F12	0.694
A13	1.405	—	—	—	—	—	—	E13	1.349	F13	0.857
A14	1.422	—	—	—	—	—	—	E14	1.276	F14	0.917
A15	1.419	—	—	—	—	—	—	—	—	F15	0.924
A16	1.412	—	—	—	—	—	—	—	—	F16	—
A17	1.419	—	—	—	—	—	—	—	—	F17	0.937
A18	1.402	—	—	—	—	—	—	—	—	—	—
A19	1.342	—	—	—	—	—	—	—	—	—	—
A20	1.206	—	—	—	—	—	—	—	—	—	—

Table B-6. Pressure data for Run 24-1 (GN₂ injection)

Run	24-1	Re/l, in.⁻¹	0.140×10^6
M	3.50	P_J, psia	7.2
P_T, cm Hg	77.2	T_J, °F	72
P_S, psia	0.195	P_J/P_T	0.48
T_T, °F	91.5		

Pressure Tap	$\frac{P}{P_S}$										
A1	1.417	B1	1.195	C1	1.434	D1	1.086	E1	—	F1	0.474
A2	1.213	B2	1.192	C2	1.161	D2	1.126	E2	—	F2	0.569
A3	1.227	B3	1.190	C3	1.187	D3	1.146	E3	1.078	F3	0.684
A4	1.215	B4	1.175	C4	1.175	D4	1.141	E4	1.109	F4	0.733
A5	1.190	B5	1.161	C5	1.158	D5	1.129	E5	1.115	F5	0.764
A6	1.178	B6	1.126	C6	1.144	D6	1.121	E6	1.109	F6	0.790
A7	1.149	B7	1.106	C7	1.152	D7	1.109	E7	1.103	F7	0.828
A8	1.126	B8	1.086	C8	1.112	D8	1.092	E8	1.092	F8	0.885
A9	1.098	B9	1.046	C9	1.098	D9	—	E9	1.086	F9	0.928
A10	1.080	B10	1.020	C10	1.057	D10	1.055	E10	1.078	F10	0.957
A11	1.072	B11	1.020	C11	1.046	D11	1.040	E11	1.049	F11	0.983
A12	1.040	—	—	C12	1.029	—	—	E12	—	F12	1.006
A13	1.040	—	—	—	—	—	—	E13	1.029	F13	1.020
A14	1.043	—	—	—	—	—	—	E14	1.009	F14	1.026
A15	1.020	—	—	—	—	—	—	—	—	F15	1.029
A16	1.029	—	—	—	—	—	—	—	—	F16	—
A17	1.011	—	—	—	—	—	—	—	—	F17	1.020
A18	1.011	—	—	—	—	—	—	—	—	—	—
A19	1.014	—	—	—	—	—	—	—	—	—	—
A20	1.023	—	—	—	—	—	—	—	—	—	—

Table B-7. Pressure data for Run 24-3 (GN₂ injection)

Run	24.3	Re/l, in.⁻¹	0.141×10^6
M	3.50	P_f, psia	14.8
P_T, cm Hg	77.7	T_f, °F	72
P_B, psia	0.195	P_f/P_T	0.99
T_T, °F	92.0		

Pressure Tap	$\frac{P}{P_B}$										
A1	1.358	B1	1.204	C1	1.375	D1	1.120	E1	—	F1	0.410
A2	1.224	B2	1.198	C2	1.172	D2	1.097	E2	—	F2	0.430
A3	1.235	B3	1.209	C3	1.172	D3	1.138	E3	0.994	F3	0.496
A4	1.232	B4	1.224	C4	1.189	D4	1.149	E4	1.075	F4	0.590
A5	1.232	B5	1.212	C5	1.195	D5	1.158	E5	1.106	F5	0.682
A6	1.232	B6	1.212	C6	1.206	D6	1.163	E6	1.135	F6	0.719
A7	1.226	B7	1.186	C7	1.198	D7	1.149	E7	1.120	F7	0.785
A8	1.204	B8	1.166	C8	1.175	D8	1.149	E8	1.120	F8	0.842
A9	1.183	B9	1.120	C9	1.158	D9	—	E9	1.126	F9	0.871
A10	1.175	B10	1.072	C10	1.123	D10	1.112	E10	1.100	F10	0.900
A11	1.143	B11	1.043	C11	1.092	D11	1.072	E11	1.086	F11	0.923
A12	1.103	—	—	C12	1.046	—	—	E12	—	F12	0.951
A13	1.086	—	—	—	—	—	—	E13	1.057	F13	0.983
A14	1.057	—	—	—	—	—	—	E14	1.037	F14	1.000
A15	1.046	—	—	—	—	—	—	—	—	F15	1.014
A16	1.014	—	—	—	—	—	—	—	—	F16	—
A17	1.014	—	—	—	—	—	—	—	—	F17	1.020
A18	1.012	—	—	—	—	—	—	—	—	—	—
A19	1.012	—	—	—	—	—	—	—	—	—	—
A20	1.029	—	—	—	—	—	—	—	—	—	—

Table B-8. Pressure data for Run 24-4 (GN₂ injection)

Run	24-4	Re/L, in.⁻¹	0.141 × 10⁶
M	3.50	P_j, psia	45.4
P_T, cm Hg	77.7	T_j, °F	74
P_S, psia	0.195	P_j/P_T	3.03
T_T, °F	92.0		

Pressure Tap	$\frac{P}{P_S}$										
A1	2.517	B1	1.282	C1	2.810	D1	1.701	E1	—	F1	0.411
A2	1.437	B2	1.126	C2	1.394	D2	0.986	E2	—	F2	0.428
A3	1.172	B3	1.224	C3	1.080	D3	1.063	E3	1.080	F3	0.440
A4	1.238	B4	1.241	C4	1.169	D4	1.144	E4	0.942	F4	0.465
A5	1.261	B5	1.244	C5	1.300	D5	1.175	E5	1.023	F5	0.477
A6	1.253	B6	1.236	C6	1.207	D6	1.172	E6	1.098	F6	0.511
A7	1.267	B7	1.244	C7	1.221	D7	1.175	E7	1.129	F7	0.557
A8	1.259	B8	1.238	C8	1.213	D8	1.184	E8	1.126	F8	0.721
A9	1.238	B9	1.224	C9	1.215	D9	—	E9	1.129	F9	0.810
A10	1.259	B10	1.207	C10	1.213	D10	1.141	E10	1.146	F10	0.842
A11	1.259	B11	1.172	C11	1.198	D11	1.161	E11	1.144	F11	0.862
A12	1.238	—	—	C12	1.167	—	—	E12	—	F12	0.876
A13	1.224	—	—	—	—	—	—	E13	1.051	F13	0.917
A14	1.213	—	—	—	—	—	—	E14	1.098	F14	0.937
A15	1.187	—	—	—	—	—	—	—	—	F15	0.960
A16	1.072	—	—	—	—	—	—	—	—	F16	—
A17	1.029	—	—	—	—	—	—	—	—	F17	0.968
A18	1.011	—	—	—	—	—	—	—	—	—	—
A19	1.009	—	—	—	—	—	—	—	—	—	—
A20	1.026	—	—	—	—	—	—	—	—	—	—

Table B-9. Pressure data for Run 24-5 (GN₂ injection)

Run	24-5	Re/l , in. ⁻¹	0.141×10^6
<i>M</i>	3.50	P_j , psia	119.5
P_T , cm Hg	77.7	T_j , °F	74
P_s , psia	0.194	P_j/P_T	7.99
T_T , °F	92.0		

Pressure Tap	$\frac{P}{P_s}$										
A1	5.916	B1	2.058	C1	5.781	D1	4.487	E1	—	F1	0.349
A2	2.095	B2	1.035	C2	3.066	D2	1.375	E2	—	F2	0.363
A3	1.107	B3	1.124	C3	0.988	D3	0.922	E3	3.326	F3	0.374
A4	1.148	B4	1.207	C4	1.032	D4	1.014	E4	1.326	F4	0.395
A5	1.230	B5	1.259	C5	1.135	D5	1.107	E5	0.914	F5	0.422
A6	1.271	B6	1.265	C6	1.213	D6	1.170	E6	0.948	F6	0.438
A7	1.287	B7	1.262	C7	1.242	D7	1.199	E7	1.020	F7	0.441
A8	1.285	B8	1.259	C8	1.225	D8	1.205	E8	1.095	F8	0.498
A9	1.280	B9	1.265	C9	1.236	D9	—	E9	1.150	F9	0.533
A10	1.280	B10	1.259	C10	1.242	D10	1.202	E10	1.158	F10	0.594
A11	1.287	B11	1.265	C11	1.245	D11	1.210	E11	1.161	F11	0.702
A12	1.289	—	—	C12	1.239	—	—	E12	—	F12	0.884
A13	1.280	—	—	—	—	—	—	E13	1.156	F13	0.922
A14	1.280	—	—	—	—	—	—	E14	1.135	F14	0.928
A15	1.270	—	—	—	—	—	—	—	—	F15	0.907
A16	1.230	—	—	—	—	—	—	—	—	F16	—
A17	1.119	—	—	—	—	—	—	—	—	F17	0.955
A18	1.020	—	—	—	—	—	—	—	—	—	—
A19	1.027	—	—	—	—	—	—	—	—	—	—
A20	1.027	—	—	—	—	—	—	—	—	—	—

Table B-10. Pressure data for Run 24-6 (GN₂ injection)

Run	24-6	Re/l , in. ⁻¹	0.140×10^6
M	3.50	P_j , psia	164.9
P_T , cm Hg	77.6	T_j , °F	74
P_s , psia	0.195	P_j/P_T	11.0
T_T , °F	92.0		

Pressure Tap	$\frac{P}{P_s}$										
A1	6.287	B1	3.537	C1	5.235	D1	5.580	E1	—	F1	0.328
A2	3.545	B2	1.066	C2	5.166	D2	2.557	E2	—	F2	0.345
A3	1.113	B3	1.060	C3	1.359	D3	0.914	E3	4.583	F3	0.351
A4	1.102	B4	1.149	C4	0.957	D4	0.951	E4	2.457	F4	0.377
A5	1.164	B5	1.221	C5	1.063	D5	1.040	E5	1.072	F5	0.379
A6	1.241	B6	1.261	C6	1.155	D6	1.109	E6	0.896	F6	0.408
A7	1.283	B7	1.276	C7	1.227	D7	1.169	E7	0.954	F7	0.405
A8	1.292	B8	1.282	C8	1.247	D8	1.210	E8	1.017	F8	0.434
A9	1.290	B9	1.270	C9	1.244	D9	—	E9	1.086	F9	0.448
A10	1.290	B10	1.276	C10	1.247	D10	1.210	E10	1.190	F10	0.484
A11	1.300	B11	1.279	C11	1.253	D11	1.218	E11	1.175	F11	0.529
A12	1.289	—	—	C12	1.244	—	—	E12	—	F12	0.726
A13	1.292	—	—	—	—	—	—	E13	1.169	F13	0.920
A14	1.289	—	—	—	—	—	—	E14	1.141	F14	0.942
A15	1.320	—	—	—	—	—	—	—	—	F15	0.962
A16	1.270	—	—	—	—	—	—	—	—	F16	—
A17	1.198	—	—	—	—	—	—	—	—	F17	0.922
A18	1.079	—	—	—	—	—	—	—	—	—	—
A19	1.020	—	—	—	—	—	—	—	—	—	—
A20	1.030	—	—	—	—	—	—	—	—	—	—

Table B-11. Pressure data for Run 24-7 (GN₂ injection)

Run	24-7	Re/l, in.⁻¹	0.140 × 10⁶
M	3.50	P_j, psia	301.3
P_T, cm Hg	77.6	T_j, °F	75
P_S, psia	0.194	P_j/P_T	20.2
T_T, °F	92.0		

Pressure Tap	$\frac{P}{P_S}$										
A1	5.055	B1	7.127	C1	3.853	D1	4.640	E1	—	F1	0.294
A2	7.400	B2	3.130	C2	7.519	D2	6.034	E2	—	F2	0.314
A3	3.017	B3	1.060	C3	4.775	D3	2.986	E3	3.873	F3	0.317
A4	1.100	B4	1.040	C4	1.458	D4	1.173	E4	5.063	F4	0.334
A5	1.109	B5	1.115	C5	0.931	D5	0.931	E5	3.640	F5	0.340
A6	1.148	B6	1.179	C6	1.075	D6	1.020	E6	1.769	F6	0.354
A7	1.188	B7	1.233	C7	1.133	D7	1.075	E7	1.014	F7	0.354
A8	1.252	B8	1.268	C8	1.173	D8	1.138	E8	0.942	F8	0.372
A9	1.280	B9	1.282	C9	1.219	D9	—	E9	1.006	F9	0.372
A10	1.301	B10	1.282	C10	1.265	D10	1.236	E10	1.081	F10	0.392
A11	1.304	B11	1.294	C11	1.294	D11	1.225	E11	1.173	F11	0.406
A12	1.304	—	—	C12	1.254	—	—	E12	—	F12	0.438
A13	1.309	—	—	—	—	—	—	E13	1.190	F13	0.516
A14	1.301	—	—	—	—	—	—	E14	1.193	F14	0.754
A15	1.304	—	—	—	—	—	—	—	—	F15	1.034
A16	1.301	—	—	—	—	—	—	—	—	F16	—
A17	1.297	—	—	—	—	—	—	—	—	F17	1.006
A18	1.251	—	—	—	—	—	—	—	—	—	—
A19	1.128	—	—	—	—	—	—	—	—	—	—
A20	1.032	—	—	—	—	—	—	—	—	—	—

Table B-12. Pressure data for Run 26-1 (GN₂ injection)

Run	26-1	Re/l , in. ⁻¹	0.287×10^6
M	2.61	P_j , psia	9.3
P_T , cm Hg	100.2	T_j , °F	73
P_S , psia	0.969	P_j/P_T	0.48
T_T , °F	101.0		

Pressure Tap	$\frac{P}{P_S}$										
A1	1.338	B1	1.044	C1	1.413	D1	1.146	E1	—	F1	0.695
A2	1.054	B2	1.033	C2	1.060	D2	1.032	E2	—	F2	0.850
A3	1.039	B3	1.036	C3	1.030	D3	1.020	E3	1.129	F3	0.895
A4	1.044	B4	1.033	C4	1.028	D4	1.019	E4	1.043	F4	0.956
A5	1.042	B5	1.032	C5	1.025	D5	1.021	E5	1.024	F5	0.993
A6	1.049	B6	1.030	C6	1.025	D6	1.022	E6	1.016	F6	1.015
A7	1.033	B7	1.030	C7	1.025	D7	1.019	E7	1.013	F7	1.010
A8	1.038	B8	1.030	C8	1.022	D8	1.022	E8	1.013	F8	1.025
A9	1.039	B9	1.030	C9	1.020	D9	—	E9	1.013	F9	1.018
A10	1.039	B10	1.030	C10	1.022	D10	1.021	E10	1.010	F10	1.019
A11	1.037	B11	1.030	C11	1.019	D11	1.021	E11	1.013	F11	1.012
A12	1.031	—	—	C12	1.019	—	—	E12	—	F12	1.004
A13	1.031	—	—	—	—	—	—	E13	1.011	F13	1.001
A14	1.031	—	—	—	—	—	—	E14	1.002	F14	1.008
A15	1.027	—	—	—	—	—	—	—	—	F15	1.002
A16	1.021	—	—	—	—	—	—	—	—	F16	—
A17	1.023	—	—	—	—	—	—	—	—	F17	1.002
A18	1.020	—	—	—	—	—	—	—	—	—	—
A19	1.016	—	—	—	—	—	—	—	—	—	—
A20	1.009	—	—	—	—	—	—	—	—	—	—

Table B-13. Pressure data for Run 26-2 (GN₂ injection)

Run	26-2	Re/l, in.⁻¹	0.287 × 10⁶
M	2.61	P_J, psia	18.8
P_T, cm Hg	100.3	T_J, °F	74
P_S, psia	0.973	P_J/P_T	0.97
T_T, °F	102.0		

Pressure Tap	$\frac{P}{P_S}$										
A1	1.569	B1	1.077	C1	1.629	D1	1.326	E1	—	F1	0.434
A2	1.075	B2	1.029	C2	1.139	D2	1.062	E2	—	F2	0.702
A3	1.032	B3	1.030	C3	1.025	D3	1.017	E3	1.271	F3	0.877
A4	1.036	B4	1.028	C4	1.023	D4	1.015	E4	1.101	F4	0.885
A5	1.035	B5	1.027	C5	1.021	D5	1.016	E5	1.032	F5	0.917
A6	1.041	B6	1.028	C6	1.019	D6	1.015	E6	1.013	F6	0.964
A7	1.028	B7	1.025	C7	1.020	D7	1.015	E7	1.007	F7	0.990
A8	1.031	B8	1.031	C8	1.017	D8	1.017	E8	1.009	F8	1.021
A9	1.031	B9	1.024	C9	1.015	D9	—	E9	1.008	F9	1.020
A10	1.033	B10	1.025	C10	1.016	D10	1.016	E10	1.006	F10	1.022
A11	1.029	B11	1.024	C11	1.015	D11	1.015	E11	1.008	F11	1.010
A12	1.027	—	—	C12	1.017	—	—	E12	—	F12	0.988
A13	1.029	—	—	—	—	—	—	E13	1.006	F13	0.995
A14	1.025	—	—	—	—	—	—	E14	0.998	F14	1.000
A15	1.020	—	—	—	—	—	—	—	—	F15	0.997
A16	1.019	—	—	—	—	—	—	—	—	F16	—
A17	1.017	—	—	—	—	—	—	—	—	F17	0.995
A18	1.014	—	—	—	—	—	—	—	—	—	—
A19	1.010	—	—	—	—	—	—	—	—	—	—
A20	1.005	—	—	—	—	—	—	—	—	—	—

Table B-14. Pressure data for Run 26-3 (GN_2 injection)

Run	26-3	Re/l , in. ⁻¹	0.285×10^6
M	2.61	P_j , psia	57.3
P_T , cm Hg	100.1	T_j , °F	74
P_s , psia	0.973	P_j/P_T	2.97
T_T , °F	103.0		

Pressure Tap	$\frac{P}{P_s}$										
A1	1.992	B1	1.575	C1	1.917	D1	1.678	E1	—	F1	0.252
A2	1.538	B2	1.092	C2	1.670	D2	1.480	E2	—	F2	0.329
A3	1.074	B3	1.031	C3	1.192	D3	1.138	E3	1.506	F3	0.392
A4	1.036	B4	1.026	C4	1.026	D4	1.023	E4	1.432	F4	0.505
A5	1.038	B5	1.025	C5	1.020	D5	1.013	E5	1.291	F5	0.743
A6	1.041	B6	1.025	C6	1.017	D6	1.013	E6	1.111	F6	0.992
A7	1.028	B7	1.023	C7	1.017	D7	1.014	E7	1.024	F7	1.029
A8	1.031	B8	1.023	C8	1.016	D8	1.014	E8	1.008	F8	0.988
A9	1.031	B9	1.023	C9	1.013	D9	—	E9	1.006	F9	0.970
A10	1.033	B10	1.021	C10	1.014	D10	1.014	E10	1.004	F10	0.978
A11	1.029	B11	1.023	C11	1.012	D11	1.013	E11	1.005	F11	0.991
A12	1.029	—	—	C12	1.014	—	—	E12	—	F12	0.989
A13	1.026	—	—	—	—	—	—	E13	1.005	F13	0.990
A14	1.024	—	—	—	—	—	—	E14	1.001	F14	0.995
A15	1.020	—	—	—	—	—	—	—	—	F15	0.985
A16	1.019	—	—	—	—	—	—	—	—	F16	—
A17	1.017	—	—	—	—	—	—	—	—	F17	0.989
A18	1.013	—	—	—	—	—	—	—	—	—	—
A19	1.010	—	—	—	—	—	—	—	—	—	—
A20	0.988	—	—	—	—	—	—	—	—	—	—

Table B-15. Pressure data for Run 26-4 (GN₂ injection)

Run	26-4	Re/l , in. ⁻¹	0.285×10^6
<i>M</i>	2.61	P_j , psia	156.2
P_T , cm Hg	100.5	T_j , °F	74
P_S , psia	0.978	P_j/P_T	8.07
T_T , °F	104.0		

Pressure Tap	$\frac{P}{P_S}$										
A1	2.115	B1	2.019	C1	2.399	D1	1.543	E1	—	F1	0.176
A2	2.055	B2	1.879	C2	1.849	D2	1.785	E2	—	F2	0.229
A3	1.865	B3	1.374	C3	1.865	D3	1.712	E3	1.446	F3	0.267
A4	1.322	B4	1.044	C4	1.630	D4	1.576	E4	1.616	F4	0.290
A5	1.041	B5	1.027	C5	1.166	D5	1.243	E5	1.594	F5	0.312
A6	1.040	B6	1.026	C6	1.022	D6	1.044	E6	1.546	F6	0.329
A7	1.025	B7	1.025	C7	1.019	D7	1.016	E7	1.466	F7	0.358
A8	1.030	B8	1.025	C8	1.018	D8	1.015	E8	1.338	F8	0.494
A9	1.030	B9	1.024	C9	1.014	D9	—	E9	1.157	F9	1.059
A10	1.031	B10	1.024	C10	1.015	D10	1.015	E10	1.010	F10	1.221
A11	1.029	B11	1.024	C11	—	D11	1.015	E11	1.007	F11	1.090
A12	1.026	—	—	C12	—	—	—	E12	—	F12	1.008
A13	1.028	—	—	—	—	—	—	E13	1.007	F13	0.988
A14	1.025	—	—	—	—	—	—	E14	1.001	F14	0.995
A15	1.020	—	—	—	—	—	—	—	—	F15	0.991
A16	1.019	—	—	—	—	—	—	—	—	F16	—
A17	1.014	—	—	—	—	—	—	—	—	F17	0.985
A18	1.013	—	—	—	—	—	—	—	—	—	—
A19	1.010	—	—	—	—	—	—	—	—	—	—
A20	1.002	—	—	—	—	—	—	—	—	—	—

Table B-16. Pressure data for Run 26-5 (GN₂ injection)

Run	26-5	$Re/l, \text{in.}^{-1}$	0.286×10^6
M	2.61	P_j, psia	212.0
$P_T, \text{cm Hg}$	100.7	$T_j, ^\circ\text{F}$	74
P_s, psia	0.978	P_j/P_T	10.9
$T_T, ^\circ\text{F}$	104.0		

Pressure Tap	$\frac{P}{P_s}$										
A1	2.715	B1	1.884	C1	3.090	D1	1.623	E1	—	F1	0.166
A2	1.980	B2	2.003	C2	1.664	D2	1.713	E2	—	F2	0.205
A3	2.020	B3	1.760	C3	1.941	D3	1.780	E3	1.443	F3	0.249
A4	1.735	B4	1.206	C4	1.828	D4	1.712	E4	1.540	F4	0.271
A5	1.038	B5	1.032	C5	1.526	D5	1.555	E5	1.634	F5	0.288
A6	1.046	B6	1.027	C6	1.091	D6	1.232	E6	1.602	F6	0.298
A7	1.030	B7	1.025	C7	1.022	D7	1.039	E7	1.561	F7	0.318
A8	1.031	B8	1.025	C8	1.018	D8	1.017	E8	1.506	F8	0.375
A9	1.024	B9	1.024	C9	1.015	D9	—	E9	1.397	F9	0.484
A10	1.035	B10	1.026	C10	1.017	D10	1.018	E10	1.068	F10	1.045
A11	1.029	B11	1.024	C11	1.015	D11	1.015	E11	1.010	F11	1.271
A12	1.028	—	—	C12	1.016	—	—	E12	—	F12	1.069
A13	1.027	—	—	—	—	—	—	E13	1.008	F13	1.010
A14	1.028	—	—	—	—	—	—	E14	1.007	F14	1.003
A15	1.020	—	—	—	—	—	—	—	—	F15	0.999
A16	1.019	—	—	—	—	—	—	—	—	F16	—
A17	1.018	—	—	—	—	—	—	—	—	F17	0.989
A18	1.012	—	—	—	—	—	—	—	—	—	—
A19	1.005	—	—	—	—	—	—	—	—	—	—
A20	1.004	—	—	—	—	—	—	—	—	—	—

Table B-17. Pressure data for Run 26-6 (GN_2 injection)

Run	26-6	Re/l , in. $^{-1}$	0.286×10^6
M	2.61	P_j , psia	300.1
P_T , cm Hg	100.7	T_j , °F	74
P_S , psia	0.976	P_j/P_T	15.5
T_T , °F	105.0		

Pressure Tap	$\frac{P}{P_S}$										
A1	3.605	B1	1.684	C1	3.894	D1	2.113	E1	—	F1	0.155
A2	1.741	B2	2.038	C2	1.669	D2	1.494	E2	—	F2	0.184
A3	2.092	B3	1.983	C3	1.853	D3	1.782	E3	1.768	F3	0.225
A4	1.994	B4	1.723	C4	1.949	D4	1.796	E4	1.403	F4	0.251
A5	1.662	B5	1.182	C5	1.837	D5	1.742	E5	1.554	F5	0.272
A6	1.141	B6	1.033	C6	1.513	D6	1.620	E6	1.647	F6	0.283
A7	1.030	B7	1.028	C7	1.104	D7	1.322	E7	1.624	F7	0.295
A8	1.035	B8	1.029	C8	1.023	D8	1.072	E8	1.600	F8	0.334
A9	1.039	B9	1.029	C9	1.019	D9	—	E9	1.561	F9	0.382
A10	1.038	B10	1.029	C10	1.019	D10	1.021	E10	1.351	F10	0.445
A11	1.031	B11	1.027	C11	1.018	D11	1.019	E11	1.057	F11	0.839
A12	1.030	—	—	C12	1.020	—	—	E12	—	F12	1.275
A13	1.030	—	—	—	—	—	—	E13	1.012	F13	1.092
A14	1.029	—	—	—	—	—	—	E14	1.009	F14	1.029
A15	1.022	—	—	—	—	—	—	—	—	F15	1.016
A16	1.021	—	—	—	—	—	—	—	—	F16	—
A17	1.019	—	—	—	—	—	—	—	—	F17	1.002
A18	1.018	—	—	—	—	—	—	—	—	—	—
A19	1.011	—	—	—	—	—	—	—	—	—	—
A20	1.007	—	—	—	—	—	—	—	—	—	—

Table B-18. Pressure data for Run 28-1 (GN₂ injection)

Run	28-1	Re/L, in.⁻¹	0.105×10^6
M	2.61	P_j, psia	3.5
P_T, cm Hg	35.4	T_j, °F	71
P_s, psia	0.351	P_j/P_T	0.51
T_{T_i}, °F	85.0		

Pressure Tap	$\frac{P}{P_s}$										
A1	1.150	B1	1.137	C1	1.092	D1	1.075	E1	—	F1	0.684
A2	1.160	B2	1.108	C2	1.108	D2	1.069	E2	—	F2	0.758
A3	1.138	B3	1.092	C3	1.099	D3	1.057	E3	1.043	F3	0.849
A4	1.111	B4	1.073	C4	1.080	D4	1.049	E4	1.049	F4	0.915
A5	1.089	B5	1.054	C5	1.061	D5	1.041	E5	1.043	F5	0.960
A6	1.063	B6	1.035	C6	1.045	D6	1.033	E6	1.037	F6	0.985
A7	1.053	B7	1.029	C7	1.037	D7	1.026	E7	1.030	F7	0.994
A8	1.041	B8	1.022	C8	1.022	D8	1.019	E8	1.024	F8	1.012
A9	1.010	B9	1.013	C9	1.011	D9	—	E9	1.022	F9	1.009
A10	1.032	B10	1.035	C10	1.008	D10	1.006	E10	1.008	F10	1.011
A11	1.042	B11	1.016	C11	0.997	D11	1.003	E11	1.006	F11	1.060
A12	1.033	—	—	C12	0.997	—	—	E12	—	F12	0.990
A13	1.031	—	—	—	—	—	—	E13	1.002	F13	0.987
A14	1.031	—	—	—	—	—	—	E14	0.997	F14	1.002
A15	1.031	—	—	—	—	—	—	—	—	F15	1.006
A16	1.030	—	—	—	—	—	—	—	—	F16	—
A17	1.034	—	—	—	—	—	—	—	—	F17	—
A18	1.030	—	—	—	—	—	—	—	—	—	—
A19	1.040	—	—	—	—	—	—	—	—	—	—
A20	1.031	—	—	—	—	—	—	—	—	—	—

Table B-19. Pressure data for Run 28-2 (GN₂ injection)

Run	28-2	Re/l, in.⁻¹	0.106×10^6
M	2.61	P_j, psia	6.4
P_T, cm Hg	35.4	T_j, °F	71
P_S, psia	0.351	P_j/P_T	0.93
T_T, °F	84.0		

Pressure Tap	$\frac{P}{P_S}$										
A1	1.195	B1	1.144	C1	1.214	D1	1.075	E1	—	F1	0.456
A2	1.172	B2	1.134	C2	1.118	D2	1.086	E2	—	F2	0.643
A3	1.160	B3	1.125	C3	1.118	D3	1.083	E3	1.053	F3	0.781
A4	1.141	B4	1.101	C4	1.101	D4	1.075	E4	1.069	F4	0.819
A5	1.111	B5	1.080	C5	1.086	D5	1.066	E5	1.062	F5	0.880
A6	1.091	B6	1.058	C6	1.074	D6	1.051	E6	1.059	F6	0.926
A7	1.070	B7	1.042	C7	1.058	D7	1.043	E7	1.053	F7	0.950
A8	1.052	B8	1.029	C8	1.035	D8	1.037	E8	1.045	F8	0.987
A9	1.043	B9	1.019	C9	1.027	D9	—	E9	1.038	F9	1.000
A10	1.035	B10	1.018	C10	1.013	D10	1.007	E10	1.026	F10	1.010
A11	1.040	B11	1.013	C11	1.003	D11	1.011	E11	1.013	F11	1.020
A12	1.031	—	—	C12	1.005	—	—	E12	—	F12	0.993
A13	1.036	—	—	—	—	—	—	E13	1.000	F13	1.000
A14	1.031	—	—	—	—	—	—	E14	0.999	F14	1.009
A15	1.029	—	—	—	—	—	—	—	—	F15	1.003
A16	1.031	—	—	—	—	—	—	—	—	F16	—
A17	1.030	—	—	—	—	—	—	—	—	F17	1.008
A18	1.030	—	—	—	—	—	—	—	—	—	—
A19	1.030	—	—	—	—	—	—	—	—	—	—
A20	1.036	—	—	—	—	—	—	—	—	—	—

Table B-20. Pressure data for Run 28-4 (GN₂ injection)

Run	28-4	Re/l , in. ⁻¹	0.106×10^6
M	2.61	P_j , psia	20.8
P_T , cm Hg	35.4	T_j , °F	72
P_s , psia	0.352	P_j/P_T	3.05
T_{T_f} , °F	82.5		

Pressure Tap	$\frac{P}{P_s}$										
A1	1.284	B1	1.157	C1	1.213	D1	1.114	E1	—	F1	0.292
A2	1.188	B2	1.167	C2	1.133	D2	1.085	E2	—	F2	0.332
A3	1.189	B3	1.157	C3	1.140	D3	1.104	E3	1.040	F3	0.357
A4	1.186	B4	1.172	C4	1.143	D4	1.117	E4	1.071	F4	0.447
A5	1.181	B5	1.165	C5	1.148	D5	1.120	E5	1.084	F5	0.630
A6	1.180	B6	1.164	C6	1.145	D6	1.122	E6	1.088	F6	0.795
A7	1.165	B7	1.130	C7	1.138	D7	1.116	E7	1.098	F7	0.874
A8	1.145	B8	1.111	C8	1.133	D8	1.108	E8	1.096	F8	0.890
A9	1.127	B9	1.068	C9	1.108	D9	—	E9	1.098	F9	0.925
A10	1.104	B10	1.034	C10	1.071	D10	1.063	E10	1.085	F10	0.959
A11	1.085	B11	1.024	C11	1.050	D11	1.024	E11	1.063	F11	0.976
A12	1.063	—	—	C12	1.021	—	—	E12	—	F12	0.986
A13	1.055	—	—	—	—	—	—	E13	1.015	F13	1.005
A14	1.045	—	—	—	—	—	—	E14	1.008	F14	1.010
A15	1.039	—	—	—	—	—	—	—	—	F15	1.016
A16	1.034	—	—	—	—	—	—	—	—	F16	—
A17	1.034	—	—	—	—	—	—	—	—	F17	1.011
A18	1.031	—	—	—	—	—	—	—	—	—	—
A19	1.032	—	—	—	—	—	—	—	—	—	—
A20	1.039	—	—	—	—	—	—	—	—	—	—

Table B-21. Pressure data for Run 28-5 (GN₂ injection)

Run	28-5	Re/l, in.⁻¹	0.106×10^6
M	2.61	P_j, psia	54.1
P_T, cm Hg	35.4	T_j, °F	72
P_S, psia	0.352	P_j/P_T	7.95
T_T, °F	82.3		

Pressure Tap	$\frac{P}{P_S}$										
A1	1.675	B1	1.127	C1	1.945	D1	0.984	E1	—	F1	0.273
A2	1.171	B2	1.187	C2	1.043	D2	1.035	E2	—	F2	0.302
A3	1.230	B3	1.198	C3	1.147	D3	1.118	E3	0.973	F3	0.318
A4	1.217	B4	1.187	C4	1.163	D4	1.126	E4	1.003	F4	0.331
A5	1.215	B5	1.183	C5	1.150	D5	1.129	E5	1.078	F5	0.355
A6	1.190	B6	1.180	C6	1.156	D6	1.135	E6	1.102	F6	0.372
A7	1.193	B7	1.182	C7	1.164	D7	1.142	E7	1.107	F7	0.407
A8	1.193	B8	1.179	C8	1.164	D8	1.143	E8	1.113	F8	0.639
A9	1.190	B9	1.158	C9	1.161	D9	—	E9	1.127	F9	0.974
A10	1.183	B10	1.123	C10	1.155	D10	1.129	E10	1.139	F10	1.051
A11	1.171	B11	1.080	C11	1.113	D11	1.078	E11	1.131	F11	0.984
A12	1.153	—	—	C12	1.091	—	—	E12	—	F12	0.926
A13	1.131	—	—	—	—	—	—	E13	1.054	F13	0.957
A14	1.100	—	—	—	—	—	—	E14	1.038	F14	1.006
A15	1.084	—	—	—	—	—	—	—	—	F15	1.006
A16	1.032	—	—	—	—	—	—	—	—	F16	—
A17	1.032	—	—	—	—	—	—	—	—	F17	1.012
A18	1.027	—	—	—	—	—	—	—	—	—	—
A19	1.030	—	—	—	—	—	—	—	—	—	—
A20	1.032	—	8	—	—	—	—	—	—	—	—

Table B-22. Pressure data for Run 28-6 (GN₂ injection)

Run	28-6	$Re/L, \text{in.}^{-1}$	0.107×10^6
M	2.61	P_j, psia	108.4
$P_T, \text{cm Hg}$	35.5	$T_j, ^\circ\text{F}$	73
P_s, psia	0.353	P_j/P_T	15.9
$T_{Tr}, ^\circ\text{F}$	82.0		

Pressure Tap	$\frac{P}{P_s}$										
A1	3.920	B1	1.116	C1	4.593	D1	1.935	E1	—	F1	0.235
A2	1.199	B2	1.127	C2	1.168	D2	1.001	E2	—	F2	0.254
A3	1.172	B3	1.211	C3	1.046	D3	1.025	E3	1.562	F3	0.270
A4	1.259	B4	1.225	C4	1.143	D4	1.098	E4	1.057	F4	0.291
A5	1.259	B5	1.212	C5	1.178	D5	1.146	E5	0.990	F5	0.302
A6	1.230	B6	1.195	C6	1.176	D6	1.157	E6	1.041	F6	0.317
A7	1.214	B7	1.195	C7	1.178	D7	1.163	E7	1.093	F7	0.331
A8	1.200	B8	1.179	C8	1.176	D8	1.170	E8	1.132	F8	0.389
A9	1.200	B9	1.197	C9	1.174	D9	—	E9	1.154	F9	0.426
A10	1.198	B10	1.184	C10	1.178	D10	1.179	E10	1.211	F10	0.542
A11	1.204	B11	1.168	C11	1.160	D11	1.151	E11	1.217	F11	0.836
A12	1.196	—	—	C12	1.160	—	—	E12	—	F12	1.136
A13	1.188	—	—	—	—	—	—	E13	1.105	F13	1.050
A14	1.180	—	—	—	—	—	—	E14	1.073	F14	1.021
A15	1.160	—	—	—	—	—	—	—	—	F15	0.960
A16	1.080	—	—	—	—	—	—	—	—	F16	—
A17	1.032	—	—	—	—	—	—	—	—	F17	0.994
A18	1.029	—	—	—	—	—	—	—	—	—	—
A19	1.031	—	—	—	—	—	—	—	—	—	—
A20	1.029	—	—	—	—	—	—	—	—	—	—

Table B-23. Pressure data for Run 28-7 (GN₂ injection)

Run	28-7	Re/l, in.⁻¹	0.107×10^6
M	2.61	P_j, psia	216.7
P_T, cm Hg	35.5	T_j, °F	73
P_S, psia	0.351	P_j/P_T	31.7
T_T, °F	82.0		

Pressure Tap	$\frac{P}{P_S}$										
A1	6.161	B1	2.544	C1	5.014	D1	4.793	E1	—	F1	0.214
A2	2.502	B2	1.102	C2	3.880	D2	2.064	E2	—	F2	0.233
A3	1.221	B3	1.123	C3	1.182	D3	1.040	E3	3.766	F3	0.238
A4	1.233	B4	1.177	C4	1.041	D4	1.011	E4	2.255	F4	0.255
A5	1.250	B5	1.214	C5	1.096	D5	1.054	E5	1.305	F5	0.268
A6	1.289	B6	1.206	C6	1.158	D6	1.100	E6	1.010	F6	0.282
A7	1.273	B7	1.206	C7	1.174	D7	1.150	E7	1.002	F7	0.284
A8	1.249	B8	1.188	C8	1.182	D8	1.182	E8	1.037	F8	0.310
A9	1.239	B9	1.203	C9	1.187	D9	—	E9	1.081	F9	0.329
A10	1.221	B10	1.199	C10	1.193	D10	1.249	E10	1.196	F10	0.349
A11	1.218	B11	1.199	C11	1.188	D11	1.236	E11	1.313	F11	0.378
A12	1.218	—	—	C12	1.190	—	—	E12	—	F12	0.475
A13	1.216	—	—	—	—	—	—	E13	1.244	F13	0.985
A14	1.211	—	—	—	—	—	—	E14	1.126	F14	1.220
A15	1.210	—	—	—	—	—	—	—	—	F15	1.165
A16	1.180	—	—	—	—	—	—	—	—	F16	—
A17	1.098	—	—	—	—	—	—	—	—	F17	1.030
A18	1.038	—	—	—	—	—	—	—	—	—	—
A19	1.034	—	—	—	—	—	—	—	—	—	—
A20	1.038	—	—	—	—	—	—	—	—	—	—

Table B-24. Pressure data for Run 28-8 (GN₂ injection)

Run	28-8	$Re/l, \text{in.}^{-1}$	0.109×10^6
M	2.61	P_j, psia	296.0
$P_T, \text{cm Hg}$	35.2	$T_j, ^\circ\text{F}$	73
P_s, psia	0.351	P_j/P_T	43.7
$T_T, ^\circ\text{F}$	81.5		

Pressure Tap	$\frac{P}{P_s}$										
A1	5.859	B1	4.331	C1	4.282	D1	4.825	E1	—	F1	0.203
A2	4.165	B2	1.486	C2	5.446	D2	3.574	E2	—	F2	0.214
A3	1.464	B3	1.150	C3	2.104	D3	1.545	E3	3.769	F3	0.218
A4	1.230	B4	1.197	C4	1.101	D4	1.085	E4	3.339	F4	0.236
A5	1.234	B5	1.230	C5	1.114	D5	1.082	E5	2.103	F5	0.242
A6	1.271	B6	1.241	C6	1.147	D6	1.114	E6	1.332	F6	0.246
A7	1.294	B7	1.240	C7	1.189	D7	1.163	E7	1.088	F7	0.264
A8	1.282	B8	1.213	C8	1.213	D8	1.203	E8	1.067	F8	0.290
A9	1.260	B9	1.227	C9	1.221	D9	—	E9	1.086	F9	0.296
A10	1.240	B10	1.224	C10	1.235	D10	1.353	E10	1.173	F10	0.309
A11	1.234	B11	1.225	C11	1.216	D11	1.342	E11	1.344	F11	0.326
A12	1.220	—	—	C12	1.230	—	—	E12	—	F12	0.378
A13	1.220	—	—	—	—	—	—	E13	1.395	F13	0.484
A14	1.222	—	—	—	—	—	—	E14	1.245	F14	0.995
A15	1.219	—	—	—	—	—	—	—	—	F15	1.238
A16	1.211	—	—	—	—	—	—	—	—	F16	—
A17	1.162	—	—	—	—	—	—	—	—	F17	1.139
A18	1.070	—	—	—	—	—	—	—	—	—	—
A19	1.032	—	—	—	—	—	—	—	—	—	—
A20	1.032	—	—	—	—	—	—	—	—	—	—

Table B-25. Pressure data for Run 30-1 (GN_2 injection)

Run	30-1	Re/l , in. ⁻¹	0.428×10^6
M	2.01	P_j , psia	12.7
P_T , cm Hg	110.3	T_j , °F	73
P_S , psia	2.72	P_j/P_T	0.60
T_T , °F	96.0		

Pressure Tap	$\frac{P}{P_S}$										
A1	1.178	B1	1.004	C1	1.251	D1	1.086	E1	—	F1	0.799
A2	1.013	B2	1.000	C2	1.015	D2	1.010	E2	—	F2	0.888
A3	1.001	B3	1.000	C3	1.002	D3	1.002	E3	1.089	F3	0.985
A4	1.003	B4	0.998	C4	1.003	D4	1.001	E4	1.026	F4	1.008
A5	1.003	B5	0.996	C5	1.002	D5	1.001	E5	1.008	F5	1.013
A6	1.013	B6	0.998	C6	1.000	D6	1.001	E6	0.999	F6	1.017
A7	0.998	B7	0.998	C7	1.001	D7	1.001	E7	0.994	F7	1.000
A8	1.008	B8	0.999	C8	1.001	D8	1.001	E8	0.998	F8	1.010
A9	1.008	B9	0.999	C9	1.000	D9	—	E9	1.000	F9	1.015
A10	1.013	B10	0.999	C10	1.003	D10	1.003	E10	0.999	F10	1.021
A11	1.003	B11	0.998	C11	1.003	D11	1.003	E11	1.008	F11	1.022
A12	1.003	—	—	C12	1.004	—	—	E12	—	F12	1.022
A13	1.002	—	—	—	—	—	—	E13	1.013	F13	0.994
A14	1.001	—	—	—	—	—	—	E14	1.004	F14	1.008
A15	0.996	—	—	—	—	—	—	—	—	F15	1.008
A16	1.000	—	—	—	—	—	—	—	—	F16	—
A17	1.009	—	—	—	—	—	—	—	—	F17	1.014
A18	1.002	—	—	—	—	—	—	—	—	—	—
A19	1.009	—	—	—	—	—	—	—	—	—	—
A20	1.008	—	—	—	—	—	—	—	—	—	—

Table B-26. Pressure data for Run 30-2 (GN₂ injection)

Run	30-2	Re/l , in. ⁻¹	0.428×10^6
<i>M</i>	2.01	P_j , psia	25.3
P_T , cm Hg	110.7	T_j , °F	74
P_S , psia	2.73	P_j/P_T	1.19
T_T , °F	97.0		

Pressure Tap	$\frac{P}{P_s}$										
A1	1.366	B1	1.018	C1	1.393	D1	1.208	E1	—	F1	0.593
A2	1.022	B2	1.000	C2	1.069	D2	1.035	E2	—	F2	0.883
A3	0.997	B3	1.000	C3	1.003	D3	1.003	E3	1.169	F3	0.910
A4	1.000	B4	0.997	C4	1.002	D4	1.001	E4	1.077	F4	0.936
A5	1.000	B5	0.996	C5	1.001	D5	1.001	E5	1.024	F5	0.980
A6	1.009	B6	—	C6	1.000	D6	1.001	E6	1.003	F6	1.011
A7	0.995	B7	0.998	C7	1.001	D7	1.001	E7	0.995	F7	1.010
A8	1.001	B8	0.999	C8	1.000	D8	1.001	E8	0.998	F8	1.022
A9	1.002	B9	0.999	C9	1.000	D9	—	E9	0.999	F9	1.020
A10	1.009	B10	0.999	C10	1.002	D10	1.003	E10	0.999	F10	1.020
A11	1.001	B11	0.997	C11	1.003	D11	1.004	E11	1.008	F11	1.022
A12	1.001	—	—	C12	1.005	—	—	E12	—	F12	1.017
A13	1.000	—	—	—	—	—	—	E13	1.014	F13	0.993
A14	0.998	—	—	—	—	—	—	E14	1.003	F14	1.006
A15	0.993	—	—	—	—	—	—	—	—	F15	1.005
A16	0.997	—	—	—	—	—	—	—	—	F16	—
A17	0.995	—	—	—	—	—	—	—	—	F17	1.011
A18	1.000	—	—	—	—	—	—	—	—	—	—
A19	1.005	—	—	—	—	—	—	—	—	—	—
A20	1.001	—	—	—	—	—	—	—	—	—	—

Table B-27. Pressure data for Run 30-4 (GN₂ injection)

Run	30-4	Re/L , in. ⁻¹	0.427×10^6
M	2.01	P_j , psia	72.4
P_T , cm Hg	110.5	T_j , °F	74
P_S , psia	2.72	P_j/P_T	3.40
T_T , °F	97.5		

Pressure Tap	$\frac{P}{P_S}$										
A1	1.599	B1	1.337	C1	1.555	D1	1.408	E1	—	F1	0.301
A2	1.318	B2	1.017	C2	1.405	D2	1.284	E2	—	F2	0.450
A3	1.009	B3	0.999	C3	1.087	D3	1.075	E3	1.305	F3	0.680
A4	1.001	B4	0.998	C4	1.005	D4	1.006	E4	1.253	F4	1.019
A5	1.000	B5	0.996	C5	1.001	D5	1.001	E5	1.171	F5	1.050
A6	1.010	B6	0.998	C6	1.000	D6	1.001	E6	1.074	F6	0.981
A7	0.995	B7	0.998	C7	1.001	D7	1.000	E7	1.014	F7	1.001
A8	1.002	B8	0.999	C8	1.001	D8	0.999	E8	1.002	F8	0.990
A9	1.004	B9	0.999	C9	1.000	D9	—	E9	1.000	F9	1.009
A10	1.010	B10	0.999	C10	1.002	D10	1.002	E10	0.998	F10	1.011
A11	1.000	B11	0.997	C11	1.003	D11	1.003	E11	1.007	F11	1.022
A12	1.001	—	—	C12	1.004	—	—	E12	—	F12	1.015
A13	0.999	—	—	—	—	—	—	E13	1.014	F13	0.991
A14	0.998	—	—	—	—	—	—	E14	1.004	F14	1.004
A15	0.993	—	—	—	—	—	—	—	—	F15	1.004
A16	0.998	—	—	—	—	—	—	—	—	F16	—
A17	0.996	—	—	—	—	—	—	—	—	F17	1.011
A18	1.000	—	—	—	—	—	—	—	—	—	—
A19	1.003	—	—	—	—	—	—	—	—	—	—
A20	1.003	—	—	—	—	—	—	—	—	—	—

Table B-28. Pressure data for Run 30-5 (GN₂ injection)

Run	30-5	$Re/L, \text{in.}^{-1}$	0.427×10^6
M	2.01	P_j, psia	205.6
$P_T, \text{cm Hg}$	110.5	$T_j, ^\circ\text{F}$	74
P_S, psia	2.72	P_j/P_T	9.66
$T_T, ^\circ\text{F}$	98.0		

Pressure Tap	$\frac{P}{P_S}$										
A1	1.501	B1	1.654	C1	1.520	D1	1.396	E1	—	F1	0.179
A2	1.657	B2	1.548	C2	1.590	D2	1.497	E2	—	F2	0.276
A3	1.520	B3	1.201	C3	1.542	D3	1.454	E3	1.333	F3	0.345
A4	1.142	B4	1.001	C4	1.395	D4	1.355	E4	1.399	F4	0.404
A5	1.001	B5	0.997	C5	1.075	D5	1.154	E5	1.381	F5	0.481
A6	1.010	B6	0.998	C6	1.002	D6	1.020	E6	1.346	F6	0.526
A7	0.995	B7	0.999	C7	1.001	D7	1.002	E7	1.288	F7	0.641
A8	1.001	B8	1.000	C8	1.001	D8	1.000	E8	1.210	F8	1.239
A9	1.002	B9	0.999	C9	1.001	D9	—	E9	1.116	F9	1.120
A10	1.010	B10	1.000	C10	1.003	D10	1.003	E10	1.010	F10	1.006
A11	1.000	B11	0.998	C11	1.003	D11	1.004	E11	1.008	F11	1.059
A12	1.001	—	—	C12	1.005	—	—	E12	—	F12	1.032
A13	1.000	—	—	—	—	—	—	E13	1.014	F13	1.018
A14	0.998	—	—	—	—	—	—	E14	1.006	F14	1.019
A15	0.991	—	—	—	—	—	—	—	—	F15	1.016
A16	0.996	—	—	—	—	—	—	—	—	F16	—
A17	0.995	—	—	—	—	—	—	—	—	F17	1.013
A18	1.000	—	—	—	—	—	—	—	—	—	—
A19	1.004	—	—	—	—	—	—	—	—	—	—
A20	1.002	—	—	—	—	—	—	—	—	—	—

Table B-29. Pressure data for Run 30-6 (GN_2 injection)

Run	30-6	$\text{Re}/l, \text{in.}^{-1}$	0.427×10^6
M	2.01	P_j, psia	296.1
$P_T, \text{cm Hg}$	110.6	$T_j, ^\circ\text{F}$	74
P_S, psia	2.72	P_j/P_T	13.9
$T_T, ^\circ\text{F}$	98.0		

Pressure Tap	$\frac{P}{P_S}$										
A1	1.662	B1	1.619	C1	1.907	D1	1.328	E1	—	F1	0.151
A2	1.680	B2	1.646	C2	1.459	D2	1.492	E2	—	F2	0.239
A3	1.630	B3	1.505	C3	1.594	D3	1.507	E3	1.278	F3	0.297
A4	1.461	B4	1.117	C4	1.542	D4	1.470	E4	1.377	F4	0.350
A5	1.059	B5	0.998	C5	1.370	D5	1.374	E5	1.413	F5	0.404
A6	1.010	B6	0.999	C6	1.056	D6	1.190	E6	1.393	F6	0.446
A7	0.995	B7	0.999	C7	1.003	D7	1.028	E7	1.368	F7	0.496
A8	1.002	B8	1.000	C8	1.002	D8	1.003	E8	1.329	F8	0.634
A9	1.003	B9	0.999	C9	1.004	D9	—	E9	1.265	F9	1.269
A10	1.010	B10	1.001	C10	1.003	D10	1.004	E10	1.083	F10	1.200
A11	1.001	B11	0.998	C11	1.004	D11	1.005	E11	1.015	F11	1.009
A12	1.001	—	—	C12	1.005	—	—	E12	—	F12	1.041
A13	1.000	—	—	—	—	—	—	E13	1.015	F13	1.030
A14	0.999	—	—	—	—	—	—	E14	1.007	F14	1.031
A15	0.993	—	—	—	—	—	—	—	—	F15	1.024
A16	0.996	—	—	—	—	—	—	—	—	F16	—
A17	0.996	—	—	—	—	—	—	—	—	F17	1.019
A18	1.001	—	—	—	—	—	—	—	—	—	—
A19	1.003	—	—	—	—	—	—	—	—	—	—
A20	1.002	—	—	—	—	—	—	—	—	—	—

Table B-30. Pressure data for Run 32-1 (GN₂ injection)

Run	32-1	Re/l , in. ⁻¹	0.143×10^6
M	2.01	P_j , psia	3.2
P_{T_1} , cm Hg	35.5	T_j , °F	70
P_S , psia	0.897	P_j/P_T	0.46
T_{T_1} , °F	81.5		

Pressure Tap	$\frac{P}{P_S}$										
A1	1.230	B1	1.050	C1	1.239	D1	1.107	E1	—	F1	0.879
A2	1.051	B2	1.023	C2	1.069	D2	1.044	E2	—	F2	0.956
A3	1.022	B3	1.025	C3	1.029	D3	1.030	E3	1.095	F3	1.000
A4	1.025	B4	1.024	C4	1.026	D4	1.029	E4	1.063	F4	1.029
A5	1.022	B5	1.023	C5	1.025	D5	1.028	E5	1.045	F5	1.023
A6	1.029	B6	1.022	C6	1.025	D6	1.027	E6	1.035	F6	1.030
A7	1.019	B7	1.020	C7	1.026	D7	1.028	E7	1.030	F7	1.032
A8	1.018	B8	1.019	C8	1.025	D8	1.030	E8	1.030	F8	1.039
A9	1.021	B9	1.018	C9	1.022	D9	—	E9	1.031	F9	1.035
A10	1.021	B10	1.017	C10	1.025	D10	1.033	E10	1.025	F10	1.029
A11	1.021	B11	1.018	C11	1.023	D11	1.023	E11	1.022	F11	1.018
A12	1.018	—	—	C12	1.024	—	—	E12	—	F12	1.011
A13	1.018	—	—	—	—	—	—	E13	1.019	F13	1.019
A14	1.016	—	—	—	—	—	—	E14	1.018	F14	1.019
A15	1.011	—	—	—	—	—	—	—	—	F15	1.030
A16	1.010	—	—	—	—	—	—	—	—	F16	—
A17	1.008	—	—	—	—	—	—	—	—	F17	1.050
A18	1.007	—	—	—	—	—	—	—	—	—	—
A19	1.009	—	—	—	—	—	—	—	—	—	—
A20	1.007	—	—	—	—	—	—	—	—	—	—

Table B-31. Pressure data for Run 32-2 (GN₂ injection)

Run	32-2	$Re/l, \text{in.}^{-1}$	0.144×10^6
M	2.01	P_j, psia	6.2
$P_T, \text{cm Hg}$	35.8	$T_j, ^\circ\text{F}$	71
P_S, psia	0.906	P_j/P_T	0.90
$T_{T_f}, ^\circ\text{F}$	81.0		

Pressure Tap	$\frac{P}{P_S}$										
A1	1.340	B1	1.075	C1	1.352	D1	1.181	E1	—	F1	0.780
A2	1.072	B2	1.021	C2	1.111	D2	1.070	E2	—	F2	0.907
A3	1.021	B3	1.020	C3	1.032	D3	1.031	E3	1.151	F3	0.970
A4	1.021	B4	1.020	C4	1.023	D4	1.023	E4	1.094	F4	1.009
A5	1.021	B5	1.019	C5	1.021	D5	1.023	E5	1.057	F5	1.030
A6	1.024	B6	1.019	C6	1.022	D6	1.024	E6	1.037	F6	1.038
A7	1.018	B7	1.019	C7	1.023	D7	1.025	E7	1.028	F7	1.040
A8	1.019	B8	1.016	C8	1.023	D8	1.026	E8	1.028	F8	1.041
A9	1.019	B9	1.015	C9	1.019	D9	—	E9	1.028	F9	1.040
A10	1.020	B10	1.016	C10	1.021	D10	1.031	E10	1.020	F10	1.030
A11	1.019	B11	1.017	C11	1.019	D11	1.027	E11	1.016	F11	1.019
A12	1.018	—	—	C12	1.021	—	—	E12	—	F12	1.017
A13	1.016	—	—	—	—	—	—	E13	1.016	F13	1.020
A14	1.016	—	—	—	—	—	—	E14	1.016	F14	1.019
A15	1.038	—	—	—	—	—	—	—	—	F15	1.027
A16	1.009	—	—	—	—	—	—	—	—	F16	—
A17	1.011	—	—	—	—	—	—	—	—	F17	1.049
A18	1.007	—	—	—	—	—	—	—	—	—	—
A19	1.008	—	—	—	—	—	—	—	—	—	—
A20	1.007	—	—	—	—	—	—	—	—	—	—

Table B-32. Pressure data for Run 32-3 (GN₂ injection)

Run	32-3	Re/l , in. ⁻¹	0.143×10^6
<i>M</i>	2.01	<i>P_j</i> , psia	19.8
<i>P_T</i> , cm Hg	35.6	<i>T_J</i> , °F	72
<i>P_S</i> , psia	0.902	<i>P_j/P_T</i>	2.89
<i>T_T</i> , °F	80.0		

Pressure Tap	$\frac{P}{P_S}$										
A1	1.609	B1	1.263	C1	1.569	D1	1.397	E1	—	F1	0.411
A2	1.246	B2	1.059	C2	1.346	D2	1.237	E2	—	F2	0.548
A3	1.050	B3	1.020	C3	1.109	D3	1.094	E3	1.298	F3	0.856
A4	1.021	B4	1.019	C4	1.030	D4	1.035	E4	1.239	F4	1.008
A5	1.021	B5	1.017	C5	1.020	D5	1.022	E5	1.160	F5	0.993
A6	1.025	B6	1.016	C6	1.020	D6	1.022	E6	1.092	F6	0.987
A7	1.019	B7	1.016	C7	1.021	D7	1.022	E7	1.048	F7	0.998
A8	1.019	B8	1.015	C8	1.022	D8	1.022	E8	1.033	F8	1.029
A9	1.019	B9	1.012	C9	1.024	D9	—	E9	1.027	F9	1.035
A10	1.020	B10	1.014	C10	1.019	D10	1.027	E10	1.016	F10	1.031
A11	1.020	B11	1.016	C11	1.017	D11	1.015	E11	1.011	F11	1.021
A12	1.018	—	—	C12	1.018	—	—	E12	—	F12	1.015
A13	1.018	—	—	—	—	—	—	E13	1.014	F13	1.018
A14	1.018	—	—	—	—	—	—	E14	1.007	F14	1.018
A15	1.012	—	—	—	—	—	—	—	—	F15	1.028
A16	1.011	—	—	—	—	—	—	—	—	F16	—
A17	1.011	—	—	—	—	—	—	—	—	F17	0.948
A18	1.011	—	—	—	—	—	—	—	—	—	—
A19	1.015	—	—	—	—	—	—	—	—	—	—
A20	1.010	—	—	—	—	—	—	—	—	—	—

Table B-33. Pressure data for Run 32-4 (GN₂ injection)

Run	32-4	Re/L , in. ⁻¹	0.142×10^6
<i>M</i>	2.01	P_j , psia	53.7
P_T , cm Hg	35.0	T_j , °F	73
P_S , psia	0.890	P_j/P_T	7.97
T_T , °F	77.0		

Pressure Tap	$\frac{P}{P_S}$										
A1	1.795	B1	1.648	C1	1.695	D1	1.546	E1	—	F1	0.258
A2	1.647	B2	1.414	C2	1.630	D2	1.509	E2	—	F2	0.330
A3	1.369	B3	1.111	C3	1.484	D3	1.409	E3	1.420	F3	0.399
A4	1.088	B4	1.023	C4	1.227	D4	1.245	E4	1.416	F4	0.479
A5	1.021	B5	1.018	C5	1.062	D5	1.098	E5	1.380	F5	0.591
A6	1.023	B6	1.016	C6	1.024	D6	1.037	E6	1.323	F6	0.794
A7	1.015	B7	1.015	C7	1.020	D7	1.025	E7	1.243	F7	1.061
A8	1.015	B8	1.014	C8	1.020	D8	1.024	E8	1.157	F8	1.118
A9	1.015	B9	1.012	C9	1.019	D9	—	E9	1.089	F9	1.049
A10	1.020	B10	1.012	C10	1.020	D10	1.028	E10	1.026	F10	1.041
A11	1.015	B11	1.016	C11	1.016	D11	1.017	E11	1.015	F11	1.014
A12	1.012	—	—	C12	1.020	—	—	E12	—	F12	1.022
A13	1.013	—	—	—	—	—	—	E13	1.015	F13	1.022
A14	1.012	—	—	—	—	—	—	E14	0.921	F14	1.021
A15	1.010	—	—	—	—	—	—	—	—	F15	1.030
A16	1.008	—	—	—	—	—	—	—	—	F16	—
A17	1.011	—	—	—	—	—	—	—	—	F17	1.048
A18	1.010	—	—	—	—	—	—	—	—	—	—
A19	1.015	—	—	—	—	—	—	—	—	—	—
A20	1.015	—	—	—	—	—	—	—	—	—	—

Table B-34. Pressure data for Run 32-5 (GN₂ injection)

Run	32-5	Re/l , in. ⁻¹	0.143×10^6
M	2.01	P_j , psia	107.5
P_T , cm Hg	35.2	T_j , °F	73
P_s , psia	0.892	P_j/P_T	15.9
T_T , °F	77.0		

Pressure Top	$\frac{P}{P_s}$										
A1	1.991	B1	1.748	C1	2.187	D1	1.484	E1	—	F1	0.182
A2	1.800	B2	1.718	C2	1.619	D2	1.588	E2	—	F2	0.246
A3	1.721	B3	1.552	C3	1.681	D3	1.570	E3	1.396	F3	0.298
A4	1.523	B4	1.221	C4	1.596	D4	1.519	E4	1.470	F4	0.339
A5	1.170	B5	1.049	C5	1.417	D5	1.423	E5	1.475	F5	0.378
A6	1.040	B6	1.021	C6	1.157	D6	1.262	E6	1.453	F6	0.424
A7	1.019	B7	1.017	C7	1.045	D7	1.109	E7	1.423	F7	0.474
A8	1.018	B8	1.018	C8	1.025	D8	1.045	E8	1.381	F8	0.694
A9	1.019	B9	1.016	C9	1.021	D9	—	E9	1.318	F9	1.180
A10	1.019	B10	1.018	C10	1.024	D10	1.031	E10	1.151	F10	1.229
A11	1.020	B11	1.019	C11	1.020	D11	1.030	E11	1.041	F11	1.114
A12	1.018	—	—	C12	1.022	—	—	E12	—	F12	1.069
A13	1.018	—	—	—	—	—	—	E13	1.019	F13	1.044
A14	1.018	—	—	—	—	—	—	E14	1.021	F14	1.049
A15	1.011	—	—	—	—	—	—	—	—	F15	1.050
A16	1.010	—	—	—	—	—	—	—	—	F16	—
A17	1.012	—	—	—	—	—	—	—	—	F17	1.044
A18	1.012	—	—	—	—	—	—	—	—	—	—
A19	1.019	—	—	—	—	—	—	—	—	—	—
A20	1.018	—	—	—	—	—	—	—	—	—	—

Table B-35. Pressure data for Run 32-6 (GN₂ injection)

Run	32-6	Re/L, in.⁻¹	0.145×10^6
M	2.01	P_j, psia	217.5
P_T, cm Hg	35.6	T_j, °F	73
P_S, psia	0.902	P_j/P_T	31.7
T_T, °F	77.0		

Pressure Tap	$\frac{P}{P_B}$	Pressure Tap	$\frac{P}{P_S}$	Pressure Tap	$\frac{P}{P_S}$						
A1	3.200	B1	1.615	C1	3.145	D1	2.131	E1	—	F1	0.152
A2	1.591	B2	1.723	C2	1.792	D2	1.452	E2	—	F2	0.176
A3	1.820	B3	1.771	C3	1.554	D3	1.516	E3	1.814	F3	0.219
A4	1.798	B4	1.694	C4	1.712	D4	1.603	E4	1.487	F4	0.251
A5	1.690	B5	1.522	C5	1.674	D5	1.577	E5	1.369	F5	0.282
A6	1.475	B6	1.191	C6	1.601	D6	1.545	E6	1.451	F6	0.310
A7	1.141	B7	1.034	C7	1.451	D7	1.482	E7	1.470	F7	0.344
A8	1.022	B8	1.007	C8	1.191	D8	1.375	E8	1.453	F8	0.419
A9	1.018	B9	1.005	C9	1.041	D9	—	E9	1.439	F9	0.505
A10	1.017	B10	1.005	C10	1.007	D10	1.012	E10	1.377	F10	0.591
A11	1.017	B11	1.006	C11	1.007	D11	1.001	E11	1.272	F11	1.090
A12	1.011	—	—	C12	1.005	—	—	E12	—	F12	1.260
A13	1.011	—	—	—	—	—	—	E13	1.020	F13	1.129
A14	1.011	—	—	—	—	—	—	E14	0.987	F14	1.072
A15	1.010	—	—	—	—	—	—	—	—	F15	1.074
A16	1.009	—	—	—	—	—	—	—	—	F16	—
A17	1.011	—	—	—	—	—	—	—	—	F17	1.077
A18	1.011	—	—	—	—	—	—	—	—	—	—
A19	1.017	—	—	—	—	—	—	—	—	—	—
A20	1.017	—	—	—	—	—	—	—	—	—	—

Table B-36. Pressure data for Run 32-7 (GN₂ injection)

Run	32-7	Re/L , in. ⁻¹	0.141×10^6
M	2.01	P _j , psia	256.4
P _T , cm Hg	34.7	T _j , °F	73
P _s , psia	0.879	P _j /P _T	38.4
T _T , °F	77.0		

Pressure Tap	$\frac{P}{P_s}$										
A1	3.700	B1	2.045	C1	3.499	D1	2.641	E1	—	F1	0.143
A2	1.951	B2	1.536	C2	2.326	D2	1.775	E2	—	F2	0.159
A3	1.592	B3	1.811	C3	1.470	D3	1.414	E3	2.158	F3	0.189
A4	1.847	B4	1.793	C4	1.659	D4	1.577	E4	1.772	F4	0.221
A5	1.810	B5	1.723	C5	1.747	D5	1.649	E5	1.473	F5	0.247
A6	1.718	B6	1.556	C6	1.714	D6	1.629	E6	1.395	F6	0.266
A7	1.520	B7	1.253	C7	1.654	D7	1.603	E7	1.484	F7	0.300
A8	1.173	B8	1.055	C8	1.524	D8	1.554	E8	1.516	F8	0.368
A9	1.035	B9	1.016	C9	1.278	D9	—	E9	1.504	F9	0.435
A10	1.019	B10	1.016	C10	1.029	D10	1.067	E10	1.473	F10	0.497
A11	1.019	B11	1.019	C11	1.018	D11	1.032	E11	1.417	F11	0.555
A12	1.014	—	—	C12	1.023	—	—	E12	—	F12	1.228
A13	1.015	—	—	—	—	—	—	E13	1.166	F13	1.268
A14	1.015	—	—	—	—	—	—	E14	1.052	F14	1.169
A15	1.011	—	—	—	—	—	—	—	—	F15	1.112
A16	1.009	—	—	—	—	—	—	—	—	F16	—
A17	1.011	—	—	—	—	—	—	—	—	F17	1.101
A18	1.010	—	—	—	—	—	—	—	—	—	—
A19	1.016	—	—	—	—	—	—	—	—	—	—
A20	1.014	—	—	—	—	—	—	—	—	—	—

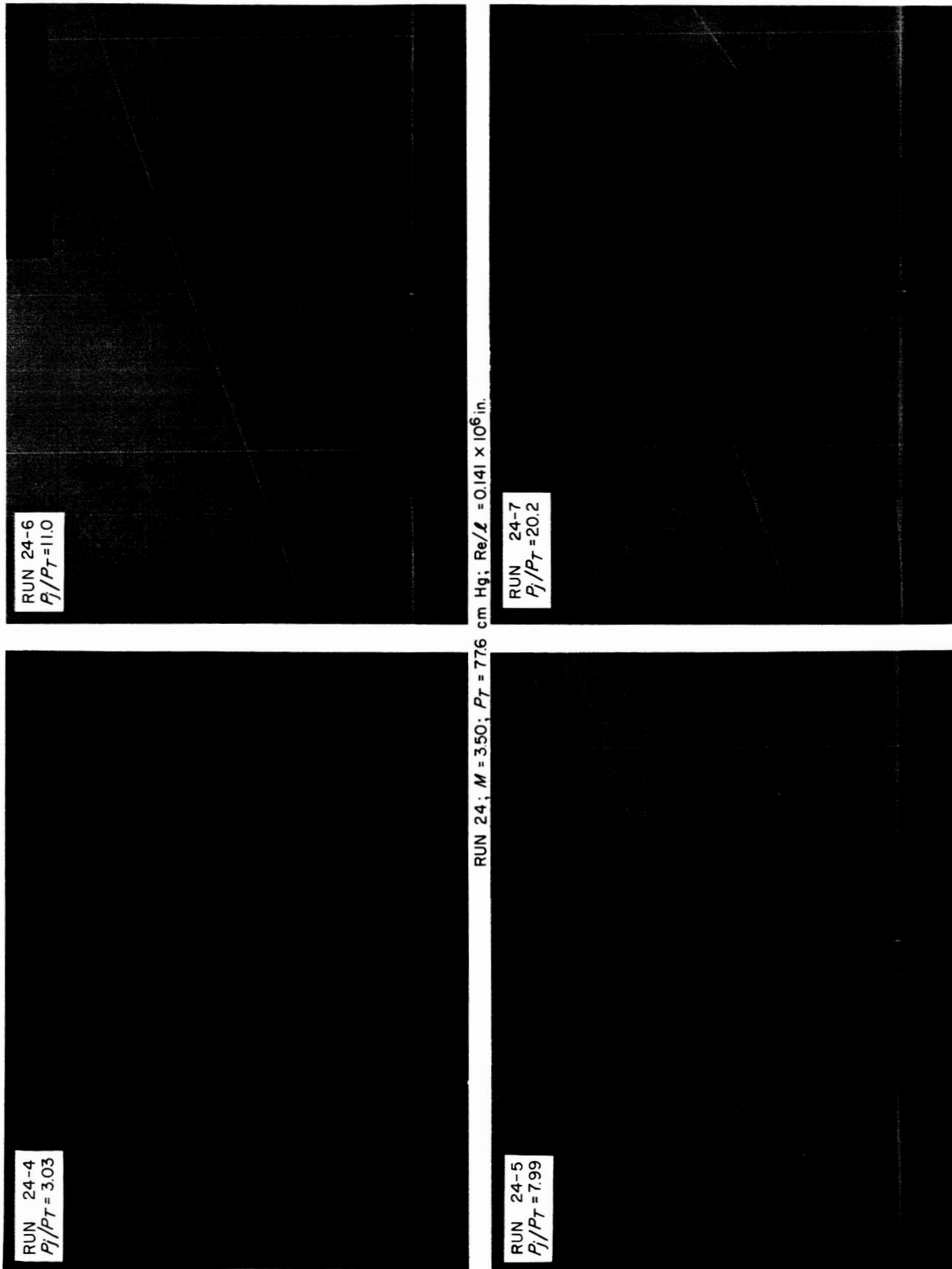


Fig. B-1. Comparison of shadowgraphs for Run 24 (GN_2 injection)

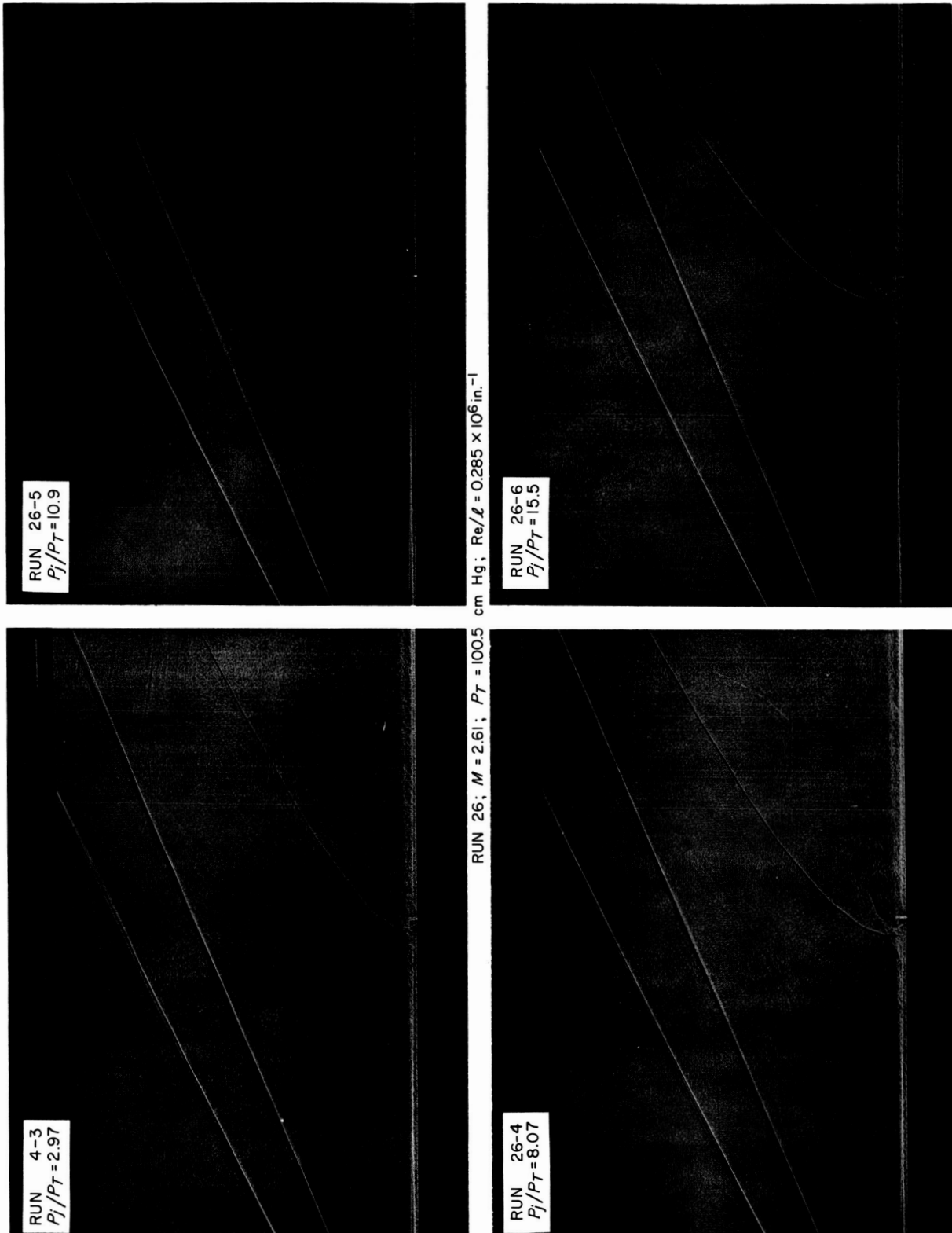


Fig. B-2. Comparison of shadowgraphs for Run 26 (GN₂ injection)

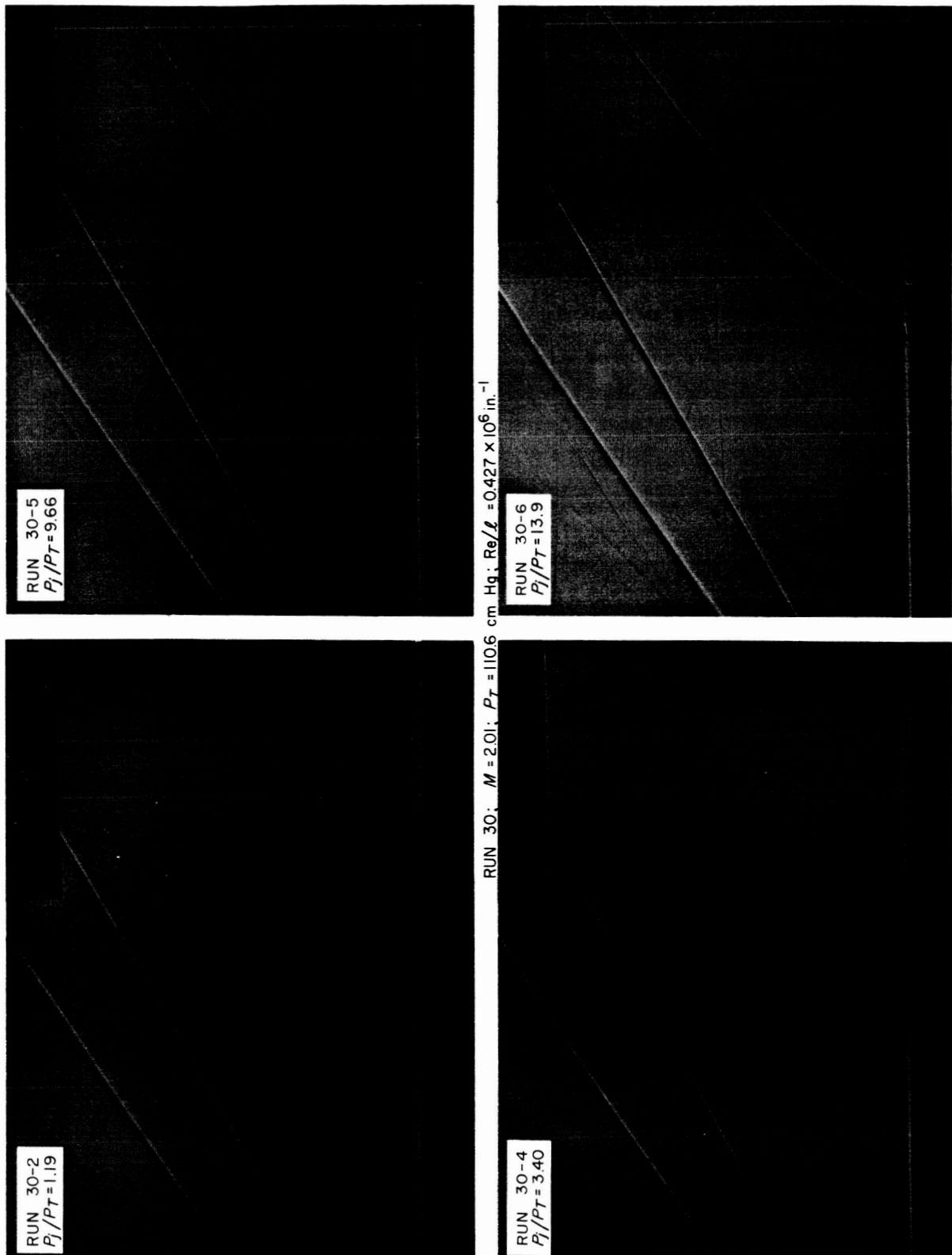


Fig. B-3. Comparison of shadowgraphs for Run 30 (GN_2 injection)

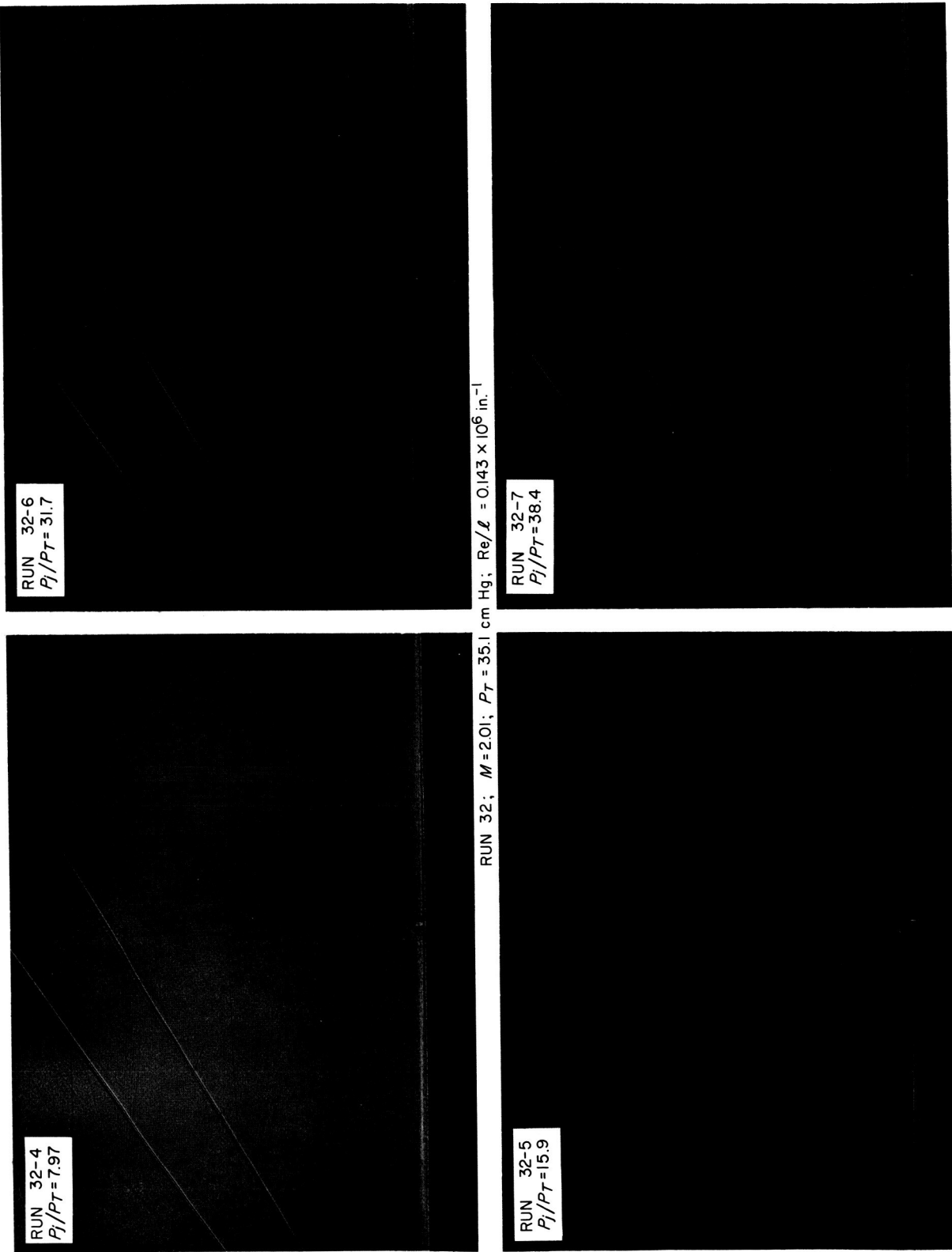


Fig. B-4. Comparison of shadowgraphs for Run 32 (GN_2 injection)

NOMENCLATURE

c_p average specific heat between t_0 and t_1

$C_{P_{sz}}$ pressure coefficient in separation zone

$h_{f\eta_0}$ heat of vaporization at surrounding pressure

M Mach number

P local static pressure

P_{exit} maximum observed plate static pressure from pressure distribution curves

P_j injection pressure

P_s tunnel static pressure

$\left(\frac{P}{P_s}\right)_{sz}$ ratio of local static pressure to tunnel static pressure in separation zone

P_T tunnel total pressure

P_{vp} vapor pressure corresponding to injection temperature

Re/l Reynolds number per unit length in free stream

Re_s Reynolds number at separation point

t_0 equilibrium temperature corresponding to the surrounding pressure

t_1 injection temperature

x percentage flash vaporization

w_c flow rate based on injector calibration

w_{fm} flow rate measured by turbine flowmeter

Δw ($w_c - w_{fm}$)

γ ratio of specific heats

REFERENCES

1. Newton, J. F., Jr. and F. W. Spaid, *Experiments on the Interaction of Secondary Injectants and Rocket Exhaust for Thrust Vector Control*, Technical Report No. 32-203, Jet Propulsion Laboratory, February 1962.
2. Kallis, J. M. and Marvin Adelberg, *Recent Advances in the Fluid Dynamics of Gas Injection for Thrust Vector and Trajectory Control*, Report No. ATN-63(3305)-3, Aerospace Corporation, July 1963.
3. Bogdonoff, S. M. and C. E. Kepler, "Separation of a Supersonic Turbulent Boundary Layer," *Journal of Aeronautical Sciences*, Vol. 22, No. 6, June 1955.
4. Dussourd, J. L. and A. H. Shapiro, "A Deceleration Probe for Measuring Stagnation Pressure and Velocity of a Particle-Laden Gas Stream," *Jet Propulsion*, Vol. 28, No. 1, p. 24, January 1958.